MINERALOGICAL STUDIES ON SOME SYNTHETIC ALLOYS AND MINERALS OF THE PLATINOID GROUP

by

SAMIRA AZIZ TOMA, B.Sc. (ALEXANDRIA), M.Sc. (CAIRO), M.I.M.M.

June 1975

A thesis submitted in partial fulfilment of requirements for the degree of Doctor of Philosophy in accordance with the Special Regulations.

ABSTRACT

Concentrates from five different localities were investigated in this study. These were alluvial concentrates from Alaska (U.S.A.), Choco (Columbia), Witwatersrand (South Africa), Urals (U.S.S.R), and eluvial nuggets from Ethiopia . The principal method of investigation was optical microscopy including quantitative reflectance and microhardness measurements. Analyses of whole grains or inclusions were carried out by electron-probe microanalysis. To help in understanding natural alloys, synthetic binary alloys of iron and platinum were studied. A series of synthetic alloys of iridium-osmium-ruthenium were prepared and studied to assist in understanding the mineralogy of similar natural alloys. The phase relationships found in the study of synthetic iridium-osmium-ruthenium alloys were used to interpret the mineralogy of the Witwatersrand concentrates. As a result some hypotheses on the origin of these placer deposits are presented.

Ferroplatinum grains differ in size morphology and optical properties. These differences are due to elements contained in solid solution. Iron and copper are invariably dissolved in the platinum, from which it is concluded that the three elements were brought together in the original magma. Iron was found to have a large effect on the reflectivity and microhardness of ferroplatinum. For naturally occurring ferroplatinum this effect is outweighed by the presence of dissolved iridium. In synthetic binary feroplatinum alloys it was found that the reflectivity decreased as the iron content increased. The microhardness of synthetic ferroplatinum increases with the increase of iron content, which reaches a maximum at the composition of Fe Pt.

Phase relations in the iridium-osmium-ruthenium system have been determined. It was found that the two phase-field determined is much narrower than reported in previous work. The microhardness of synthetic hexagonal alloys is greater than cubic alloys. Hardness changes in naturally occurring alloys are interpreted according to the various mechanisms of hardening in solid solution. Data on the microhardness and reflectivity of native iridium were also obtained.

CONTENTS

LIST OF MAPS.

LIST OF TABLES

LIST OF FIGURES

APPENDIX 4.

ACKNOWLEDGMENT

I wish to express my gratitude to my supervisor, Professor D.D. Hawkes, for his guidance and encouragement during the course of this research.

I am also indebted to Dr. D. Vaughan for helpful criticism, and to Dr. S. Murphy of the Department of Metallurgy for his advice in the preparation of synthetic alloys. I am particularly grateful for his valuable help in reading the manuscript for these synthetic alloys. My thanks also go to the technicians in the Department of Geological Science and the Department of Metallurgy for their help.

I would like to express my gratitude to Professor A.P. Millman, University College Cardiff, for suggesting the topic of research. My great thanks also go to Mr. G.A. Kingston, University College Cardiff, for lending me some samples from his own collections.

CHAPTER I

1.1. INTRODUCTION

This investigation is principally a study of the mineralogy of the platinoid group metals with particular reference to the various alloy forms of platinum, osmium, iridium and ruthenium in various concentrates. The aim of this work was to :-

a. Collate data on recorded platinum occurrences throughout the world and make mineralogical and geological comparisons between them.

b. Enlarge and clarify present knowledge of platinum mineralogy, particularly that of the alloys.
This involved preparation of synthetic alloys, and chemical analysis of these and natural samples, followed by determination of quantitative reflectance and quantitative microhardness, X-ray diffraction patterns and microscopic properties.

c. Examine and interpret the various forms of platinoid mineral intergrowths to clarify aspects of mineral genesis, especially with those forms of controversial origin.

1.2. DISCOVERY AND USES OF THE PLATINUM GROUP ELEMENTS.

The oldest known object containing platinum is an ancient Egyptian ornament. The platinum probably came from a placer deposit. Platinum is also found in some ancient ornaments from Abyssinia and other localities in the far and near East. It is also possible that the Greeks sometimes confused it with the mineral electrum. In Columbia, the pre-Columbian Indians of Ecuador worked platinum together with gold.

The first known reference to platinum was made in 1517 by Julius della Scala, who called it "Orichalcum". He found it impossible to melt this metal which was said to be found between Mexico and the Darient Coast (Columbia). In 1640 Alvaro Alonso described a metal as a "grey brilliant and lustrous stone and very difficult to work because it is not attacked by fire". In 1741 an Englishman who lived in Jamaica described a metal similar to silver which was impossible to melt by fire, but only by means of a special fluid that was known to the Indians of those regions. Crude platinum arrived in Europe from South America in 1735, although early export from Columbia was restricted by the Spanish government. The first complete melting of platinum was reported by Lavoisier in 1783, which was shortly after the discovery of oxygen. The fusion was achieved by heating platinum on charcoal in a blast of the new gas. One can visualize the difficulties that early chemists had in reaching a temperature of 1773°C, the melting point of pure platinum. Its properties were described early in 1750 by B. Brownrigg and W. Watson. Pure platinum was first isolated by Mardgraff in 1757.

Osmium and iridium were described by S. Tennant in 1803. Their names come respectively from Greek words Osme (smell), on account of the penetrating odour of the volatile oxide, and Iris (rainbow), because of the different colours displayed by its salts. Palladium and rhodium were discovered by Wollaston in 1803. The former is named after the asteroid Pallas, discovered in the same year, and the latter from the Greek word meaning rose because of the colours of its salts. The name ruthenium, from Ruthenia, the latin name for Russian, was first used by Ossan in 1828 to designate a platinum residue.

The use of platinum metals in modern jewellery dates from about 1909 by replacing gold in most of its applications. The higher ductility of the alloys, hardened with iridium or ruthenium ensured the durability of jewellery. Platinum metals act as catalysts in oxidation, reduction, hydrogenation and de-hydrogenation reactions. One of the principal uses of platinum is as a catalyst in oil refining which replaces the old cracking system used before the war. It is also used as a catalyst in the production of nitric acid which is used to produce fertilizers and explosives and many other processes such as the production of pharmaceuticals, vitamins and antibiotics. The major application of platinum in the electrical industry is in contacts and for electrodes in spark plugs. Thermocouples and thermo-elements usually consist of platinum alloyed with other metals such as rhodium, iridium or ruthenium, depending on the temperature to be measured. Platinum has had an interesting history in connection with the development of the internal combustion engine. It was originally used for the tube in hot ignition; then came high-tension electrical ignition with platinum-iridium contacts in the spark coil circuit and magnets. More recently platinum has been used in catalyst materials used to reduce the exhaust emissions of motor vehicles.

Rhodium-platinum alloys are used for the windings of high temperature electric resistance furnaces. The addition of rhodium gives an alloy particularly suitable for high-temperature work. Brazing alloys which contain palladium are frequently used in gas turbines, jet engines and frames because they are relatively free from corrosion at high temperatures. One of the common uses for platinum and platinum alloys is in electro-plating. The rhodium plating, which gives a pleasing, uniform and non-tarnishing coat, is known as the best for finishing jewellery. The high reflecting power of a rhodium coating is being used in lighting equipment and search lights. Platinum, palladium and rhodium plating is being especially applied to such articles as watch cases, coffee services, medals etc.

Platinum metals are extensively used in dentistry because of their resistance to corrosion and excellent mechanical properties.

1.3 BRIEF BACKGROUND ON THE GEOCHEMISTRY OF THE PLATINOIDS

The platinum metals are six of the heavier metals of group VIII (Table 1.1) which are usually divided into the light platinum metals ruthenium, rhodium, palladium, and the heavy platinum metals osmium, iridium and platinum. The presence of one or more of the platinum metals in a mineral phase, generally as a major constituent, gives rise to the term "Platinoid" for that phase. The commercial use of the term "Platinum" generally refers to the whole group of elements. The atomic radii of these metals are very similar. Because of this similarity, as well as similarity of crystal structure, and chemical and physical properties (Table 1.2), the platinum metals form a geochemically coherent group of elements. They are invariably found together in nature and readily substitute for one another in mineral lattices. This factor results in their most common mineral forms being the native metals, alloys of these metals (Table 1.3), and alloys with base metals of similar atomic radii and structure, such as copper, nickel, iron, cobalt, mercury, tin and the precious metals gold and silver. Thus native platinum, ferro-platinum, osmiridium (cubic-Ir-Os), iridosmine (hexagonal Os-Ir) and other rare minerals are important platinum sources.

The platinum metals also combine with sulphur, arsenic, tellurium, bismuth, and antimony to give a variety of less common sulphides, arsenides, tellurides, bismuthides, and antimonides (Table 1.4). Notable amongst these being braggite(Pt, Pd, Ni) S, cooperite, (Pt S), laurite (Ru, Os) S_2, sperrylite (Pt As_2), and stibio-palladinite (Pd_3Sb).

Platinum metals also occur in other minerals in trace quantities as in the base-metal sulphides, pyrrhotite, pentlandite, and chalcopyrite and to a lesser degree in silicates and oxides. However, it is evident from the increasing number of platinoid minerals which are being found, that they occur as discrete platinoid minerals rather than substituting in the lattices of the base metal sulphides or rock-forming silicates.

PLATINOID METALS

26 Fe 55.85	27 Co 58.94	28 Ni 58.71	29 Cu 63.54
44 Ru 101.1	45 Rh 102.91	46 Pd 106.4	47 Ag 107.8
76 Os 190.2	77 Ir 192.2	78 Pt 195.09	79 Au 197.0

GROUP VIII GROUP I B

(Table 1.1)

Platinoid metals in the periodic table

	LIGHT			HEAVY		
Properties	Ru	Rh	Pd	Os	Ir	Pt
Atomic radius (Å)	1.33	1.34	1.37	1.35	1.35	1.38
Crystal system	hexagonal C.P.	cubic F.C.	cubic F.C.	hexagonal C.P.	cubic F.C.	cubic F.C.
Lattice parameter (Å)	ao=2.7058 c/a=1.5824	3.7957	3.8825	ao=2.7304 c/a=1.5785	3.8312	3.9161
Reflectivity (%)	62.0-70.0	65.0-70.0	69.0-80.0	64.0-74.0	65.0-72.0	65.0-73.0
Microhardness (VHN)	220-300	422-800	190-475	474-790	464-739	423-795
Specific gravity	42.2	41.44	42.02	22.5	22.5	21.45
Melting point(°C)	2400	1966	1554	2700	2454	1773.5
Resistivity (μ - ohm.cm) 0°C	7.16-7.6	4.51	10.0	9.5	4.9	9.83

Table 1.2.

Close similarity of the platinoids in physical, chemical and structural properties.

Name	Composition	System
Ferroplatinum	FePt	isometric
Osmiridium	IrOs	isometric
Iridosmine	OsIr	hexagonal
Platinum	Pt and traces of others	isometric
Allopalladium (Rare)	PdHg and traces of others	hexagonal
Norilskite	PtFeNiCu ?	?
Palladium	PdAs and traces of others	isometric
Rhodium	Rh Os or Ir	?
Potarite	PdHg (or $Pd_3 Hg_2$?)	tetragonal
Rhodite	RhAu	isometric
Porpezite	PdAu	isometric
Platiniridium	PtIr	isometric
Palladiplatinum	amount PdPt	isometric
Aurosmiridium	Ir Os Au and traces of Ru and Au.	?

Alloys of the platinoids.

Table 1.3

	NAME	COMPOSITION	SYSTEM
SULPHIDES	Braggite	(PtPdNi) S	tetragonal
	Vysotskite	(PdNi) S	tetragonal
	Cooperite	Pt S	tetragonal
	Laurite	(RuOs) S_2 + Ir	isometric
	Hollingworthite	(RhPdPtIr) $(AsS)_2$	?
	Roseite (rare)	(OsIr) S	?
	Erlichmanite	OsS_2	cubic
	Unnamed (1)	(Ru,Rh,Os) S	cubic
		c.f.Alaska Fig.2.1	
	Unnamed (2)	Ir. Sulphide	cubic
	Unnamed (3)	(Pt,Ir,Os,Ru) S	
ARSENIDES	Sperrylite	Pt As_2	Isometric
	Osarsite	Os As S	Monoclinic
	Arsenopalladinite	Pd_3 As or Pd_5 As_2	Tetragonal
TELLURIDES	Kotulskite	Pd Te Bi	Hexagonal
	Merenskyite	(Pd Pt) $(Te\ Bi)_2$	Trigonal
BISMUTHIDES	Insizwait	Pt Bi_2	?
	Froodite	Pd Bi_2	Monoclinic
	Polarite	Pd Bi	Tetragonal
	Michenereite	Pd Te Bi	Isometric
ANTIMONIDES	Geversite	Pt Sb_2	Isometric
	Stibiopalladinite	Pd_3 Sb	?

Table 1.4

Chemical compounds of the platinoids.

1.4. DISTRIBUTION OF DEPOSITS OF PLATINOID METALS.

Platinum metals have been found as natural alloys all over the world. The principal countries in which platinum metals have been found are listed alphabetically in Table 1.5 (after Mertie 1969). These countries are shown in Map 1.1. Most of these occurrences are not economic deposits and are only of scientific interest. The most significant deposits are related to basic and ultrabasic rocks, but some are associated with granitic rocks.

Recently Stumpfl 1974 summarised his researches in depth, and discussed the genesis of platinum deposits, especially those of primary deposits. Most of the samples studied in this work are from placer deposits and the distribution of placer deposits will be discussed in more detail.

Platinoid placers are commonly derived from dunite or serpentinite, in which these metals are sparsely and irregularly distributed. In non-glacial regions it may be inferred that the original lodes could be discovered by tracing the alluvial deposits upstream. Commonly, the general country rock may thus be recognised, but workable lodes cannot be located. This may result from one or more of the three following causes :-

1. The original rocks from which placers were derived may have been completely eroded, so that no platiniferous source rocks remain in this area.
2. The present country rock may be platiniferous, but may represent the uneroded low grade roots of lodes that were richer in their upper horizons.
3. All the original source rocks may have been of extremely low grade, and the placers may have been concentrated from such sources over a very long period of time. Under such circumstances representative source rocks, even if preserved, would not constitute workable lodes.

The formation of placers is possible under any of these conditions but workable lodes can so rarely be located from placer fields, that it is concluded that the platinum metals in placers have been concentrated generally from source rocks in which these metals were sparsely and widely disseminated.

Heavy metals, such as platinum or gold, rarely migrate far downstream from their bed rock sources, unless they are so fine-grained as to be moved by swift water or floated by surface tension.

Generally, however, ordinary detrital grains of platinum work rapidly downwards through alluvial deposits, and come to rest near, or against bed rock. If the bed rock has a well-developed cleavage or fracture, the precious metals may penetrate 10 feet or more. Only very high water that cuts to bed rock, or a rejuvenation of the stream, will again move these metals. Even under these conditions their migration down stream is not great. Hence, excepting some special environment such as glaciation, placers of the precious metals may be assumed to lie within a few miles of their bedrock sources. If placer paystreaks are very long, it may be suspected that the metals have been distributed downstream by repeated lowering of the base level of erosion or as a result of glaciation.

Platinum placers consist of alluvial deposits that contain the alloys of the six platinum metals . Most of the placer grains consist of two intergrown or intermixed alloys, each of variable composition. Some of the alluvial platinum comes from placers that yield both gold and platinum e.g. the stream placers of Columbia.

Commonly gold and platinum occur in separate alloys, one of gold and silver and the other of five or six platinum metals. This fact is not generally revealed by bulk analyses of placer platinum, where small amounts of gold are reported merely as a part of the precious metals content.

In this investigation, electron micro-probe analyses of placer deposits from Choco in Columbia, show that platinum metals are intergrown with gold. Also samples from Witwatersrand show that gold is intergrown and alloy with platinum metals. It is also noticed that the size of the grains of gold and platinum are the same. These observations and the results of the microscopic investigation agree with the previous suggestion by Mertie (1969). Platinum placers and gold placers can be classified as follows:-

1. Residual placers, which can be present stream valleys, or old stream valleys.
2. Residual and eluvial placers.
3. Beach placers, which may be present beaches, or ancient beaches.
4. Deltaic and outwash deposits.
5. Glaciofluvial deposits.
6. Aeolian deposits.
7. Lithified placers.

1.5. LOCATIONS OF PLATINOIDS STUDIED IN THIS THESIS

Placer deposits from Alaska, Columbia, Ethiopia, Witwatersrand and Urals have been selected for detailed study for the following reasons:-

1. The placer deposits of Alaska are the only commercial platinum deposits in the United States, and previous analyses were commercially based and do not provide information for scientific study.
2. The gold-platinum placers of Columbia have not been adequately described before.
3. The Ethiopian deposits have been investigated in this study because of their national importance, because the presence of platinum minerals in Ethiopia leads to considering the presence of platinum minerals in the Egyptian Black Sand which was studied before by the writer as part of an M. Sc. these project.

4. Special attention has been paid to placers of the Witwatersrand because , although they are the world's principal source of osmiridium, very little information is available on their mineralogy, mode of occurrence and chemical composition. However, Cousins (1973) has discussed the genesis and mode of occurrence of the platinoids in the Witwatersrand system. In 1974, Stumpfl published his paper on the genesis of platinum deposits in general and the primary deposits in particular.

5. The Urals deposits constitute one of the major deposits in the world, but there is no detailed information about their mineralogy in English, most of the available data being in Russian.

1.6. PREVIOUS MINERALOGICAL WORK ON THE PLATINOIDS.

The first scientific work on platinoid deposits was carried out by Louis Duparc (1920), a French geologist who worked for many years on different deposits, especially in the Urals. The development of the electron microprobe by Castaing (1960), marked a new era in the history of the study of opaque minerals, and especially of the platinum ores. In Russia, Zvyaginstev (1963), studied the close association of platinum deposits with hydrothermal veins and reported several new minerals. Stumpfl (1962), investigated the Driekop platinum pipe (Transvaal) and he suggested that some deposits may have been formed at a lower temperature than previously supposed. He also found a number of new platinum antimonides and tellurides which indicated low temperature deposition in frequent association with platinum and copper; a discovery which is of great interest since copper may be used as a path finder in geochemical prospecting for platinum. A further publication by Stumpfl (1974), summarised earlier work in that field and put forward additional ideas on the genesis of platinum deposits. Kingston (1966) , studied the platinoid bismuthotellurides at the Merensky Reef which led him to consider paragensis and geochemical relations, and he suggested a more complicated association and origin than was first thought possible.

He also reported and studied three new minerals. Special mention should also be made of Genkin, Shuraviev and Zmirnova (1962), (1963), in the U.S.S.R for their contribution to the study of platinoid minerals. They also reported new phases such as moncheite and kotulskite, and proposed different views on the paragensis and geochemistry of the ores. Of special importance in studies of the Sudbury ores are the investigations of Hawley (1958), (1962), whereas Rucklidge (1969), found a new palladium - bismuthotelluride from three Canadian localities. Koen (1964), studied rounded platinoid grains from the Witwatersrand, suggesting that the rounded shapes of these grains are due to their water - worn nature and suggested for them a detrital origin. Cousins study (1973), of the platinoids in the Witwatersrand system on the other hand, led him to the belief that the Witwatersrand platinoids represent a very mature stage of chemical attrition, and that the water (of the detrital origin) was saline. From the Californian sands, Snetsinger (1971), found a new mineral, calling it erlichmanite, which is defined as a cubic disulphide in which osmium is the most abundant metal. He compared the new mineral with Western Ethiopian "roseite". A recent paper by Mihalik, Jacobsen and Hiemstra (1974), describes platinum minerals from an hydrothermal environment.

In (1972) Cabri summarised literature and tabulated the major and minor phases in the platinum group of metals, and in 1973, he and others recorded a new platinum-iron-copper mineral from localities in British Columbia. The two new minerals which Harris (1974), found from Papua and New Guinea are ruthenarsenite (Ru As) and iridarsenite ($Ir\ As_2$).

TABLE 1.5. DISTRIBUTION OF PLATINUM METALS

Albania
Algeria
Argentina
Australia
    New Guinea (Australian)
    New South Wales
    Queensland
    Tasmania
    Victoria
Brazil - 6 states
Burma
Canada - 10 provinces
    Alberta
    British Columbia
    Manitoba
    Newfoundland
    Northwest Territories
    Nova Scotia
    Ontario (principal deposits)
    Quebec
    Saskatchewan
    Yukon
Ceylon
Chile (Island of Chiloe)
China (Mongolia)
Columbia - 2 departments
    Choco
    Narino
Cuba
Czechoslovakia
Dominican Republic
Ecuador
Egypt
Ethiopia
Finland (Lapland)
France
Germany
Ghana
Great Britain
    Cornwall
    Ireland
    Scotland
Greenland
Guatemala
Guiana (French)
Guyana
Honduras
Hungary
India
    Assam
Indonesia
    Borneo
    Java
    Sumatra
Iran
Italy
Kenya
Malagasy Republic (Madagascar)
Malawi (formerly Nyasaland)
Mexico
New Caledonia
New Guinea
    Papua
    Territory of New Guinea
New Zealand
Norway
Panama
Peru
Philippine Islands
Portugal
Puerto Rico
Republic of the Congo
    Katanga
Republic of South Africa
    Cape of Good Hope Province
    Orange Free State
    Witwatersrand
Rhodesia
Romania
Sierra Leone
Somali Republic
Spain
Surinam
Sweden
Union of Soviet Socialist Republics
    Noril'sk district
    Petsamo district
    Ural Mountains
    Other districts
United States - 12 states
    Alaska
        Goodnews Bay district
        Twenty-one other localities
    Arizona - 3 counties
    Arkansas
    California - 34 counties
    Colorado - 5 counties
    Delaware
    Georgia
    Idaho - 8 counties
    Maryland - Baltimore County
    Missouri
    Montana - 5 counties
    Nevada - 3 counties
    New Mexico
    New York
    North Carolina - 3 counties
    Oregon - 13 counties
    Pennsylvania
    South Dakota
    Texas
    Utah - 2 counties
    Washington - 6 counties
    Wyoming - 3 counties
    Venezuela

*After Mertie (1969)

- 1. ALASKA
- 2. MANITOBA
- 3. BRITISH COLUMBIA
- 4. CALIFORNIA
- 5. GUIANA
- 6. BRAZIL
- 7. ARGENTINA
- 8. REPUBLIC OF SOUTH AFRICA
- 9. RHODESIA
- 10. ZAIRE
- 11. KENYA
- 12. SOMALIA
- 13. SIERRA LEONE
- 14. ETHIOPIA
- 15. GHANA
- 16. FRANCE
- 17. GERMANY
- 18. U.S.S.R.
- 19. INDIA
- 20. PHILIPPINE ISLANDS
- 21. JAPAN
- 22. N.AUSTRALIA
- 23. S.AUSTRALIA
- 24. NEW ZEALAND
- 25. TASMANIA
- 26. NETHERLANDS EAST INDIES
- 27. MADAGASCA
- 28. CHILE
- 29. COLOMBIA
- 30. NYASALAND
- 31. NEW GUINEA

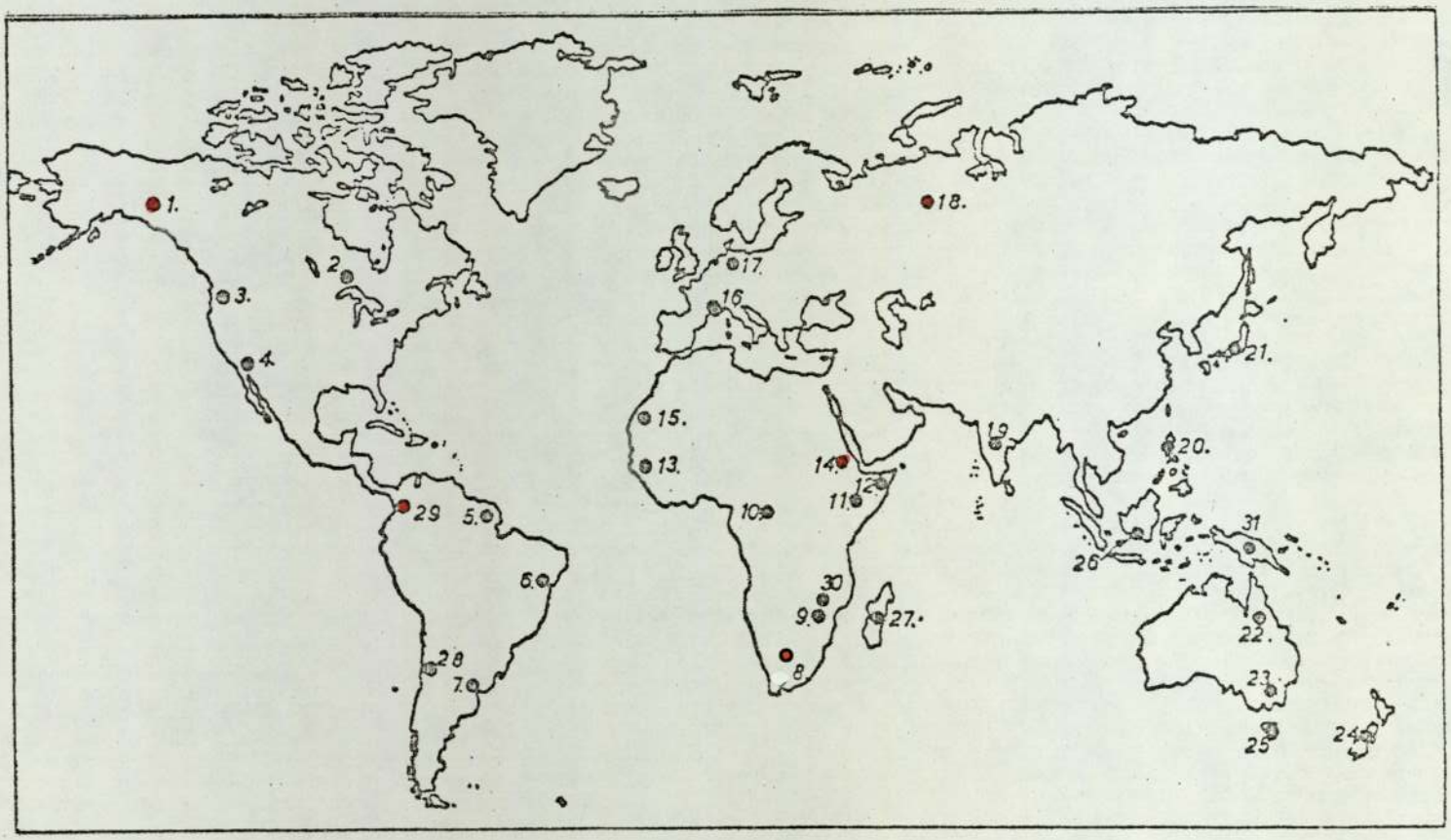

Localities of Platinum throughout the World

● Localities of samples being studied in this investigation

(MAP 1.1)

CHAPTER 2.

ALLUVIAL PLATINOID DEPOSITS OF ALASKA

2.1. GEOLOGICAL SETTING - (c.f. Map 1.1.).

According to Mertie (1969) all the platinum metals so far found in this district occur in placers within the valley of the Salmon River and its western tributaries that head in the dunite of Red Mountain (Map 2.1.). The tributaries of the Salmon River that head in the Paleozoic sedimentary rocks and the overlying rocks are quite devoid of platinum. These include Quartz Creek, on the west side of the Salmon Valley, and Medicine Creek, Snow Gulch, Anita Creek, and Happy Creek on the east side. This localization of the platinum metals in Red Mountain led to a search for deposits of these metals along the west side of this mountain. No large volume of eluvial and alluvial deposits blanket its western slopes, and extends to Kuskokwim Bay.

Alluvial deposits of the platinum metals might also be expected to exist along the north side of Red Mountain, particularly because the dunite crops out along the north side of the Smalls River. Platinum Creek, has two tributaries from the north, called Fox Gulch and Squirrel Creek. The Paystreak on Platinum Creek included stream placers and others that would more properly be classed as beach placers, though the two types were not distinctly defined. According to the U.S. Geological Survey the length of the Platinum Creek is about 2 miles. At the mouth of the Fox Gulch, the width of this paystreak was 200 feet, and at the confluence with Salmon River it had a width of 400 feet. The total length of the paystreaks of Platinum Creek, Fox Gulch, and Squirrel Creek was about 3.5 miles. The platinum metals occurred in the lower few feet of gravels, and on the surface of bedrock, and for a few feet within the cracks and crevices of fractured bedrocks. These metals consist of fine grains, which are larger than those recorded from the paystreaks of Salmon River.

According to Mertie 1940, 1969, the bedrock formations of the area exclusive of intrusive rocks, comprise highly folded sedimentary rocks with some tuffaceous beds, overlain by lavas and tuffs, all of which are believed to be of late Palaeozoic age. In late Mesozoic or Tertiary time these rocks were invaded by ultrabasic intrusives, and at a somewhat later date by granitic rocks. The ultrabasic rocks are of two general types, of which one is composed largely of olivine and the other of pyroxene with variable, but distinctly smaller, amounts of olivine. The olivine rock, or dunite, is the principal bedrock of Red Mountain, and about a quarter of it is altered to serpentinite. Olivine bearing pyroxenite forms the ridge south-west of Susie Mountain. The granitic rocks occupy the long ridge south-east of the head waters of Small River. The dunite and serpentinite are the bedrock sources of the platinum metals that are recovered from the placers of Salmon River and its tributaries. The granitic rocks are believed to be the sources of a small amount of gold that is also contained in the placers. Platinum metals have not been found in place, but much has been learned regarding their occurrence and character in bedrock from the disposition and patterns of the areal drainage system and from analyses of the platinum metal at many recorded sites in the valleys. The Tertiary history of this region, from the time of the invasion by granitic rocks to the end of the Pliocene epoch, is obscure, but it seems probable that during most of this period the area was above sea level. Much more information, however, is available regarding the Quaternary period, though the regional geologic history during the Pleistocene epoch has proven to be a complex problem.

2.2. MINERALOGY OF THE ALASKAN CONCENTRATES.

Five polished sections have been investigated under the reflected light microscope during this research. The ferroplatinum grains from Alaskan samples are large and angular when compared to other localities studied. They are creamy white in colour, and of high reflectance. Iridosmine, is found as hexagonal-shaped lamellae,

with non-careous boundaries, intergrown within the ferroplatinum matrix. Some of these lamellae are very fine and they are parallel to certain crystallographic planes of the ferroplatinum . Some iridosmine grains are small and rounded, or forming rod like shapes as shown from Fig.2.2. Osmiridium also is found intergrown within the ferroplatinum matrix. Osmiridium is found to be less common than the hexagonal phase iridosmine. Laurite (Ru S) grains are found as small grey inclusions in the ferroplatinum. These grains of laurite can be easily differentiated by having high relief and being much harder than the ferroplatinum (Fig.2.3). A rare sulphide mineral which is new, has been found during this study, the optical properties of which are as follows :-
Subround grain, bluish grey in colour, with high relief, harder than ferroplatinum, and with reflectivity of 53%. Analysis by the electron micro-probe shows that it is a sulphide of (Ru,Rh,Os) with low iridium content of about 1% (Fig.2.1.).

No associated gold has been found. Also no accessory minerals such as pyrite, chalcopyrite, magnetite and chromite have been found in the polished sections. The range of reflectivity in the Alaskan samples is 63-68%, and the microhardness ranges from 278-670 at 100g.

Eight ferroplatinum grains from Alaska samples have been selected for quantitative analysis by the electron micro-probe analyser. The results of these analysis are tabulated in Table 2.1. Also quantitative reflectance and microhardness measurements of these grains are included in the same table.

Comparison between analyses by the electron micro-probe and bulk chemical analyses are discussed in Chapter 7.

2.3. DISCUSSION OF ALASKA CONCENTRATES.

In samples from Alaska, it appears that the separation process used for these concentrates was very good, therefore associated minerals were very rare. Since the intergrown minerals are also uncommon, comparatively little can be concluded about the formation of the deposits. The original magma from which these minerals were derived must have been rich in iron and copper because the dissolved iron and copper content are high. The absence of replacement or of intergrown minerals suggests that platinoid grains have suffered little alteration, since they were exposed by erosion of the host rock. The sharply angular shapes of the grains and the position of the placer deposits close to the source rocks, indicates that they have been transported only a short distance. Therefore the time since they were exposed is comparatively short. This, coupled with the geologicaly non-severe environment accounts for the unaltered state of deposits.

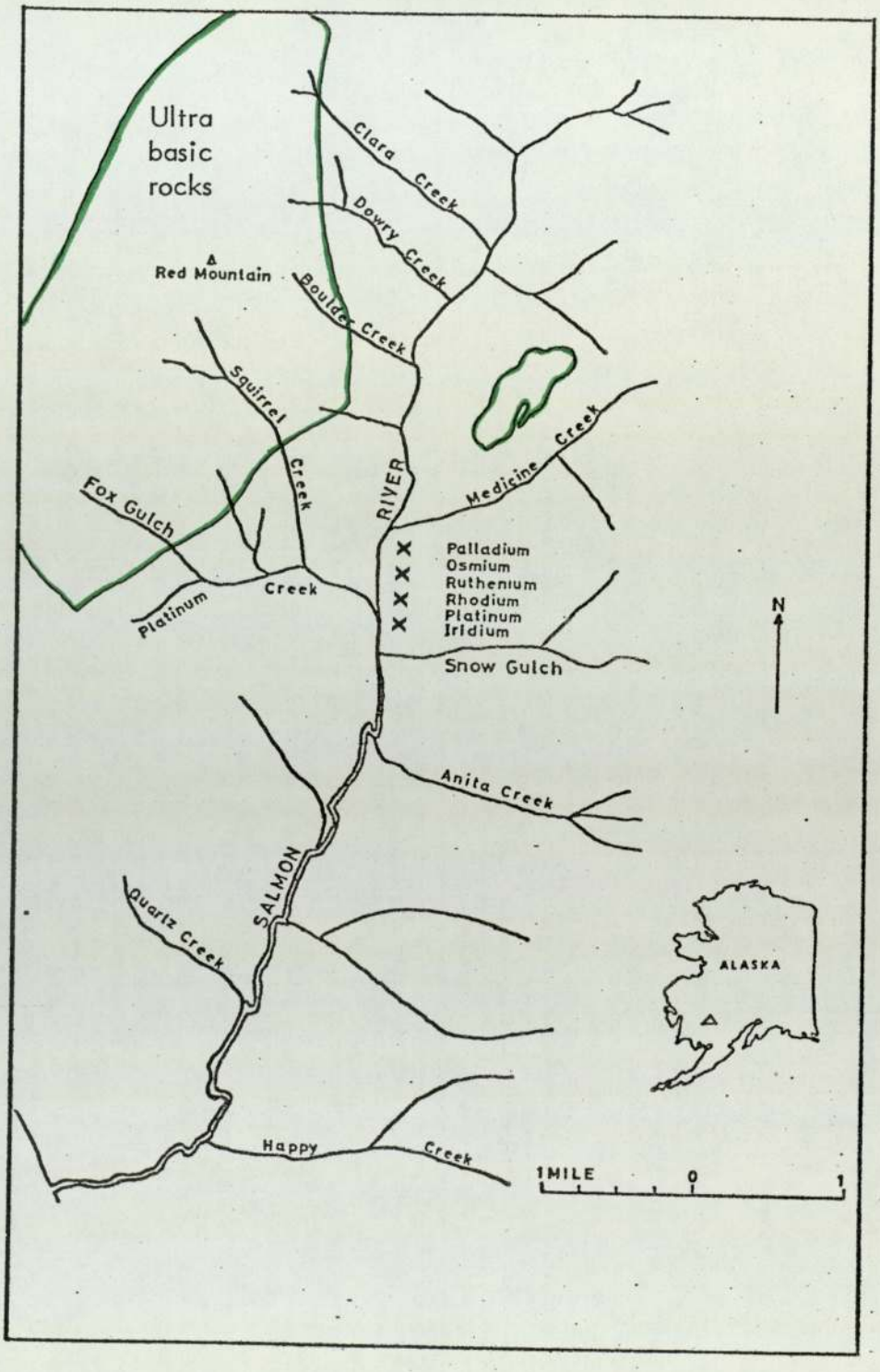

Map 2.1.

Locations of Platinoids in the Salmon River and its tributaries in Alaska.

Grain No.	Pt	Fe	Cu	Ir	Os	Total	R % (589 nm)	HVN (100) g
1.	89.50	7.70	.58	1.55	.638	99.96	66.90	314
2.	87.57	7.40	1.46	2.10	1.30	99.83	65.56	408
3.	88.20	7.70	.76	1.90	.75	99.31	66.14	330
4.	87.10	6.70	1.95	2.50	1.59	99.84	68.46	612
5.	90.40	8.10	.50	.20	.75	99.95	66.24	314
6.	87.00	6.70	2.10	2.76	1.20	99.76	63.40	278
7.	91.30	5.20	.59	2.30	.45	99.84	65.78	
8.	85.10	13.60	.63	.11	.39	99.83	63.11	670
Average	88.27	7.89	1.07	1.68	0.884	99.79	65.70	418

Microprobe analysis, reflectance, and microhardness data for naturally occurring alluvial platinum from Alaska

(Table 2.1)

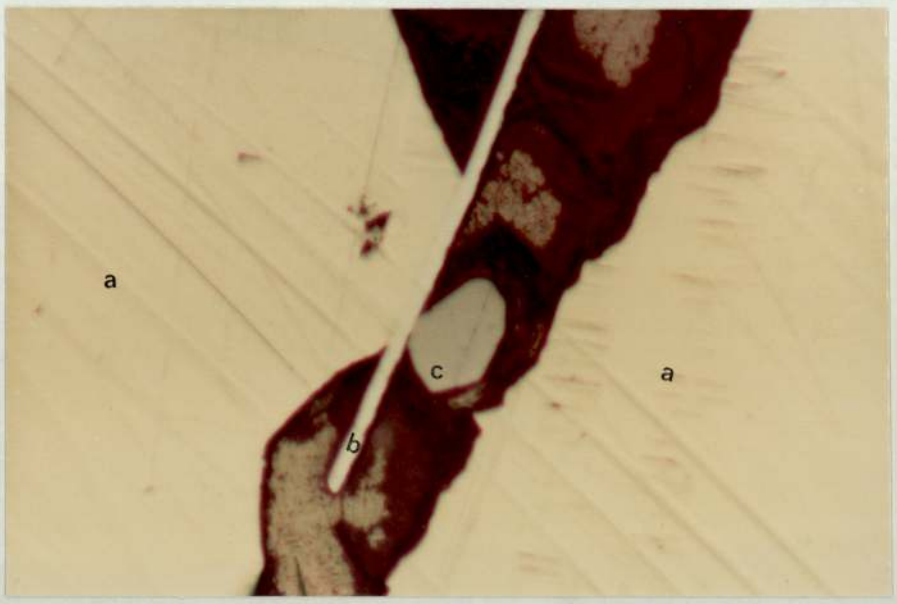

Fig. 2.1

Reflected light photomicrograph showing :

a. Bright creamy ferroplatinum grains c.f. Table 2.1
grain No. 1.

b. Iridosmine rod.

c. A rare mineral, bluish grey in colour, isotropic, high relief $R\%_{589} = 53$.

Electron micro-probe analysis shows that it is a sulphide of (Ru, Rh, Os) with a low iridium content (1%).

Locality : Alaska.

Magnification X 560.

Fig 2.2.

Reflected light photomicrograph showing iridosmine as, fine lamellae of different orientations, included in the ferroplatinum matrix.

Locality : Alaska.

Magnification X560.

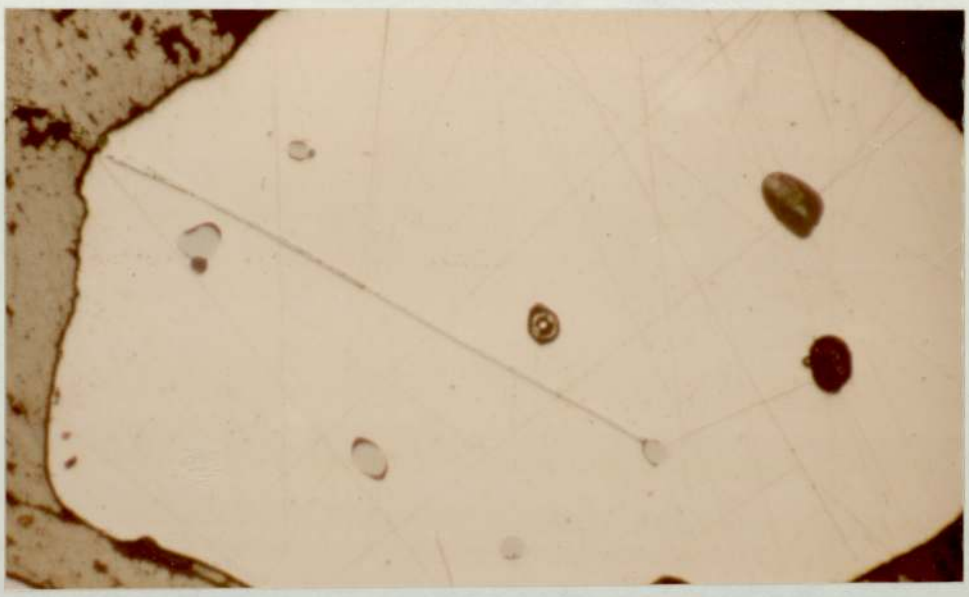

Fig 2.3

Reflected light photomicrograph of rounded grains of (medium-grey) laurite enclosed in the ferroplatinum matrix.

Electron probe microanalysis shows that the laurite contains approximately 12% Os.

Locality : Alaska.

Magnification X 280.

CHAPTER 3.

ALLUVIAL PLATINOID DEPOSITS OF CHOCO, COLUMBIA (c.f. Map 1.1.).

3.1. GEOLOGICAL SETTING.

The gold-platinum placers of the Choco district lie mainly in the valleys of the San Juan and Atrato Rivers. The San Juan River, which is the principal site of the platinum metals, flows southwards, and then veers westwards in Southern Choco to flow to the Pacific Ocean. The Atrato flows north. The drainage patterns of the San Juan and Atrato Rivers within the piedmont province, together with the principal streams which lie between these two rivers and the Pacific Ocean, are shown in Map 3.1. The platiniferous district of Choco can be divided into two provinces, that of the north, called Atrato, and that of the south called San Juan from which the studied samples have been obtained.

From studying the distribution of the platinum-bearing rivers of Choco the distribution seems to be grouped about a common centre, namely Cerro Iro (as shown on south east of Map 3.1). The hills consist of igneous rocks of the family of the gabbros and the diorites which are mainly composed of felspars. Further to the west these gabbros are followed by a zone of basic rocks without felspars such as dunite and pyroxenites. They are in contact with siliceous rocks compacted and metamorphosed, that form a mixed zone followed by tertiary sediments mainly constituted of argillite, sandstone and conglomerates. All the region is covered by an alluvial formation called "Caliche". This is a gravel mainly constituted of sandstone which in some placers is argillaceous and which supports the humus and the vegetation. The platiniferous centre is thus formed of dunites and pyroxenites, which in Choco are disposed in breccias or lenses.

According to most of the geologists who have studied this area, the age of the rocks is from Precambrian to Tertiary, and strike generally northward, through in the upper valley of the San Juan River the statigraphic sequence within the area whose drainage is shown in (Map 3.1), comprises undifferentiated Mesozoic,Cretaceous, and Tertiary rocks.

Precambrian and post-Jurassic intrusives are also present. The formations of genetic significance are two sedimentary formations described as upper and lower Tertiary in age, and a band of post-Jurassic intrusive rocks that lie east of the Tertiary rocks.

The gold-platinum placers of the Choco district are mainly in the valley of the San Juan River and the Atrato River and their tributaries. The San Juan basin is the principal source of platinum metals, as most of the Atrato basin deposits are predominantly gold placers. All the deposits of the platinum metals so far found in Columbia are gold-platinum placers, in which the ratio of gold to platinum varies from valley to valley.

Certain isolated mountains along the west flanks of the Cordillera Occidental, are known from previous geological studies to be the site of intrusive rocks that include ultrabasic rocks, which are considered to be the primary source of the platinum metals in Choco district. Platinum in Columbia has been reported from the ultrabasic rocks of several localities, (e.g. Antioquia, Tolima etc), but always following a line which probably extends from Chile, across Peru, Equador and Columbia to the Caribbean Sea.

According to Kunz (1921), "the platinum which is found in the gravels from the erosion of Tertiary platiniferous conglomerates is mainly constituted of ultrabasic rocks". More recently Singewald (1950), reported that the principal gravels of the San Juan Valley, are fine-grained basic rocks, diorite, and they contain also shales derived probably from the Cretaceous and early Tertiary rocks.

3.2. MINERALOGY OF THE CHOCO CONCENTRATES.

Ten polished sections of concentrates from Choco were examined in this study. Ferroplatinum grains from Choco are characterised by a creamy white colour witha yellowish tint. The grains are large and angular. Iridosmine is commonly enclosed in the ferroplatinum grains which may be irregular in shape (Fig.3.1), or in the form of coarse lamellae, (Fig.3.2.). They form bodies precipitated within the ferroplatinum, and are characterised by their smooth and non-careous boundaries. Sometimes they are crystallised in special crystallographic planes (Fig. 3.3.). Osmiridium (cubic Ir-Os alloys) is found as small inclusions in the ferroplatinum grains, it is less common than the hexagonal (Os-Ir alloys) iridosmine. This may be due to the close similarity in optical properties of osmiridium and ferroplatinum grains. In plain polarised light, they both have nearly the same colour, both are isotropic, very close in reflectivity, but osmiridium is harder than ferroplatinum. Native iridium was found in Choco samples forming small bodies within the ferroplatinum grains. It is pure white, isotropic, high in reflectance and harder than the ferroplatinum. Some platiniridium laths were found in Choco samples which are platinum with more than 20% iridium, but they are not common. Qualitative analysis by the micro-probe was used.

Laurite (Fig. 3.4.) is a common mineral in the Choco samples. It is found as euhedral and irregular grains enclosed in the ferroplatinum matrix. Cooperite (Fig. 3.5) was found to replace ferroplatinum. Also braggite was found as single grains, and enclosed in the ferroplatinum. Sperrylite is also found, intergrown with the ferroplatinum. It is differentiated from the ferroplatinum by its higher hardness and lower reflectance compared to the ferroplatinum grains. Gold is found as separate grains i.e. associated with the ferroplatinum. Also magnetite (Fig. 3.6.) chromite (Fig.3.7) and chalcopyrite are found to be associated with the ferroplatinum.

Six grains of ferroplatinum were selected for quantitative analysis, using the electron probe-micro analyser. The results of these analyses are tabulated in Table 3.1. Also quantitative reflectance and microhardness measurements of these grains are included in the same table.

Comparison between the analyses using the electron micro-probe and the bulk analyses for Choco samples are shown in Chapter 7.

3.3. DISCUSSION OF CHOCO CONCENTRATES.

Samples from Choco are the purest ferroplatinum alloys in all the deposits studied. Since the dissolved iron and copper are the lowest content in the concentrates studied, the original magma from which these minerals were derived was poorer in both elements. The ferroplatinum grains are sharp edged and replacement minerals are irregularly distributed within them, which suggests they were formed simultaneously. The presence of sulphide minerals as a major constituent of the concentrates shows that the original magma from which these minerals were derived was rich in sulphur i.e. rich in platinum, rich in sulphur, poor iron and copper. The Choco deposits are known to be old, but the lack of surface replacement on the grains shows that they have not been subjected to severe conditions since their deposition.

Gold is found as separate grains associated with the ferroplatinum. There is no evidence of alloying with each other. It is possible for gold to dissolve in ferroplatinum at high temperatures as shown by some of the Witwatersrand concentrates. This lack of alloying suggests that the platinum and gold were segregated in the magma.

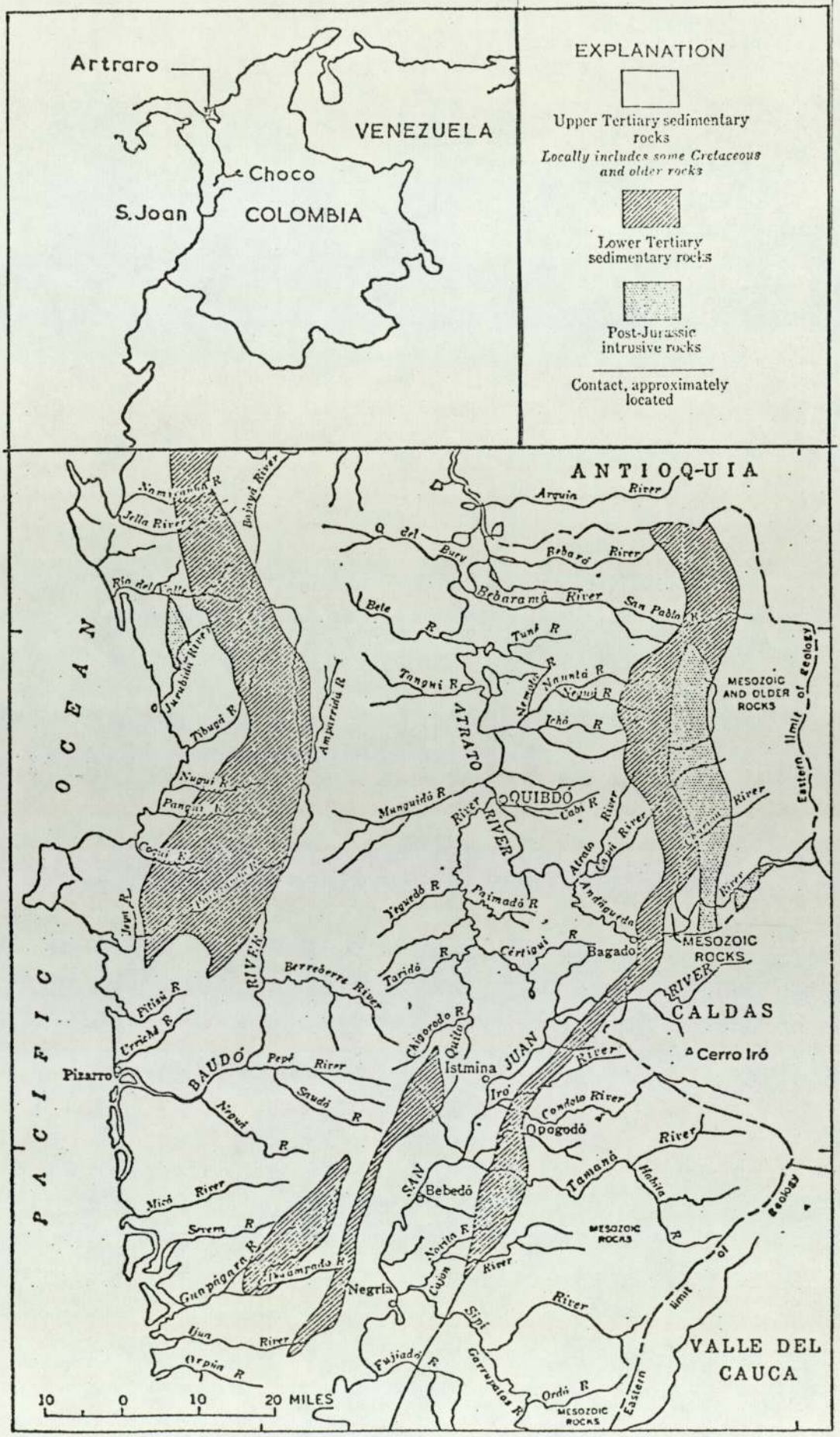

Map 3.1.

Choco district in Columbia.

Grain No.	Pt	Fe	Cu	Ir	Os	Total	R% 589	HVN 100
1	91.6	6.78	0.63	0.53	0.78	100.32	63.2	397.5
2	92.04	6.84	0.57	-	-	99.45	63.1	465.9
3	94.79	4.76	0.45	-	-	100.0	63.1	487.7
4	93.7	4.78	0.37	-	1.1	99.95	59.9	503
5	88.2	6.7	0.44	0.81	0.7	96.85 + Ni	60.1	338.7
6	94.95	4.66	0.38	-	-	99.99	63.3	414.6
Average	92.5	5.8	.47	.22	.43		62.1	434.6

(Table. 3.1)

Microprobe analyses, reflectance and microhardness data for naturally occurring platinum grains from Choco.

- Not detected.

Fig. 3.1

Reflected light photomicrograph, showing irregular shapes of iridosmine in a ferroplatinum matrix.

Locality : Choco.

Magnification X 380.

Fig. 3.2

Reflected light photomicrograph, showing coarse lamellae of iridosmine in ferroplatinum and ferroplatinum in iridosmine.

Locality : Choco.

Magnification X 380.

Fig. 3.3

Reflected light photomicrograph showing iridosmine with a very high content of iridium in the ferroplatinum matrix. Iridosmine crystallises in special crystallographic directions.

The grey, pinkish phase is a sulphide of (Ru, Rh, Os).

Locality : Choco.

Magnification X 560.

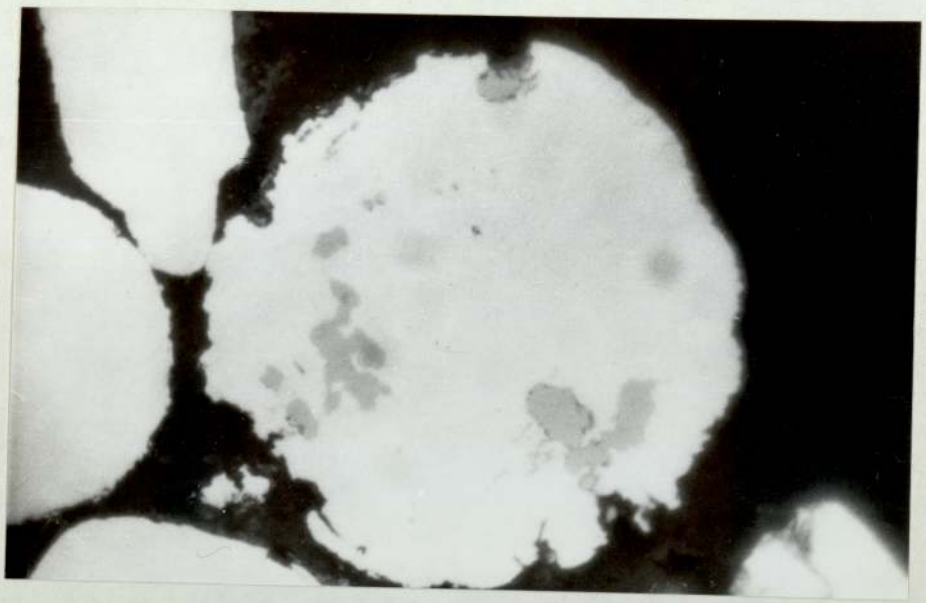

Fig. 3.4

Reflected light photomicrograph of anhedral (dark grey), grains of laurite (Ru S)and no other elements were detected by electron micro-probe analysis. The matrix is ferroplatinum with approximately 8% iron.

Locality : Choco.

Magnification X 480.

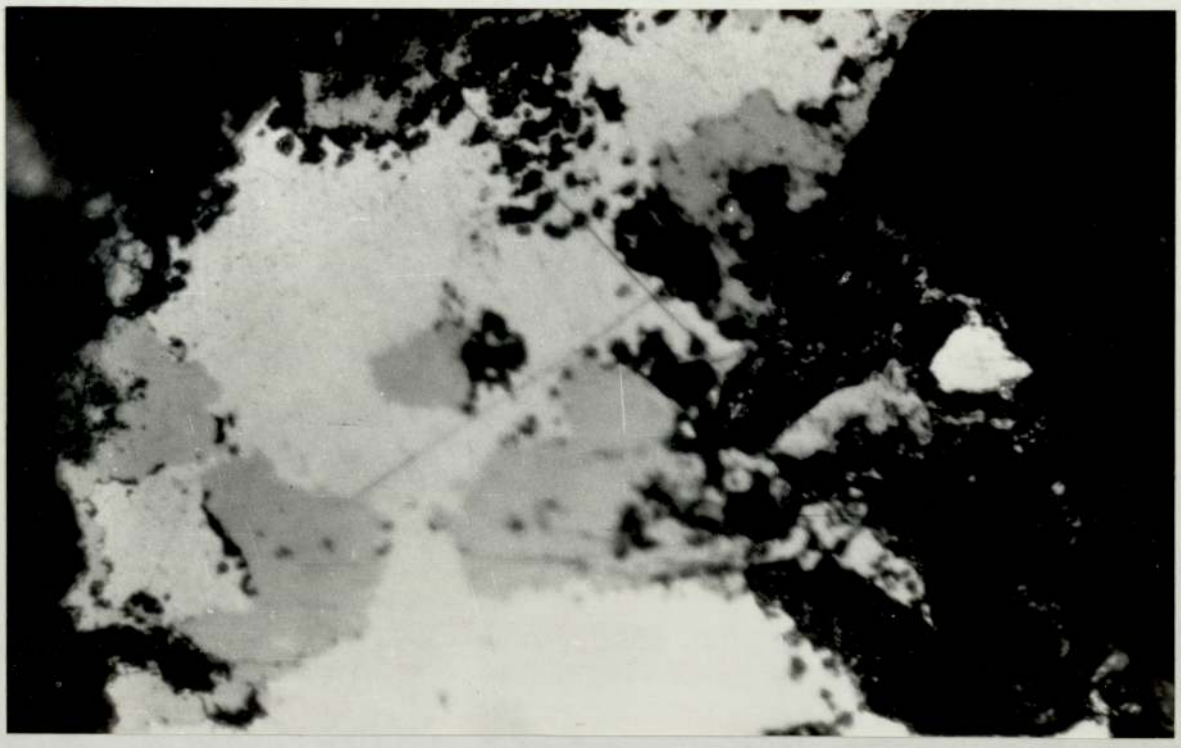

Fig. 3.5

Reflected light photomicrograph showing replacement of ferroplatinum by Cooperite (Pt S).

Locality : Choco.

Magnification X 560.

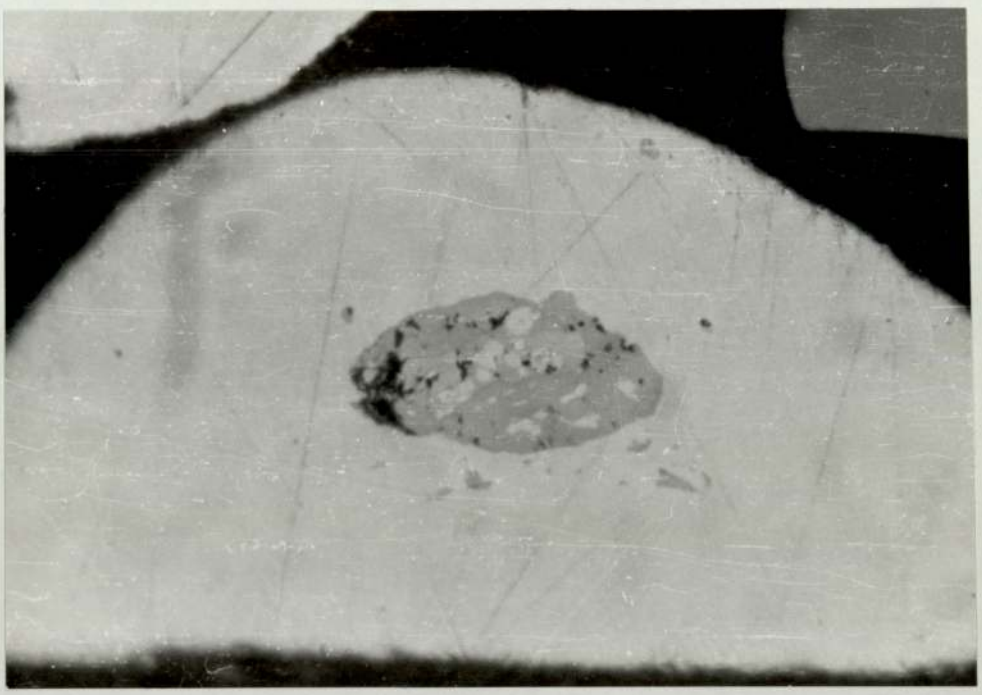

Fig. 3.6

Reflected light photomicrograph showing magnetite in the ferroplatinum and ferroplatinum in magnetite.

Locality : Choco.

Magnification X 480.

Fig. 3.7

Reflected light photomicrograph, showing chromite, intergrown and associated with ferroplatinum.

Locality : Choco.

Magnification X 220.

CHAPTER 4

ELUVIAL NUGGETS OF ETHIOPIA (c.f. Map 1.1.).

4.1. GEOLOGICAL SETTING.

The geology and general distribution of platinum and gold in the ultrabasic complex of the Yubdo district, in the Wallaga province of Ethiopia, have already been described by Duparc et.al. (1927), Molly (1928, 1959), Augustithis (1965), and Otteman and Augustithis (1967). These have shown this ultrabasic mass to be of a Uralain type consisting of a central zone of platiniferous dunite enclosed by a less platiniferous pyroxenite. The dunite is overlain for the most part by a hard, brownish rock consisting of secondary silica, iron oxides and residual chromite which is believed to be derived from the dunite by some form of hydration alteration and leaching of magnesia, Augustithis (1965). This altered rock, which is also platiniferous, was first described by Duparc et.al. (1927), who named it "birbirite". A lateritic eluvium occurs as a layer ranging in thickness from 2-10m, forming a capping over the dunite, birbirite and pyroxenite. In the past, economic quantities of platinum have been obtained from this eluvium, especially from those parts overlying the dunite, in the form of small nuggety grains, Molly (1959). The grades of the primary source rocks and the birbirite are uneconomic.

The presence of platinum in Ethiopia led to consideration of the presence of platinum in the black sands of Egypt, since these black sands were derived mainly from the Abyssinia plateau and were carried by the Blue Nile and the White Nile which are the main sources of the River Nile (Map 4.1.).

4.2. MINERALOGY OF ELUVIAL FERROPLATINUM NUGGETS FROM ETHIOPIA.

Two polished sections of ferroplatinum nuggets from Ethiopia were examined during this study.

Under the reflected light microscope eluvial ferroplatinum nuggets from Ethiopia are found to consist of a ferroplatinum matrix within which euhedral osmium crystallizes in the form of fine and coarse lamallae. These native osmium lamellae are readily identified by their strong anistropy (brown-orange-red) (Fig. 4.1.). Laurite grains are also included in the ferroplatinum matrix. Other platinoid sulphides such as (Rh, Ir, Fe) sulphide and (Rh, Ir, Pt) sulphide are shown by qualitative analysis using the electron micro-probe. The platinoid sulphides are grey in colour with angular shapes and are intergrown with the ferroplatinum nuggets.

Two electron micro-probe analyses of ferroplatinum nuggets from Ethiopia have been obtained. Quantitative reflectivity and microhardness measurements for the same analysed area are tabulated in Table 4.1. .

The comparison between the micro-probe analyses and the bulk analyses are shown in Chapter 7.

4.3. DISCUSSION OF THE ETHIOPIAN NUGGETS.

Since the eluvial nuggets from Ethiopia are sharp edged and angular this suggests that they are in situ. The absence of replacement or surface attack confirm the idea of being in situ, and the sharp edges suggest they had not been moved from the place of origin. According to Otteman and Augustithis (1967), the nuggets are found in the lateritic covers of ultrabasic rocks and in birbirites. Birbirite is a reddish, iron-bearing, quartzitic rock named by Duparc et. al. (1927) after the Birbir River which cuts through the pyroxenite massive of Yubdo.

The presence of the intergrown sulphide in the ferroplatinum matrix and the presence of intergrown iridosmine suggest that

sulphur was present in the original melt and the sulphides crystallised at the same time with the ferroplatinum.

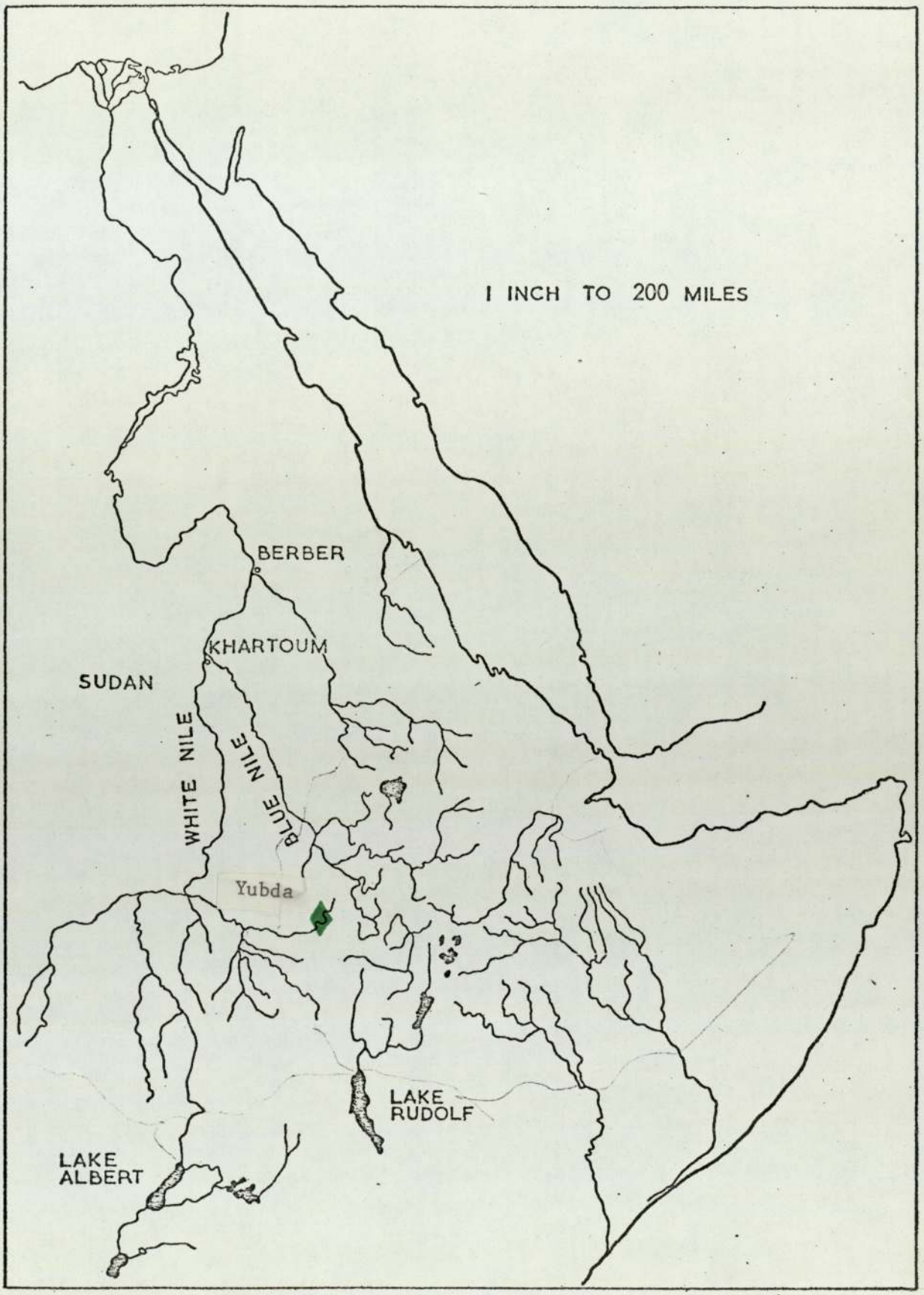

Map 4.1

Western Ethiopia where the eluvial platinum is near the Sudan border.

Analysis No.	Pt	Fe	Cu	Ir	Os	Total	R % 589nm	HVN 100
1.	88.8	7.95	0.9	1.15	1.1	99.9	54.6	333.6
2.	90.7	6.2	0.6	1. 5	0.9	99.9	61.9	299.1
Average	89.75	7.0	.75	1.3	1.0		60.75	316.35

Microprobe analysis, reflectance and microhardness data for platinum nuggets from Ethiopia.

(Table 4.1).

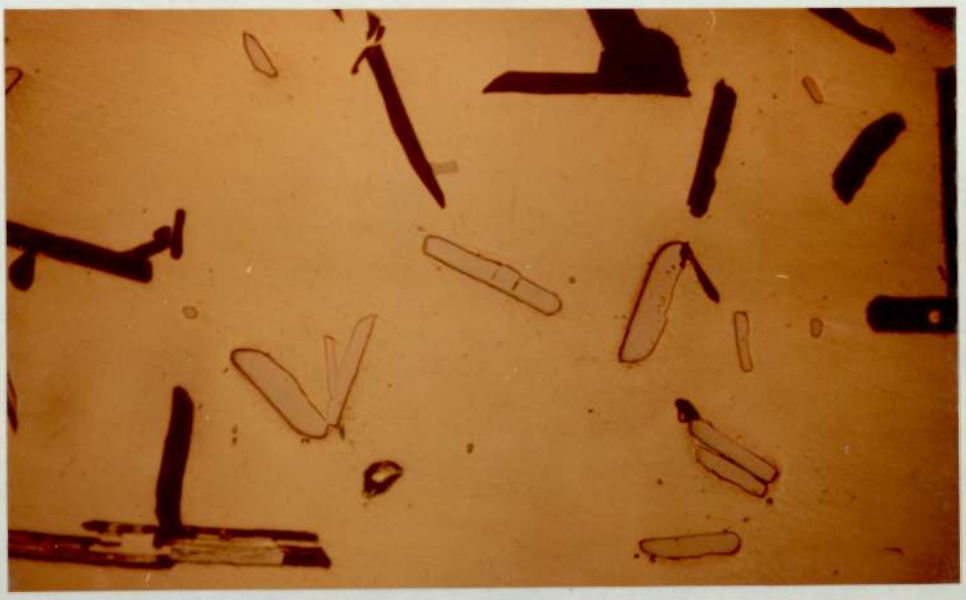

Fig. 4.1

Reflected light photomicrograph showing iridosmine which is strongly anistropic, the nicols half-crossed to show the (brown-orange-red) colour of the anistropy.

The osmium content of these iridosmine is from 60 to 70%.

Locality : Ethiopia.

Magnification X 560.

CHAPTER 5.

PLACER DEPOSITS OF WITWATERSRAND.

5.1. GEOLOGICAL SETTING.

The gold deposits of the Witwatersrand consist of lithified placers that are mined as lode deposits. Osmiridium in this area, according to Wagner (1929), was first identified by William Bettel in concentrates from the conglomerate (banket) of the New Rietfontein Mine, in Orange Free State, in 1892. Osmiridium is a by-product of gold mining.

The Witwatersrand system, consisting of bedded rocks of terrestrial origin, rests uncomformably upon the rocks of the Swaziland system, which is the basal complex of this region. The Ventersdorp system, overlying the Witwatersrand system, consists of andesitic lavas and pyroclastics, and both systems are considered to be of late Precambrian age. According to Furon (1963), the thickness of the Witwatersrand system is about 28,000 ft, and according to Coetzee (1960) the thickness of these two systems is about 40,000 ft. Many local disconformities and unconformities exist in the Witwatersrand system, and the beds therefore show divergent thickness at different localities. The auriferous conglomerates of the Witwatersrand are ancient lighified placers, which comprise numerous strata with an aggregate thickness of about 2,000 ft, and a maximum individual thickness of about 65 ft. The rocks of the Witwatersrand system, in the Transvaal and Orange Free State, are folded into a large syncline with a major axis trending east-west which has a length of about 110 miles and a width of about 45 miles. In the Johannesburg area these rocks form the north flank of the syncline and dip steeply south, though they flatten with depth to 30° .

Near Parys the synclinal structure is modified locally by a quaquaversal anticline. Owing to erosion and to the cited dome, the rocks of the Witwatersrand system crop out mainly at four separate areas, that is , near Johannesburg, Heidelburg, Parys, and in an area between Ventersdorp and Klerksdorp.

The gold and platinoid metals of the Witwatersrand occur in thin beds of conglomerate and grit, known as reefs, which form the upper part of the Witwatersrand system. Several groups of these reefs have been recognised (Map 5.1.). The beds of conglomerate in the Upper Witwatersrand system range in thickness from an inch to 15ft. , in the Main Reef group from 1 to 10ft. The placer platinoid metals are exceedingly scarce, but are most prevalent in the Main Reef Leader on the Far East Rand, less so on the West Rand, and are least plentiful in the Central Rand, where all the reefs of the Main Reef group are thickest. Both gold and osmiridium are found to be most plentiful in conglomerates that have large pebbles. In the Main Reef Leader, these pebbles have a mean diameter of 2", and consist mainly of quartz, with less quartzite, chert and slate. The sandy matrix, in which the noble metals mainly occur, contains a large volume of secondary pyrite. Other ore minerals that are present in small amounts are pyrrhotite, galena, sphalerite, chalcopyrite, cobalt arsenide, uraninite, and the platinum metals. The sandy matrix has been recrystallised, with the development of secondary quartz, sericite, chlorite, chloritoid, carbon, and rutile, but these are probably original accessory minerals of the conglomerates. Less resistant accessory minerals, such as the iron ores, have been destroyed in the process of recrystallisation,and probably constitute the sources of the pyrite. The gold is exceedingly fine grained, and has not in general retained its original detrital form. The platinoid metals, however, have resisted recrystallisation and show rounded outlines, or at least rounded edges of the crystalline grains, that indicate their detrital origin.

The platinum metals are exceedingly fine grained and range in size (at one mine) according to Wagner (1929), from 0.04 to 0.19mm in diameter.

5.2. MINERALOGY OF THE PLACER DEPOSITS OF WITWATERSRAND

Ferroplatinum is not a common phase in the Witwatersrand concentrates, but samples were obtained from Klerksdorp gold mine. The grains are small in size compared to other localities. They have sub-rounded edges and are not easy to differentiate from osmiridium grains which are the commonest platinoid phase in the Witwatersrand concentrates (Fig. 5.1.). Ferroplatinum grains in most cases are found intergrown with other platinoid phases such as braggite, cooperite or other sulphides of rhodium, iridium, osmium etc. Because each grain in Witwatersrand concentrates is composed of more than one phase they are somewhat complex (Fig. 5.2.). Many grey and greyish-white varieties of platinoid sulphides both isotropic and anisotropic segregated at the surface of the ferroplatinum grains, could be identified by the probe analysis. Osmiridium and ferroplatinum particularly are closely similar under the reflected light microscope, and because of the small size of the grains and the large number of different phases present are difficult to identify except by probe analysis. Beside the rounded grains which are the major phase, there are some larger grains with sharp edges.

Iridosmine is the most common platinoid phase in the Witwatersrand gold-bearing conglomerate. It is found in the polished section, of the concentrates as separate grains and not enclosed in the ferroplatinum, unlike the samples from other localities. These grains are roughly spherical with a strong anisotropic core indicating a high osmium and ruthenium content, surrounded by isotropic phase, low in osmium and rich in iridium and platinum. Other grains are composed of three phases, (Fig. 5.3) as follows:-

a. Bluish-white in colour, weakly pleocheorioc, strongly anisotropic phase with a high osmium and ruthenium content.

Chemical composition is as follows:-

Os=65.9% Ru=15% Ir=12% Pt=8%

Followed by phase (b) which is richer in iridium and lower in osmium.

b. White in colour with a very faint, bluish tint, weakly anisotropic.

Chemical composition is as follows:-

Os=40% Ru=34.6% Ir=17.2% Pt=8.6%

c. Pure white phase, isotropic, at the border of the grain.

Chemical composition is as follows:-

Os=13.9% Ru=12.1% Ir=59.8% Pt=14.3%

Iridosmine was sometimes associated with osmiridium in wavy, alternating bands which cross from one side of the grain to another or form concentric bands. An example is shown in Fig.5.4. .

Other accessory minerals were found to be of two type intergrowths and replacement. The intergrowths were usually in the form of small particles distributed inside the osmiridium or ferroplatinum grains. Laurite was frequently found in this form (Fig.5.5.) Pyrrhotite in ferroplatinum is shown in Fig.5.6. . A magnetite particle enclosed in ferroplatinum is shown in Fig. 5.7 .

Replacement of ferroplatinum grains by platinoid sulphides was very common. A rounded ferroplatinum grain with extensive surface replacement by laurite is shown in Fig. 5.8 . Other sulphides were observed to replace ferroplatinum; for example Fig. 5.9 shows attack of a ferroplatinum grain by rhodium, palladium, and iridium sulphides in three places.

In many cases the surface sulphide layer has interposed a layer of gold between it and the unaffected centre, (Fig.5.10 and Fig. 5.11). In some cases only a gold core exists, (Fig. 5.12). One of the minute grains in Fig. 5.13 in which replacement and intergrowth occur are shown in the same grain.

Magnetite, galena, chalcopyrite, pyrrhotite and uraninite were associated with the concentrates.

Koen (1964) described two kinds of iridosmine from Witwatersrand area, based on his microscopic study. He called them iridosmine 1 (very high in osmium) and iridosmine 11 (less osmium content than iridosmine 1. Koen explained the origin of these grains in the Witwatersrand as of detrital origin. The presence of iridosmine 1 and iridosmine 11 in the same grain which was found by Keon confirm the presence of a naturally occurring iridium-osmium alloy lying in the 2-phase field of the equilibrium diagram.

Qualitative analyses for 50 grains were carried out using the electron micro-probe analyser. Eight grains were selected for quantitative analysis, only five being ferroplatinum. The results of the analyses, reflectance and microhardness measurements are also tabulated in Table 5.1. Grain 1,2, 3 and 4 were too small to measure the microhardness. Seven grains from Witwatersrand osmium-iridium-ruthenium alloys which are quantitatively analysed by the electron micro-probe are included in Table 11.1 in the iridium-osmium-ruthenium Chapter. Comparison between mineral analysis and bulk analysis are found in Chapter 7.

5.3. DISCUSSION OF THE WITWATERSRAND PLACER DEPOSITS.

The detrital origin of the gold and platinum metals of the Witwatersrand is favoured by practically all South African geologists who have had a professional familiarity with these ores.

The acknowledged fact of recrystallisation, with solution redeposition of the gold, however, has led some to believe that the noble metals are epigenetic and hydrothedral in origin, with sources extraneous to the conglomerate. Probably the most ambitious formulation of an epigenetic hypothesis was made by Graton (1930), who, notwithstanding his many contributions to the theory of ore deposits, was unfamiliar with placers. Consequently he failed to evaluate the evidence for a detrital origin of these deposits. In particular, he overlooked the rounded and sub-rounded form of the grains of platinum metals. A few other geologists, in particular Davidson (1953 and 1955), have also accepted Graton's interpretation. Evidently, owing to their great resistance to the chemical processes attendant upon weathering, the grains of osmiridium, unlike the detrital gold, have not been dissolved and redeposited, but instead have maintained their original form and character. It is generally admitted that the gold and osmiridium were deposited simultaneously. It therefore follows, without the cogent collateral evidence, that all the precious metals of the Witwatersrand originated as detrital deposits.

The exact sources of the gold and platinum metals are not definitely known, though granitic intrusives within the Swaziland system are known to be mineralised with gold, tin and columbite. Most geologists familiar with these deposits believe that these metals were transported for a long distance to the north-west or north-north-west from bedrock sources that are now either eroded or overlapped by younger geological formations. It is certain that these bedrock sources are not directly related to the platinum-bearing intrusives of the Transvaal, as the former are millions of years older than the latter. Probably the noble metals of the Witwatersrand were contained in sediments that were

transported by and deposited from a large river that built a delta close to the sea.

Cousins (1973) examined the mineralogy of concentrates from many sources in the Witwatersrand. He concluded that the deposits were of placer origin, but have been extensively modified since deposition. He also concluded that the original minerals are considered to be sulphides of the platinum group metals, which have suffered chemical attrition.

The results of the present investigation do not fully agree with this view. There seems little doubt, that the rounding of the grains is caused by wear rather than by chemical reactions. This is shown by the many grains which show two-phase structures passing from one side of a rounded grain to another (Fig. 5.3.). A two-phase accretion alloy could only occur as concentric shells of different phases lying approximately parallel to the rounded surface. Structures which resemble accretion deposits do exist, as for example the grain marked "a" in Fig. 5.4.. However, banding bears little relationship to the shape of the grain and a magmatic origin for these structures is suggested instead.

Rejection of the accretion hypothesesis does not mean that no alteration to the deposits has occured during the long time since they were placers. There is clear evidence that alteration of platinoid grains to sulphide minerals has taken place after deposition. This is shown by the attack of rounded (i.e. eroded) grains to give an envelope of base-metal sulphide (Fig. 5.7), laurite (Fig. 5.8), complex (Rh, Pd, Ir) sulphide (Fig. 5.9), or cooperite (Fig. 5.10). In each case micro-probe analysis has shown that the principal components of the sulphide envelope are present also in the enclosed metal grains and are the components most likely to form sulphides.

Since the sulphide appears to start from the mantle and not from the core and it grows inwards, it is suggested that the sulphide minerals are formed selectively from the platinoid metal grains. This is the opposite mechanism to that put forward by Cousins (1973), who proposed that the Witwatersrand platinoids are derived from primary sulphide particles.

Strong supporting evidence that selective sulphidisation has occurred is provided by Fig. 5.10 to 5.12 . A layer of gold separates the sulphide layer from the ferroplatinum core in Fig. 5.10 . (The rhodium rich phase "a" is of no importance to the argument and has probably been precipitated subsequent to the formation of the composite grain).

Since the core phase "b" contains an appreciable gold content, and gold does not readily form sulphides, sulphide formation would be expected to enrich the core in gold as only platinum sulphide can be formed. Gold does not form a continuous solid solution with platinum except at very high temperatures so the formation of a discrete gold layer would be expected. The position of the layer at the base of the sulphide envelope indicates that the platinoids diffuse faster in gold than does sulphur. Ferroplatinum must have been able to diffuse through the thick gold layer to join the sulphide phase so the temperature must have been sufficiently high for this to take place, even slowly.

A similar case is shown in Fig. 5.11 where osmiridium has changed to braggite with an interposed gold film.

It is presumed that Fig. 5.12 shows the end result of a complex platinoid grain attacked by sulphide. Here an irregular core of gold is surrounded by an envelope of platinoid metal sulphide.

It is notable that an interposed gold layer only appearswhere the platinoid metal contains dissolved gold. One of the smaller rounded grains of Fig. 5.12 is an example of sulphide replacement, but no gold layer is present and it contains no dissolved gold as shown from the analysis by the electron micro-probe. It appears from this evidence that at least some of the gold from the Klerksdorp gold mine is derived from a gold-bearing platinoid metal by selective sulphidation subsequent to placer deposition.

The source of the sulphide mineralisation is not known. However, the platinoid metal grains frequently contain particles of sulphide minerals enclosed in the grains.

For example laurite inclusions in the ferroplatinum are shown in Fig.5.5. and 5.13 (b). A complex (Rh Ir) sulphide was also identified in Fig. 5.13 (a). In Fig. 5.6 pyrrhotite particles are shown in ferroplatinum, and in Fig. 5.13 (b) laurite appears in osmiridium. Some of the grains are rounded and since the sulphides are grown randomly and not round the border it is probably that particles have been precipitated from solid solution during cooling of the magma, rather than in situ in the placer deposit . If the original magma contained sulphur, sulphide minerals could be associated with the platinoid metal grains in the placers. Subsequently the sulphur may have been displaced chemically from these minerals and have then attacked the platinoids.

The mineralogy of the unaltered platinoid metal grains gives some information on conditions in the original magma from which these metals were derived.

The iridium-osmium-ruthenium phase diagram (Chapter 12) obtained from the results on the synthetic alloys helps to understand these conditions. Unfortunately some of the natural alloys contain large amounts of both iridium and platinum and as only a ternary diagram is available this leads to difficulty in its use. In order to represent four component alloys on a ternary diagram, the platinum and iridium contents were added together and minor amounts of other elements were ignored. This procedure is justified as platinum and iridium have the same crystal structure, the same number of electrons in the outermost shell (6s) and adjoin each other in the periodic table. Their Goldschmidt atomic diameters differ by only 2%. These factors indicate that their effects on the phase equilibria optical and mechanical properties ought to be similar.

The average of the bulk analyses of Witwatersrand concentrates (Table 7.1) gives :- (Ir + Pt) = 46.4%, Rh=0.7% Os=37.9%. The remaining 15% is probably Fe, Cu, Au, S and minor amounts of other elements. Ignoring these elements and normalising the Ir + Pt, Rh and Os contents to 100% and converting to atomic % allows the mean composition of the platinoid contents of the magma to be put on the ternary phase diagram. Such an alloy of composition 54% Ir + Pt, 45% Os, 1% Ru would begin to feeze at approximately 2,700°C (Fig. 12.8) and the first crystalline material to form would be close-packed hexagonal with a composition near 75% Os. Freezing would be completed at about 2,600°C. The products would be primary β (cph), partially dissolved during the peritectic reaction, and surrounded by α (fcc). The compositions of the β and α phases would be approximately 53% Os, 0.5% Ru, 44.5% Ir = Pt and 45% Os, 1.0% Ru and 54% Ir + Pt respectively.

Cases where the actual alloy composition was the same as the mean composition would be rare, but even if the local composition was very different from the mean, any concentrated alloy which was two-phase after solidification would have first formed the close-packed hexagonal phase surrounded by the face center cubic phase. Furthermore, it has been found experimentally that the hardness of osmiridium alloys, both natural and synthetic is lower than of close-packed hexagonal iridosmine, (Fig. 12.16 , 12.18 and Table 11.3). In the course of erosion and transportation such a structure would be broken into small particles. The fractures would pass preferentially through the softer phase (core) , surrounded by a mantle of eroded osmiridium.This condition describes some of the platinoid grains in the Witwatersrand concentrates e.g. Fig 5.2.

Where solidification of the platinoid metals occurred in regions of the magma poor in these elements, the phase structure would depend on the rate of coming of different elements. Different elements would be supplied at varying rates by connection and diffusion of individual atoms. Since a certain critical nucleus size must be attained before a particle becomes stable, a magma with low concentration of platinoids could contain atoms in supersaturated solution at temperatures below the normal freezing point. A small, growing crystallite in one part of the magma could have layers of very different concentration formed on its surface during its growth. Solid state diffusion would of course start immediately after layer formation, but in cases where there was complete solid solubility between elements it would disapper entirely. Otherwise the bands would gradually attain the correct composition of each phase in equilibrium with the other at the temperature of the magma at that time.

During subsequent slow cooling the compositions of the bands would alter gradually as dictated by the phase diagram. Some bands would thicken and very thin ones might disappear. Alloys with a mean composition like that, will be entirely in the close-packed hexagonal or face centered cubic field. Banding arising as described above should disappear by diffusion unless the cooling was rapid.

Evidence for this type of freezing process is widespread in the Witwatersrand concentrates. The bands of the hexagonal and cubic phases can be distinguished in Fig. 5.3 for example. Note that the region marked "b" is actually a fine structure of alternating bands of hexagonal and cubic phases . In each case the band is presumbaly in equilibrium with the band on each side of it. If two adjoining bands could be analysed quantitatively in the electron probe-micro analyser, useful information on the phase relationships could be obtained. In no case was this possible during the present study. The analyses of the blue and white bands in region "b" of Fig. 5.3 are not useful because it is not known with what the phases are in equilibrium with, since the bands were too small to analyse.

Another example is shown in Fig. 5.4. Here the hexagonal bands are much less regular. The overall hexagonal shape of the grain suggests that the grain was formed as a hexagonal phase; optical microscopy showed that the bluish anisotropic bands are hexagonal and the off white isotropic bands are cubic. The most probable explanation of this is that the bands were formed as described earlier but at temperatures higher than the peritectic temperature for the alloy as a whole, so that the whole grain was hexagonal. Cooling would have to be rapid to prevent the elimination of the concentration differances by diffusion. As the hexagonal crystal cooled through the peritectic change the bands rich in

osmium and ruthenium would remain hexagonal but the bands in iridium would change to the cubic structure. If the subsequent cooling rate were slow the bands would reach the equilibrium concentration as shown by the phase diagram. If the rate of cooling is fast then a considerable displacement in composition might occur. The presence of banding coupled with the overall hexagonal shape of the crystal is good evidence that some parts of the magma cooled at a rapid rate.

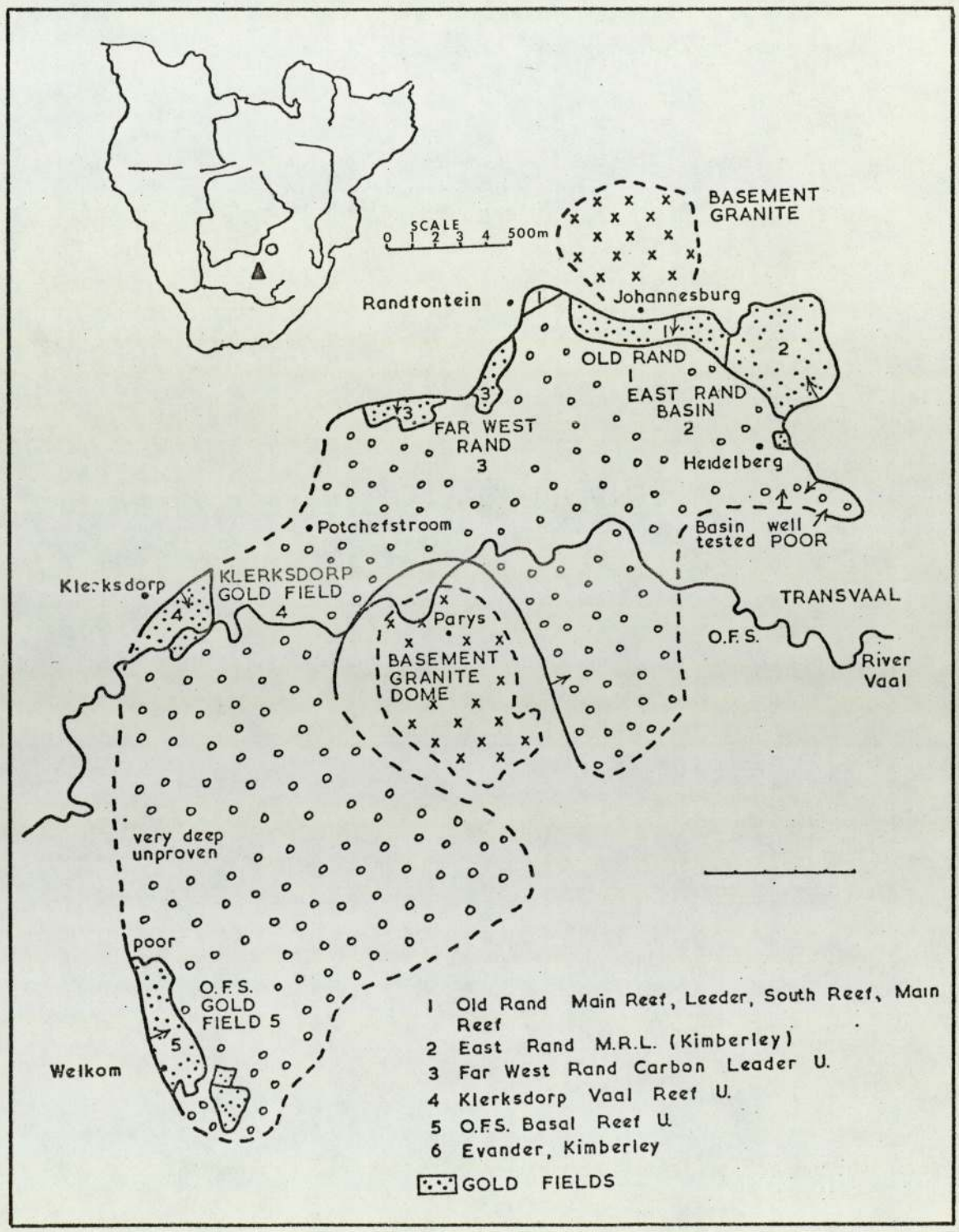

Map. 5.1

Gold mines in Witwatersrand where platinoid is a by-product.

Grain No.	Pt	Fe	Cu	Ir	Os	Total	R% 589 mm	VHN 100
1	83.5	7.5	0.49	8.5	-	99.99	72.8	
2	64.88	2.17	-	26.5	6.1	99.85 +.2 Ni	73.1	
3	42.1	9.96	-	22.6	25.1	100.16 + .4 Ni	68.9	
4	92.1	7.96	-	-	-	100.06	64.1	
5	91.4	8.0	.51	-	-	99.91	65.0	498
6	90.4	7.2	2.30	-	-	99.9	65.0	598
7	94.1	5.2	0.50	-	-	99.8	69.1	432
8	88.9	10.2	0.84	-	-	99.94	57.1	419
Average	80.9	7.3	.58	7.2	3.9		66.9	

(Table 5.1.)

Microprobe analyses, reflectance and microhardness data for naturally occurring platinum from the Witwatersrand.

- Not detected.

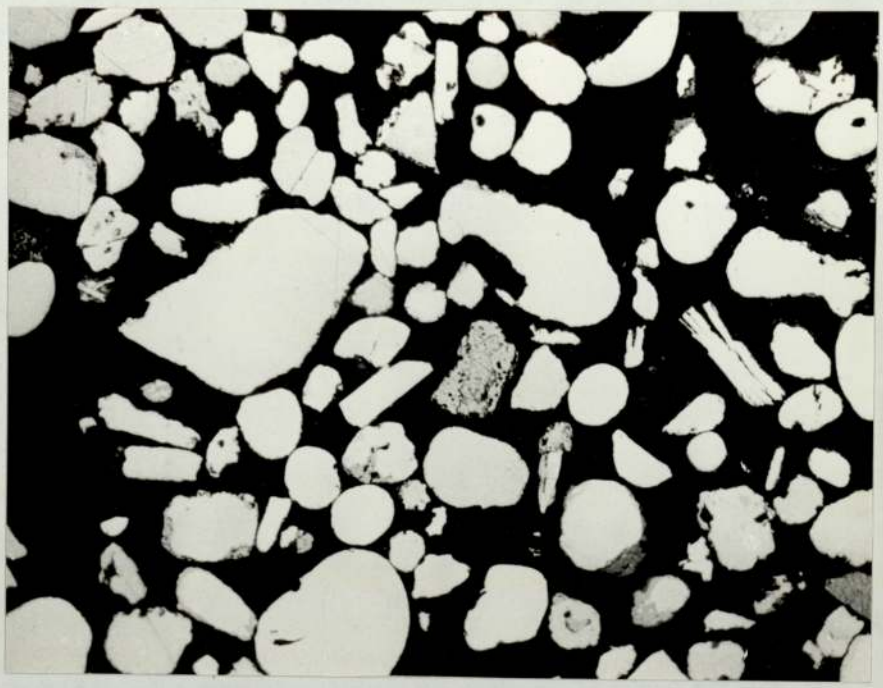

Fig. 5.1

Reflected light photomicrograph showing rounded, and anhedral grains from concentrates of the Witwatersrand Klerksdorp gold mine.

Magnification X 330.

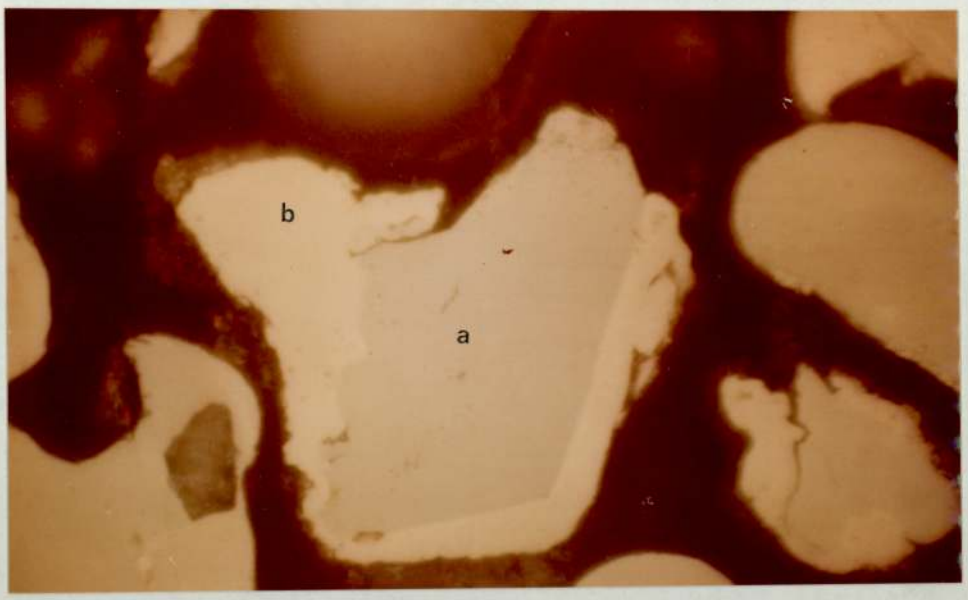

Fig. 5.2

Reflected light photomicrograph showing naturally occurring, alloy consisting of two phases :-

a. Osmium-iridium alloy, with high osmium content, (irodismine).

b. Iridium, platinum rich phase with minor ruthenium and osmium, (osmiridium).

The X-ray distributions for the elements present are shown in the following figures.

Locality : Witwatersrand.

Magnification X 560.

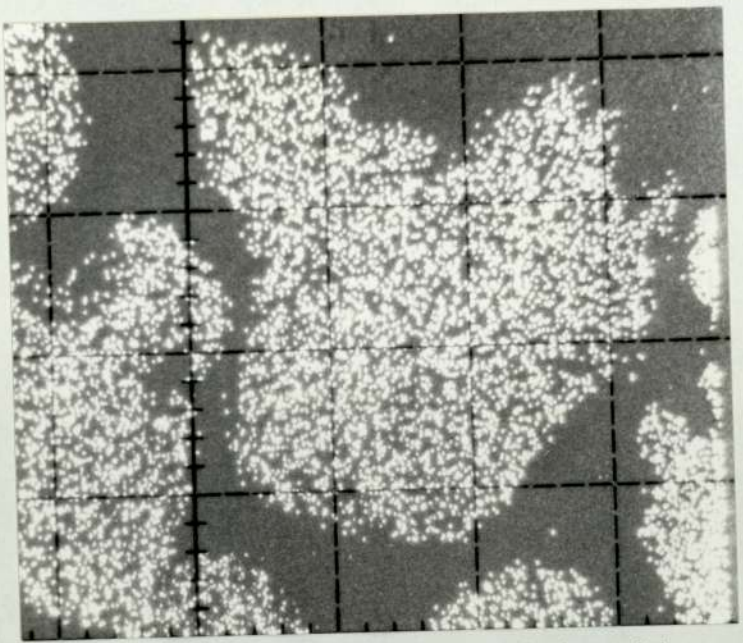

X-ray distribution for Ir in Fig. 5.2 phase (a) and (b).

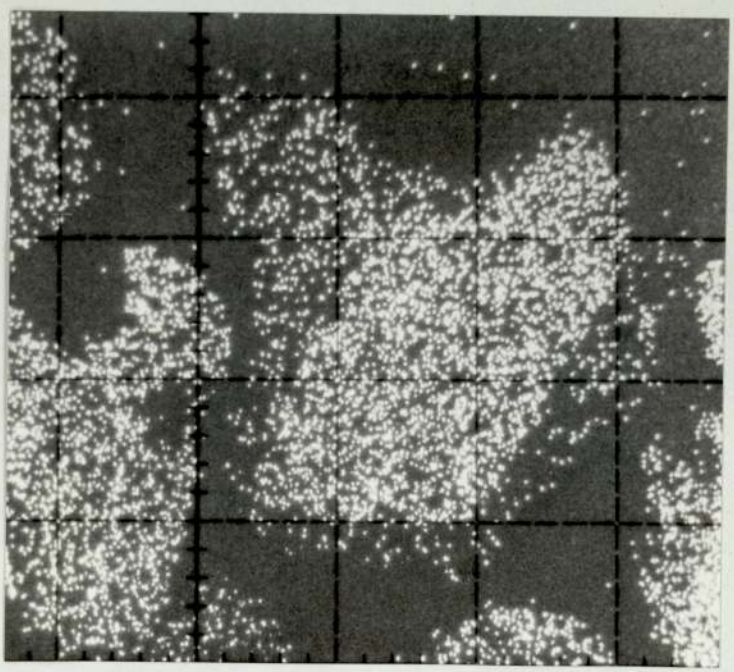

X-ray distribution for Os of Fig. 5.2.

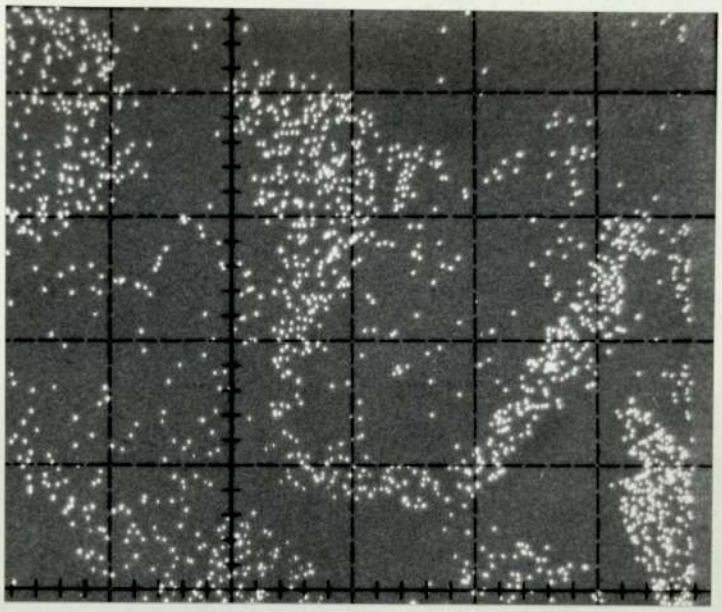

X-ray distribution for platinum in Fig. 5.2

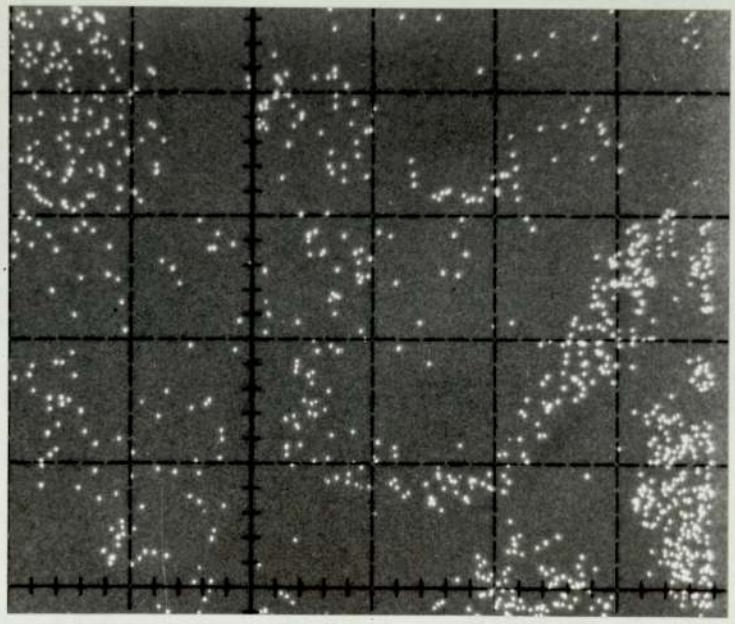

X-ray distribution of ruthenium in Fig. 5.2.

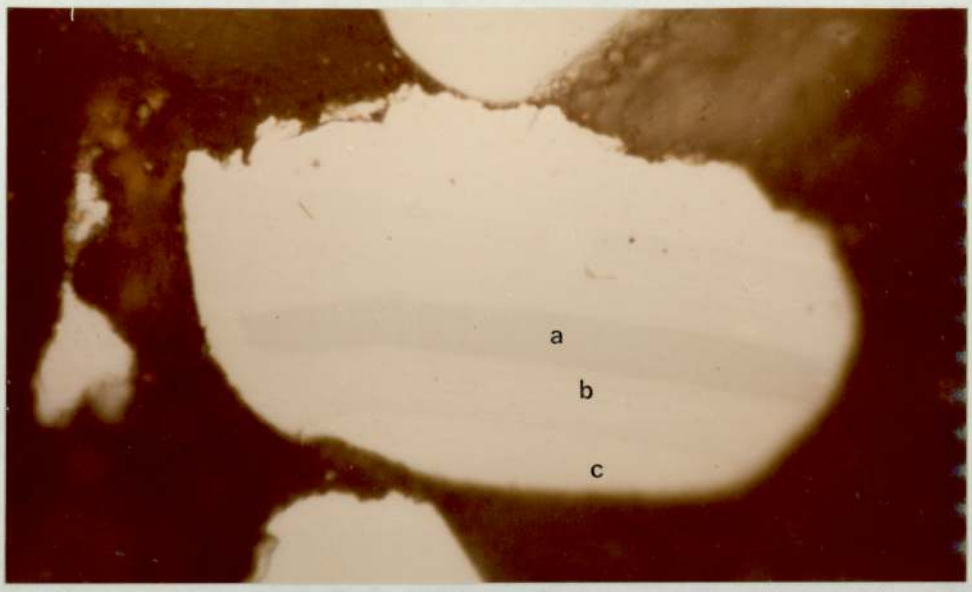

Fig. 5.3

Reflected light photomicrograph showing a naturally occurring, alloy consisting of three phases :-

a. Bluish-white in colour, weakly pleocheorioc, strongly anistropic.
Chemical composition is as follows:-

Os= 65.9% Ru= 15% Ir= 12% Pt= 8%

b. White in colour with a very faint, bluish tint, weakly anistropic.
Chemical composition is as follows:-

Os= 40% Ru= 34.6% Ir= 17.2% Pt= 8.6%

c. Pure white, isotropic.
Chemical composition is as follows:-

Ir= 59.8% Pt= 14.3% Os= 13.9% Ru= 12.1%

Locality : Witwatersrand.

Magnification X 560.

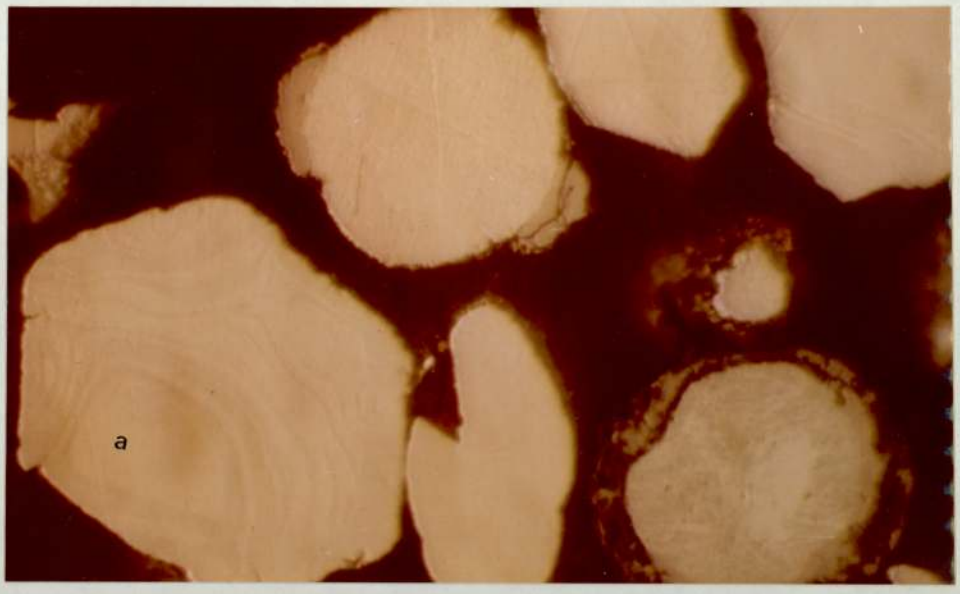

Fig. 5.4

Reflected light photomicrograph showing naturally occurring, alloys of osmium-iridium-ruthenium. Grain (a) , represents an alloy lying in the two-phase field of the osmium-iridium equilibrium diagram i.e. it consists of a hexagonal phase blue anistropic bands and a cubic phase . White areas in the grain which is isotropic.

Locality : Witwatersrand.

Magnification X 560.

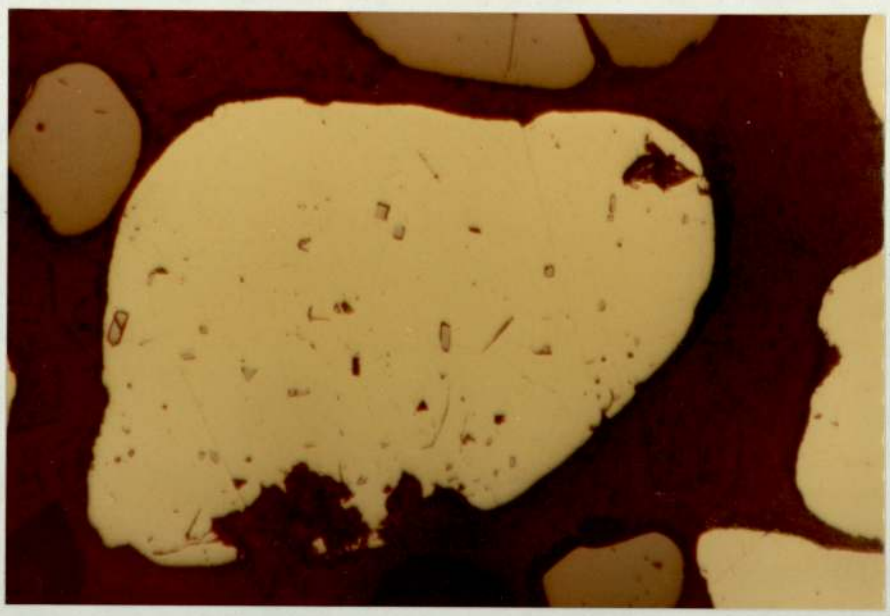

Fig. 5.5

Reflected light photomicrograph of small, euhedral, (pinkish grey) grains of laurite (Ru S) with minor amounts of osmium and rhodium, enclosed in the ferroplatinum matrix.

Locality : Witwatersrand.

Magnification X 320.

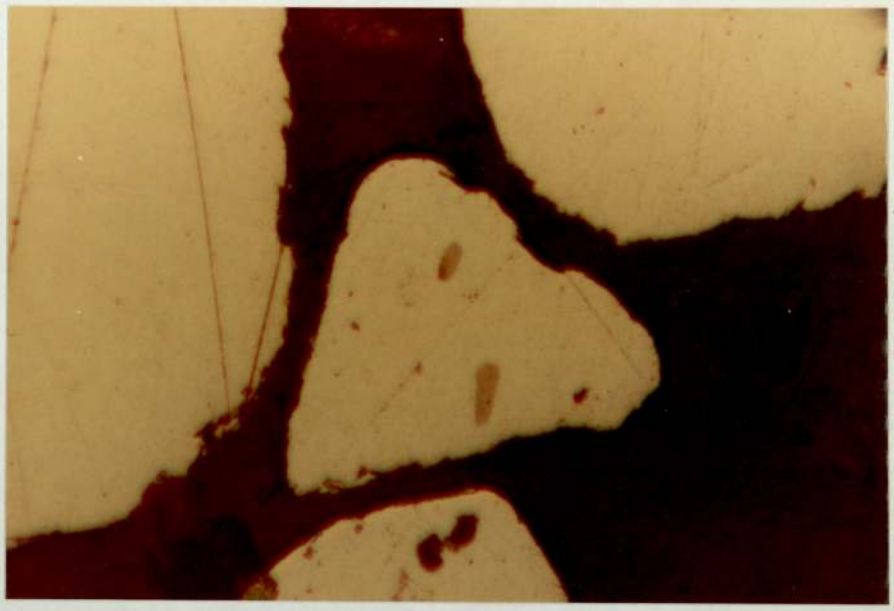

Fig. 5.6

Reflected light photomicrograph showing pyrrhotite FeS, intergrown with ferroplatinum.

Locality : Witwatersrand.

Magnification X 480.

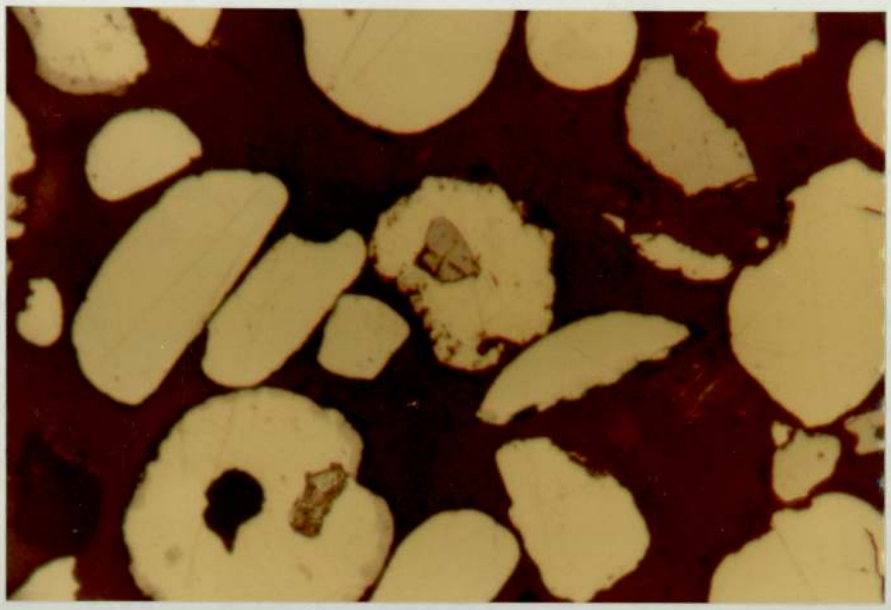

Fig. 5.7

Reflected light photomicrograph showing magnetite particles enclosed in the ferroplatinum. The ferroplatinum grain has been slightly replaced at the borders by iron sulphide.

Locality : Witwatersrand.

Magnification X 330.

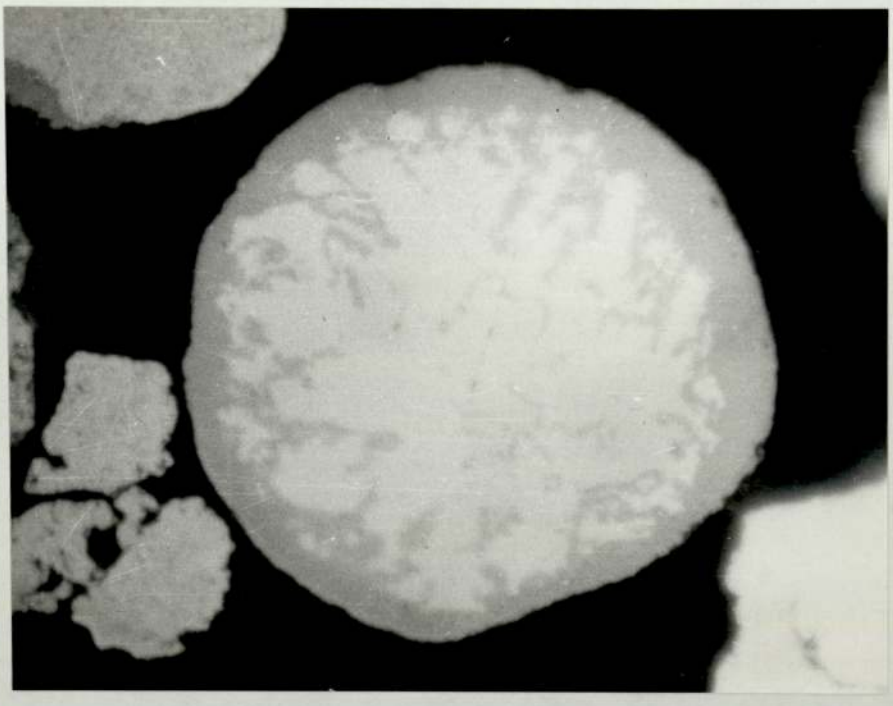

Fig. 5.8

Reflected light photomicrograph showing a rounded grain of naturally occurring ferroplatinum, in the border of which has been replaced by laurite.

Locality : Witwatersrand.

Magnification X 560.

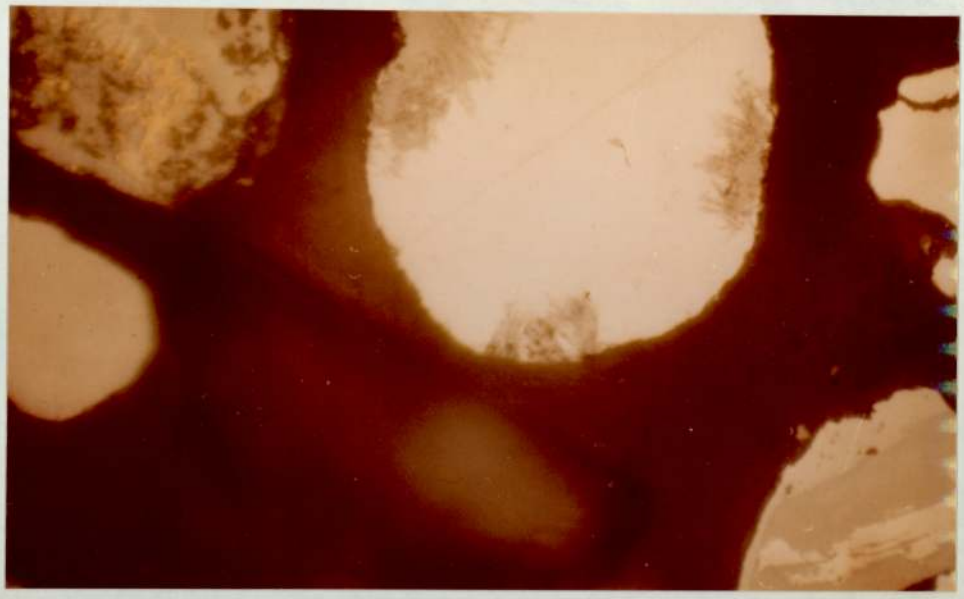

Fig. 5.9

Reflected light photomicrograph showing selective replacement by sulphides of Rh, Pd, Ir, to a ferroplatinum grain.

X-ray distributions of the elements present are shown in the next page.

Locality : Witwatersrand.

Magnification X 560.

X-RAY DISTRIBUTION OF ELEMENTS PRESENT IN FIG.5.9

S

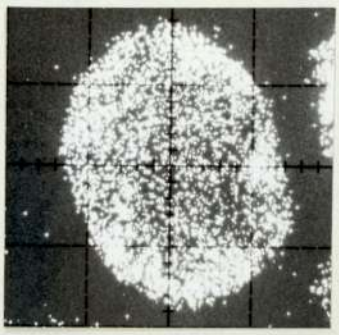

Pd

Fe

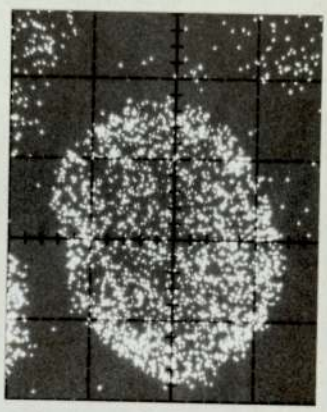

Ir

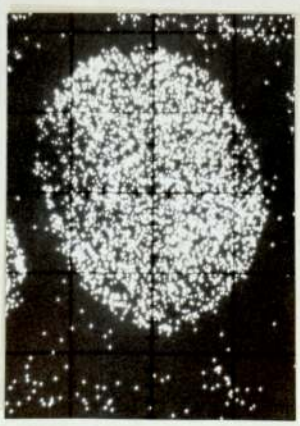

Pt

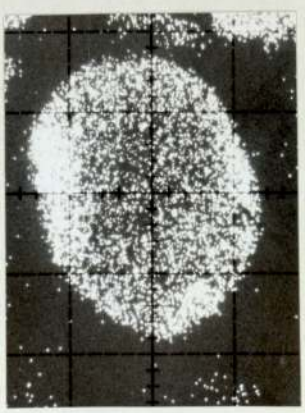

Rh

Fig. 5.10

Reflected light photomicrograph showing a typical complex grain from Witwatersrand, showing :-

a. Phase, white in colour, isotropic.

$R\%_{589} = 74$ $VHN_{100} = 810.$

Electron micro-probe analysis is as follows:-

Rh = 46.5% Ru = 33.2% Ir = 14.9% Os = 5.1% Pd trace.

b. Greyish white in colour , isotropic phase.

$R\%_{589} = 67$ $VHN_{100} = 475.$

Electron micro-probe analysis is as follows:

Pr = 81.7% Au = 12.9% Fe = 5.9%

c. Gold phase surrounding phase (b)

Electron micro-probe analysis show that gold dissolved in platinum.

Au = 94.8% Pt = 5.1%

d. Cooperite, grey strong anistropic phase.

Electron micro-probe analysis is as follows:-

Pt = 88.87% S = 11.1%

X-ray distribution for the elements present in each phase are shown.

Magnification X 480.

X-RAY DISTRIBUTION OF ELEMENTS

PRESENT IN FIG.5.10.

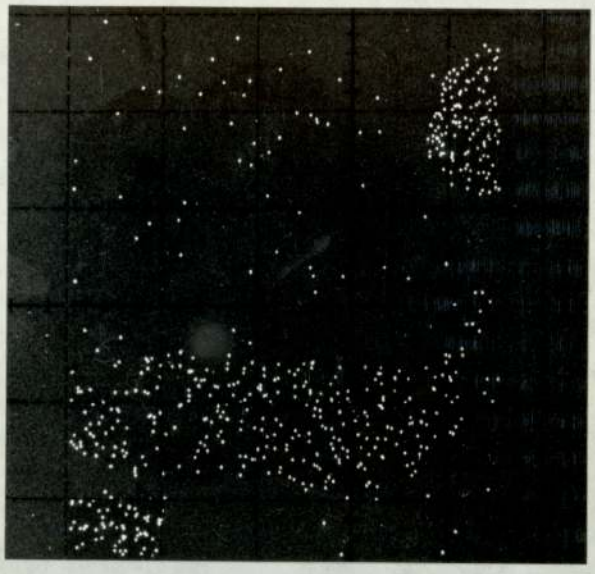

Ir.Mag. X800

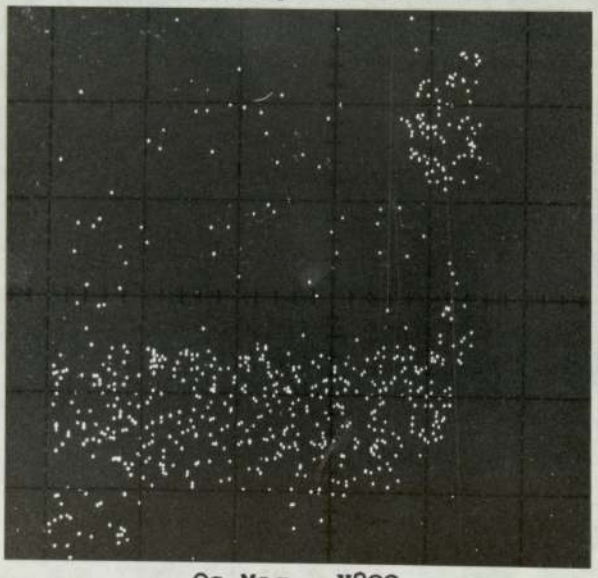

Os.Mag. X800

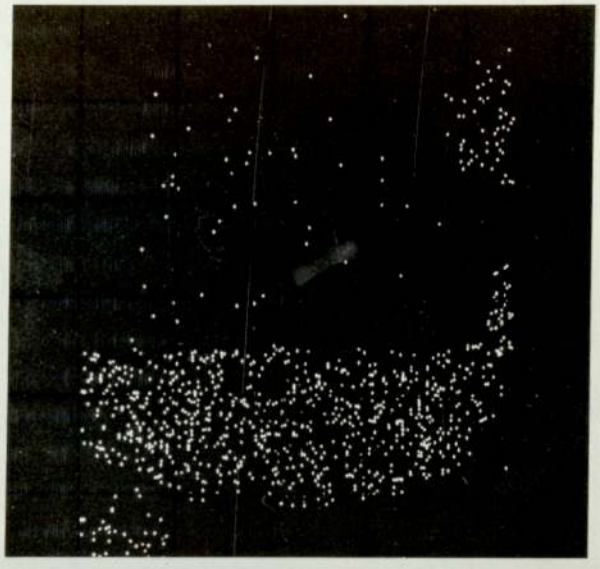

Rh.Mag. x 800

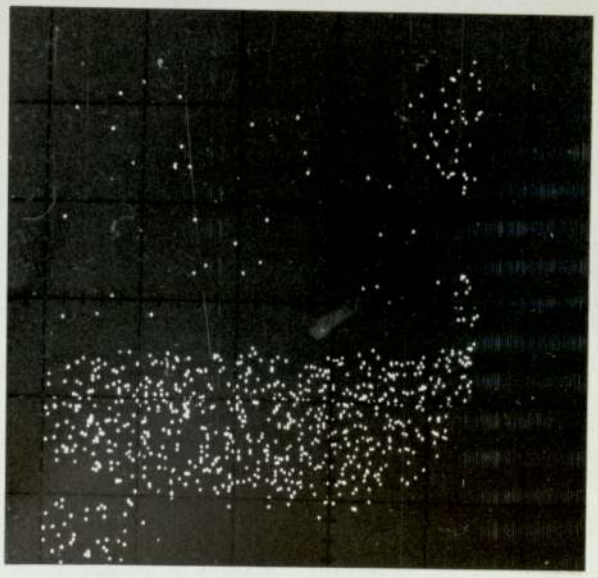

Ru.Mag x 800

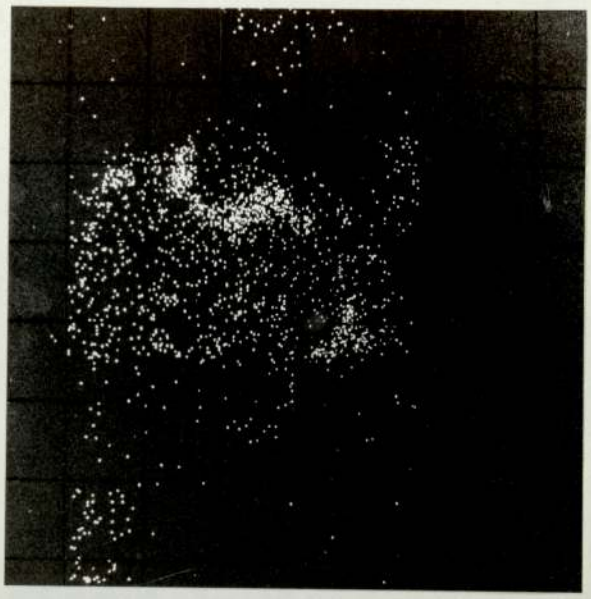

Au. Mag. x 800

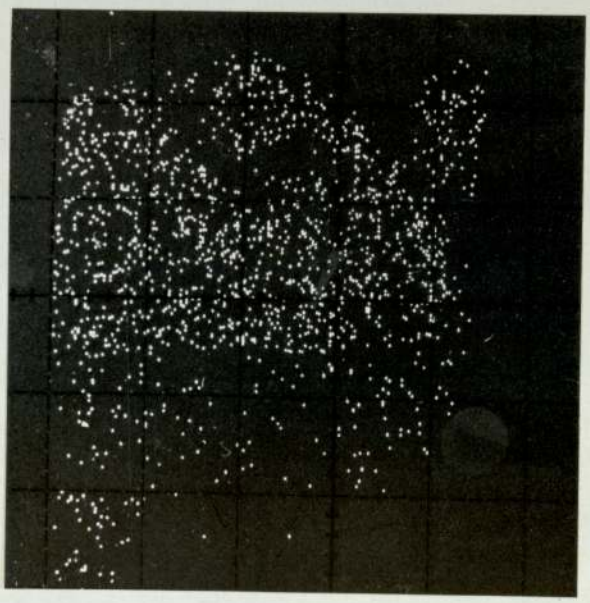

Pt. Mag. x 800

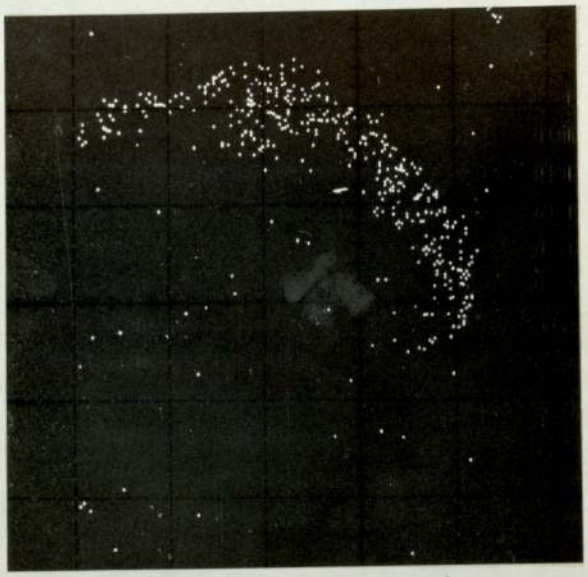

S.Mag. x 800

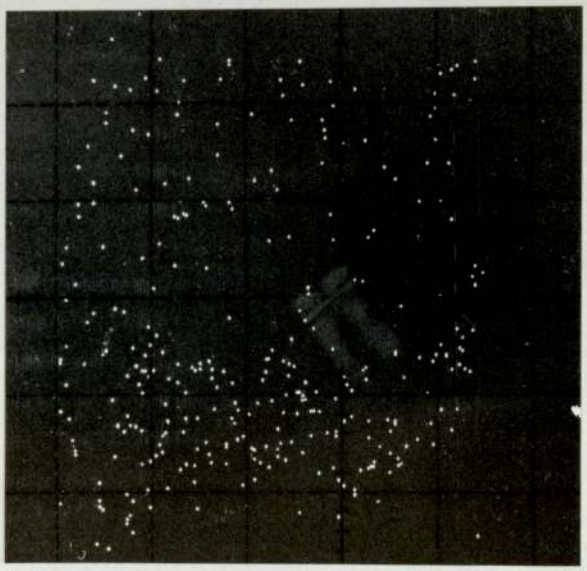

Pd.Mag x 800

Fig. 5.11

Reflected light photomicrograph showing three phases intergrown together in one grain.

a. Osmiridium.

b. Gold.

c. Braggite.

Locality : Witwatersrand.

Magnification X 560.

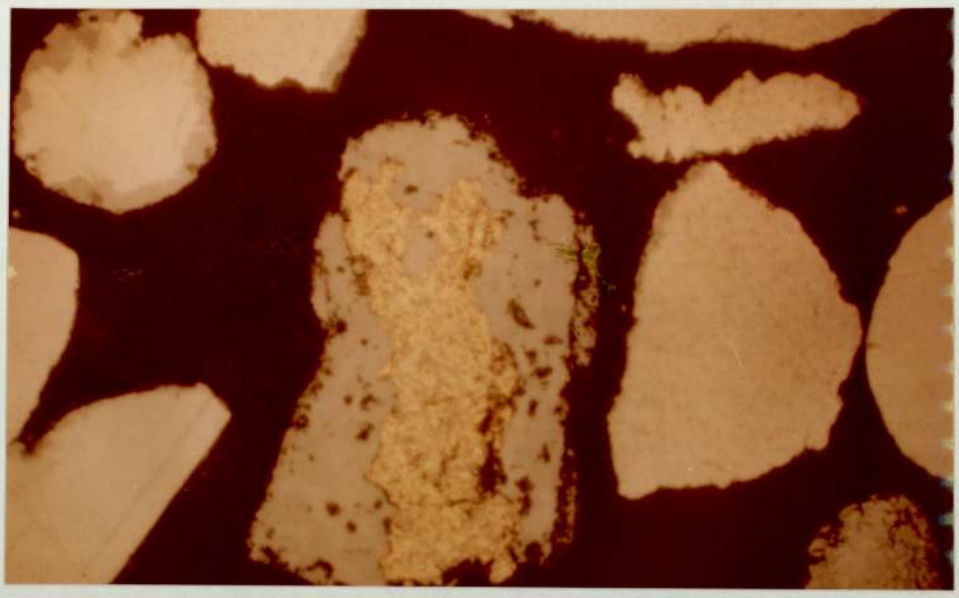

Fig. 5.12.

Reflected light photomicrograph of gold enclosed by anistropic sulphides of Pt, Ir, Os, Ru as shown from the electron micro-probe analysis for this grain.
Locality : Witwatersrand.
Magnification X 560.

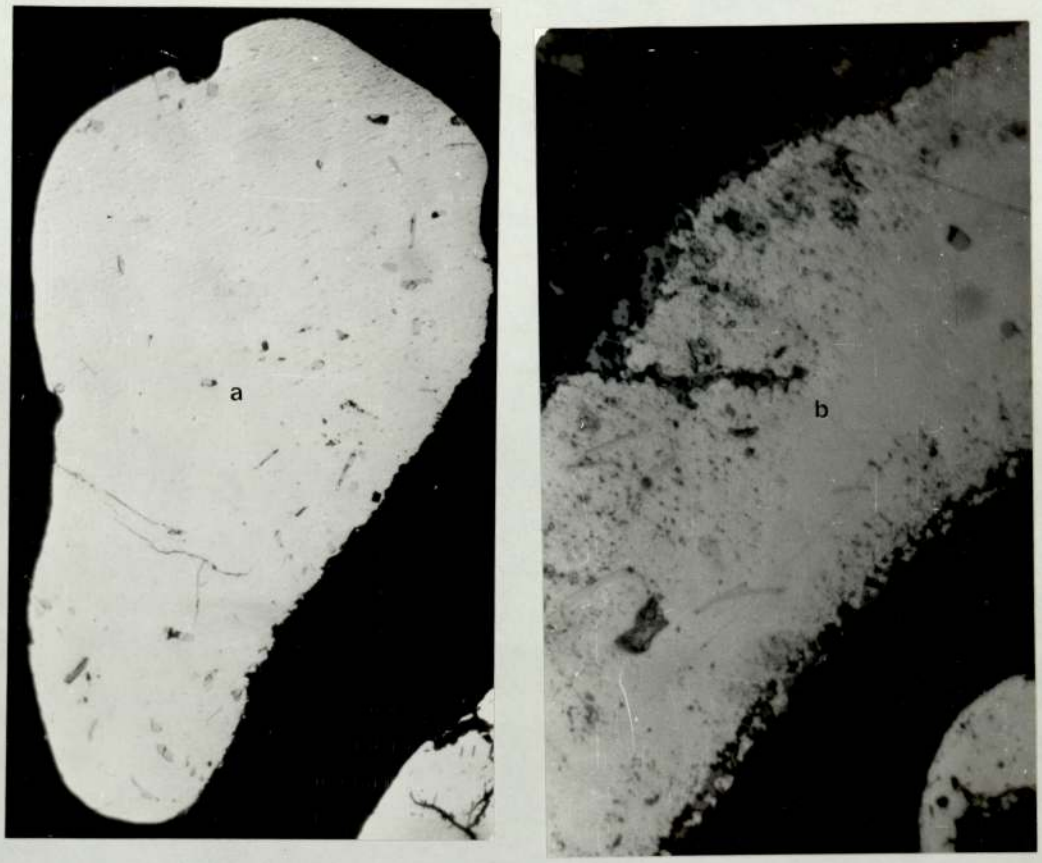

Fig. 5.13

Reflected light photomicrograph showing minute inclusions in the platinoid metals grains. These can only be identified by the electron microprobe.

a. Ferroplatinum grain containing laurite, and thin long particles of (Rh Ir) sulphide.

b. Osmiridium grain containing laurite, iridosmine, and chromite.

Locality : Witwatersrand.

Magnification : x 560.

CHAPTER 6.

ALLUVIAL PLATINOID METALS IN THE URALS.

6.1. GEOLOGICAL SETTING.

The alluvial platinoid metals were first discovered in the Ural mountains in the year 1819. Since then Ural platinum took first place on the world markets. According to Betechtin (1961) platinum is usually associated with the dunite rocks which together with diallagites, gabbros, diorites and granites form a continuous zone which extends over some 600 km. in a braod strip along the axis of the Ural mountains. Duparc and Tikonowitch (1920) divided this area into eleven dunitic and five pyroxenitic centres. These dunitic centres and the principal rivers that drain this stretch of the Ural Mountains are shown in Map 6.1. A list of the headwater streams is given in the figure.
Eight of these dunitic centres are on the Asiatic side of the Urals. Two are on the European side, and one, (the Tegil area) is on both sides. The richest platinum area in the Urals is the Nischni-Tagil (Map 6.2). The geology of Nischni-Tagil had been described in a number of essays in Russian. These descriptions can be summarised as follows:-

The dunite mountains together with the other mountain ranges within this platinum-containing area, are situated on the western edge of a zone of intrusive rocks which mainly consists of gabbro. It is characteristic that in the middle of dunite, no harzburgite occurs. Map 6.2 shows gradual transition at the central mass of dunite into the surrounding pyroxenite (diallagite) and then gabbro.

The transition is occasionally accompanied by the appearance of plagioclase-containing pyroxenite (Tylait). Gabbro is succeeded eastwards by diorite (sometimes syenite), then by quartzdiorite and finally granite.

All these intrusive rocks merge gradually into one another; only occasionally a more complicated set-up is found. These regions represent different parts of an originally complete magma of gabbroidal composition.

According to Betechtin (1961), platinoids are paragenetically joined to chromite in such a way that whenever one speaks of primary platinum deposits, one actually refers to accumulations of chromite within the dunite-ore. This however, does not mean that all chromite deposits have a platinum content which can be mined. So-called "empty" deposits have been found too, which contain practically no platinum at all. Normally, chromite occurs at the 1-2% level as an accessory mineral of the dunite ore in the shape of fine idiomorphous grains.

6.2 MINERALOGY OF THE ALLUVIAL DEPOSITS FROM THE URALS.

Ferroplatinum grains from the Urals concentrates are large and angular shape, similar to the Alaskan ferroplatinum, but different from the small grains of the Witwatersrand. The Urals concentrates are characterised by associated minerals more than the other localities studied. The associated minerals are as follows :- Magnetite, ilmenite-hematite, chromite, pyrite, chalcopyrite, cubanite, sphalerite, and pyrrhotite. Minerals such as sperrylite (Fig. 6.1) are found to be associated and intergrown. Laurite (Fig. 6.2) is found as small inclusions in the ferroplatinum matrix. Braggite and cooperite were found to be intergrown with the ferroplatinum, and also associated with it.

Concentrates from the Urals contain iridosmine enclosed in the ferroplatinum matrix, (Fig. 6.3). The particle shapes are

similar to those from Choco and Alaska, but the iridosmine differs in colour (whiter) and exhibits, weaker anistropy. It forms rod-like or needle shapes. Osmiridium is also found enclosed in the ferroplatinum.

Native iridium is a naturally occurring member of the osmium-iridium-ruthenium alloy group. It occurs as small inclusions in the ferroplatinum matrix (Fig. 6.4). It is a common mineral in the Ural samples in contrast to other localities studied. It is pure white in colour, isotropic, higher in reflectance and harder than ferroplatinum. Electron microprobe analyses for two grains from the Urals, together with reflectance and microhardness data are included in Table 6.2. Eight ferroplatinum grains are selected for quantitative electron microprobe analysis. The results of these analyses are tabulated in Table 6.1. Also quantitative reflectance and microhardness measurements are included in the same table.

Comparison between analyses by the electron micro-probe and bulk analyses for the Urals ferroplatinum are discussed in Chapter 7.

6.3. DISCUSSION OF THE URAL CONCENTRATES.

The origin of the Ural concentrates is exhaustively discussed in the Russian literature and the primary deposits from which these concentrates are derived are well known.

From this study, chromite was found to be enclosed and associated with the ferroplatinum. The presence of chromite suggests that the primary origin which was rich in chromite belongs to the earliest formation of the cooling dunite magma.

The sharp edges of the ferroplatinum grains suggest that they have not travelled a long distance ie. the primary origin from which they were derived is very close to the place of deposition. The presence of native iridium as small inclusions in the ferroplatinum grains suggests that the original melt was rich in iridium.

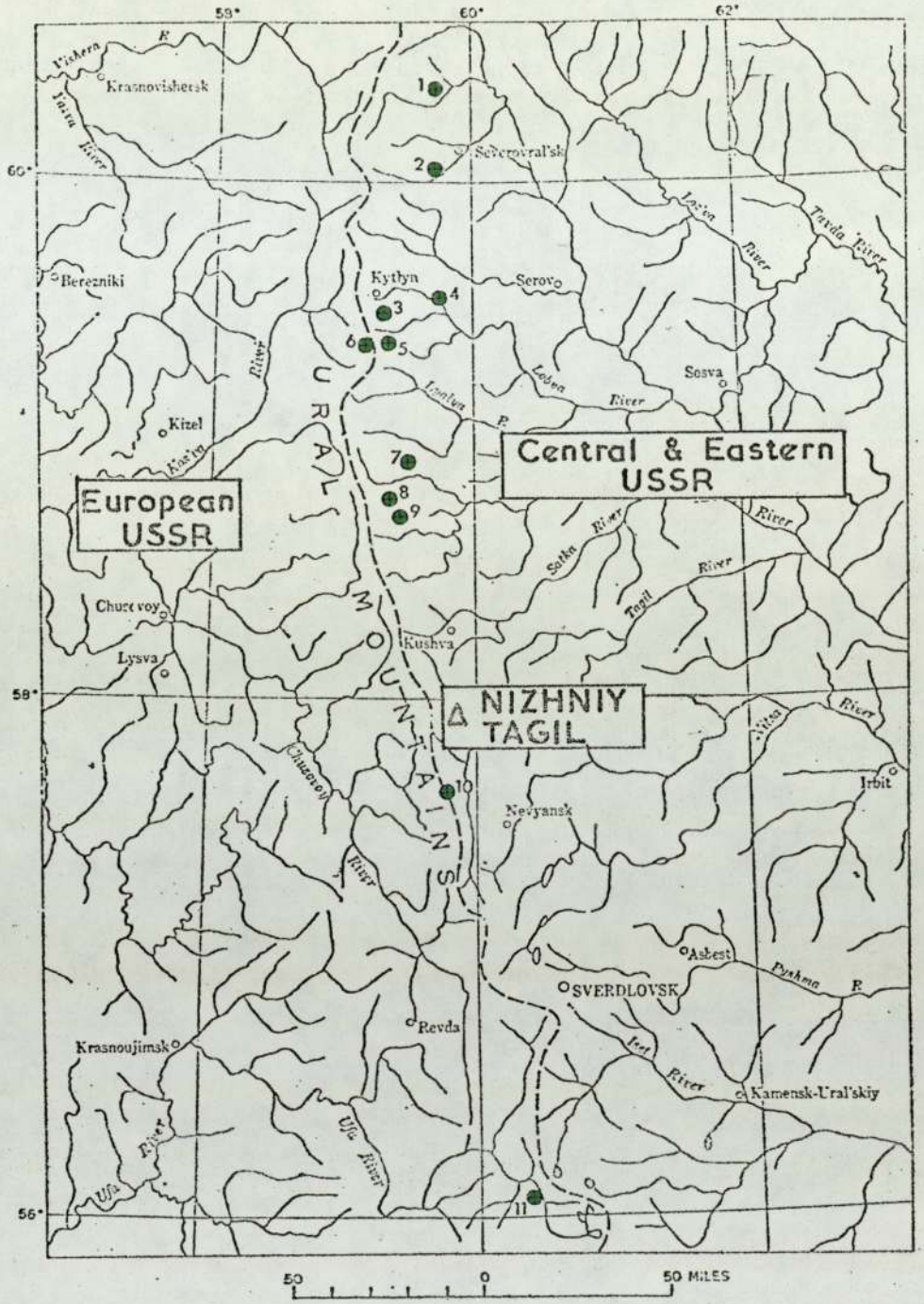

Map. 6.1.

Locations of dunites and pyroxinites in the Urals from which all the Urals platinum comes.

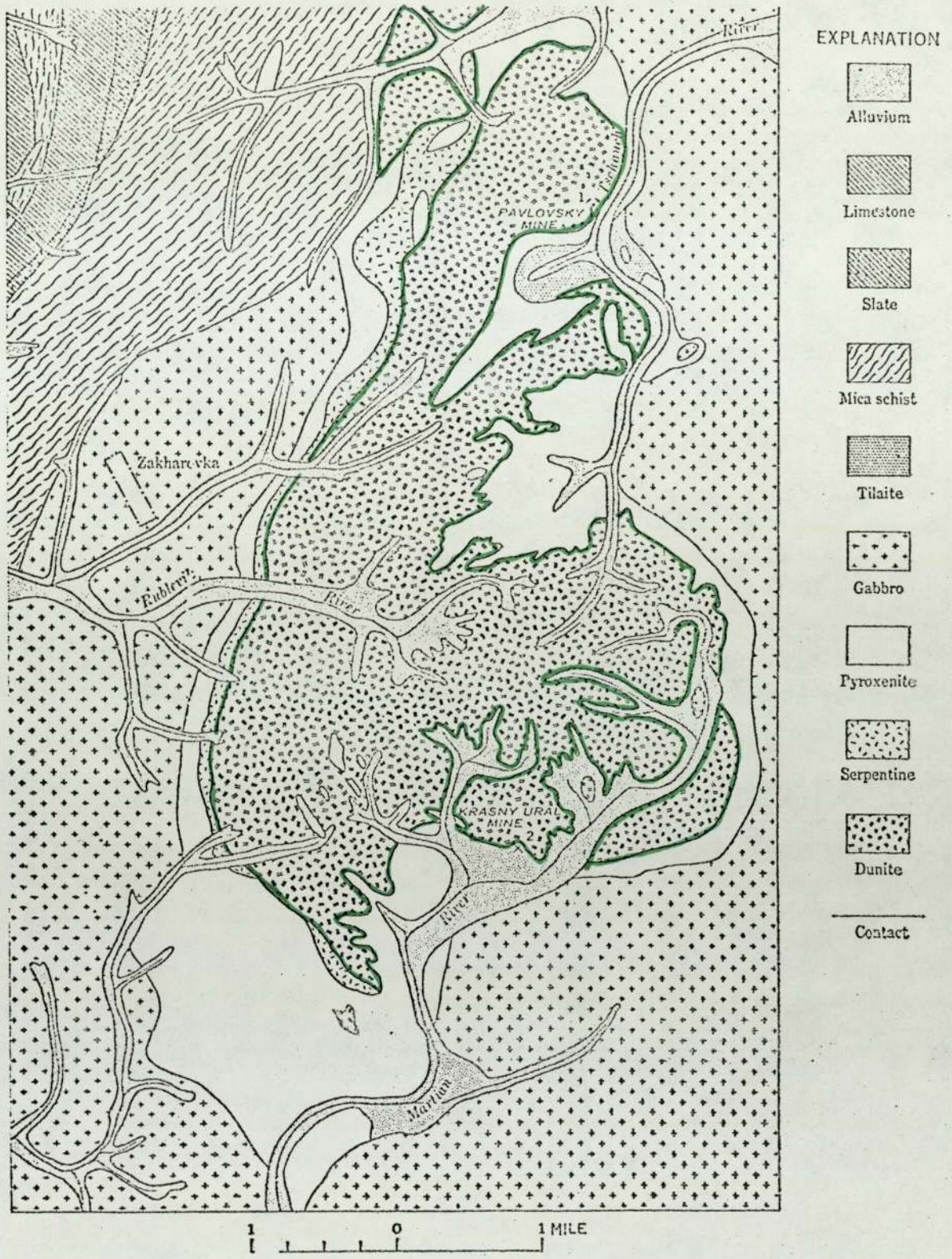

Map. 6.2.

Nizhniy-Tagil dunite massif (from Betechtin, 1961), the richest platinum area in the Urals. (See previous map for general location).

Grain No.	Pt	Fe	Cu	Ir	Os	Total	R % 589 nm	HVN 100 g.
1.	89.60	6.86	.45	1.71	1.37	99.99	67.00	292
2.	85.02	10.15	0.84	2.66	1.32	99.99	59.00	275
3.	90.95	6.40	0.81	1.06	1.06	100.3	67.40	238
4.	88.44	6.86	0.70	3.57	1.24	100.84	69.80	582
5.	88.67	6.36	0.89	1.77	1.87	99.56	66.30	284
6.	89.68	6.86	0.56	1.51	0.88	99.49	66.50	473
7.	92.1	4.30	.46	1.25	1.70	99.81	67.30	137
8.	82.80	8.60	0.39	8.00	-	99.79	72.00	582
Average	88.40	7.00	.64	2.70	1.20		66.90	358

Microprobe analysis, reflectance and microhardness data for naturally occurring alluvial platinum from Urals

(Table 6.1).

Grain No.	Electron microprobe analyses						R % 589	VHN
	Ir	Os	Pt	Fe	Cu	Total		
Grain 1.	80.9	8.7	9.3	.9	.5	100.3	78%	663 (100)
Matrix.	8.0	-	79.9	9.8	2.5	100.2	72%	625 (100)
Grain 2.	64.71	19.42	13.00	1.15	.96	99.24	72%	840 (100) 783 (50)
Matrix.	6.4	2.3	81.2	9.4	.6	99.9	70%	596 (100)

(Table. 6 .2).

Electron microprobe analyses, reflectance and microhardness data for native iridium from the URALS.

Fig. 6.1

Reflected light photomicrograph showing sperrylite (Pt As) grain intergrown with chalcopyrite.

$R\%_{589} = 54$ $VHN_{200} = 1269.$

X-ray distribution for the elements present are shown in the following figures.

Locality : Urals.

Magnification X 280.

X-ray distributions of Pt, As and S of Figure.6.1.

Mag. 150 - Pt.

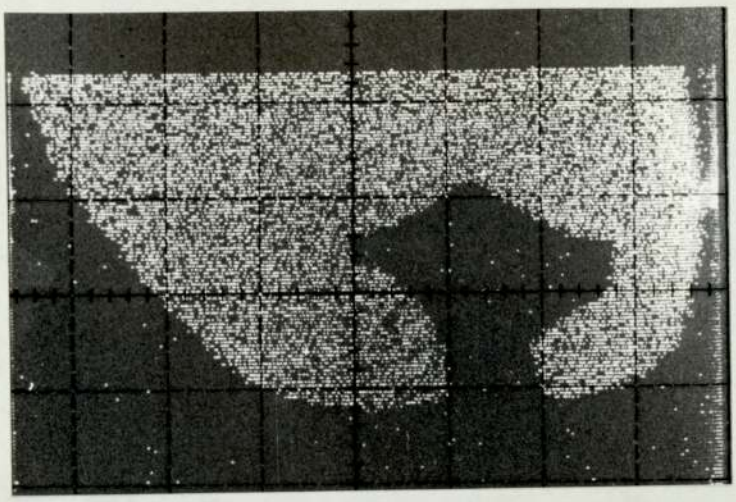

Mag. 150 - As

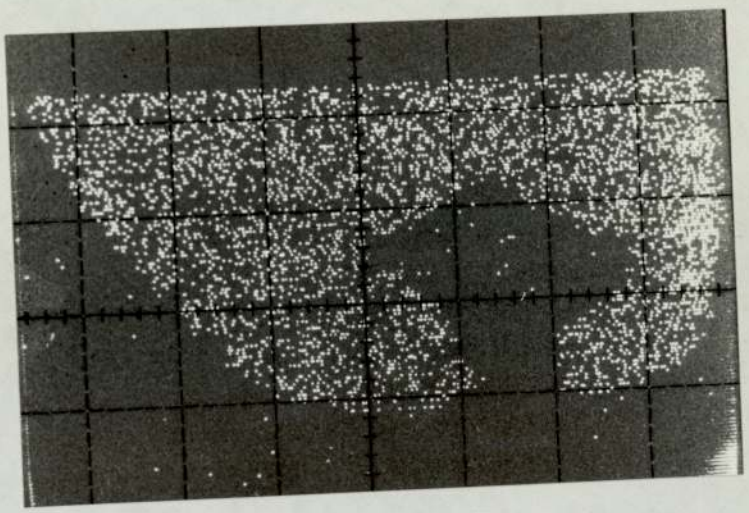

Mag. 600 - S

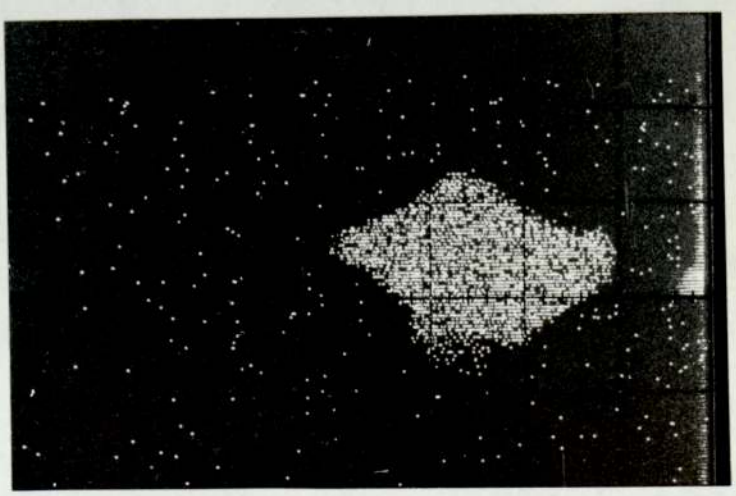

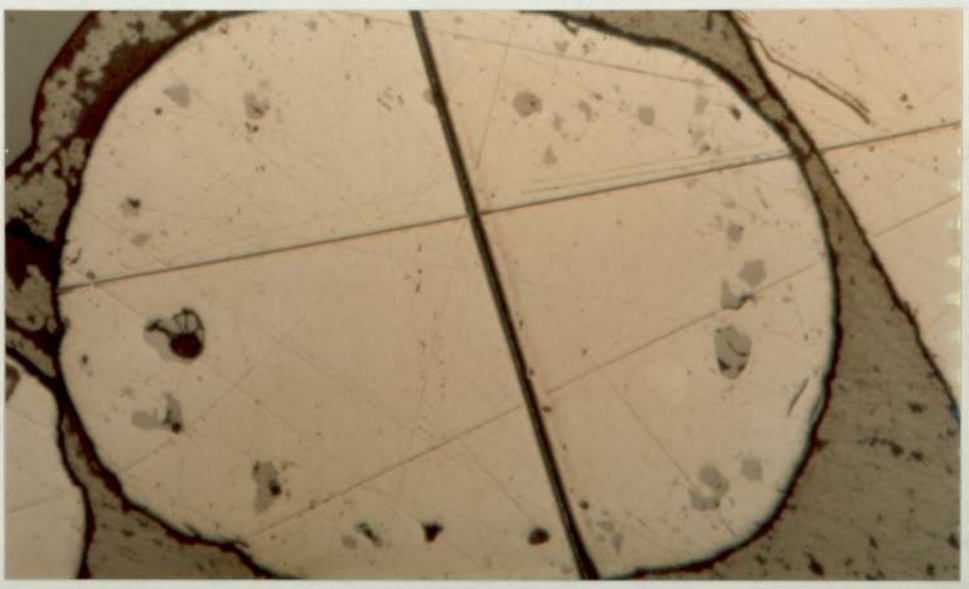

Fig. 6.2

Reflected light photomicrograph of anhedral grains of laurite, (grey) enclosed in the ferroplatinum matrix.

Locality : Urals.

Magnification X 220.

Fig. 6.3

Reflected light photomicrograph showing, iridosmine, enclosed in the platinum matrix in different orientations.

Locality : Urals.

Magnification X 560.

Fig. 6.4

Reflected light photomicrograph showing, native iridium as ex-solved bodies in the ferroplatinum matrix. Reflectance, microhardness measurements and electron micro-probe analysis are shown in Table 6.2, grain 1.

Locality : Urals.

Magnification X 560.

CHAPTER 7.

CHEMICAL COMPOSITION OF FERROPLATINUM.

7.1. PREVIOUS WORK.

According to different analyses for crude platinum from various parts of the world, (kindly supplied by Messrs. Johnson, Matthey and Co. Ltd), native platinum is nearly always found to contain iron, which may be up to 25% and often contains minor iridium, copper, palladium, rhodium and ruthenium. Most of the previous analyses have been obtained from impure material which was not investigated microscopically, with the result that it is not possible to determine which of these elements are present in solid solution, and which are present as inclusions or impurities. Previous analyses have called platinum "polyxene" when its iron content is less than 11%. The name polyxene is derived from a Greek word meaning "entertainer of many guests", in allusion to the many elements which accompany it. Ferroplatinum with more than 10% of iron is frequently magnetic. Numerous analyses of native platinum from various parts of the world show that the composition ranges for the different constituents are as follows:-

Platinum -	60 - 90%
Iridium up to -	7%
Palladium up to -	3%
Copper up to -	4%
Osmiridium (Ir + Os) up to -	27%
Rhodium up to -	2%
Gold up to -	2%
Iron up to -	2 - 6%

A small amount of nickel and cobalt may be present.

According to the previous analyses, the amount of osmium in native platinum reaches 27%. It appears that much of the osmium is found as inclusions of osmium minerals (iridosmine and osmiridium) enclosed within the ferroplatinum but not dissolved with it. However, rhodium and palladium appear to be alloyed with the platinum.

Native platinum is often cubic and the magnetic properties show variation with the iron content.

During this study the name ferroplatinum is used for native platinum which contains more than 4% iron.

7.2 CHEMICAL COMPOSITIONS OF MINERALS AND BULK CONCENTRATES.

A large number of naturally occurring ferroplatinum grains were examined under the reflected light optical microscope from the five localities studied. Some of these grains were subsequently analysed in the electron-probe microanalyser. The results are grouped according to the place of origin and are tabulated in Tables 2.1, 3.1, 4.1, 5.1 and 6.1. In Table 7.1 is shown the commercial bulk analyses of the concentrates from the five localities studied in this work. Table 7.2 shows bulk analyses of the Choco concentrates according to Wokkitel. Table 7.3 shows the bulk analyses of concentrates from alluvial deposits from various localities supplied by Messrs. Johnson Matthey & Co. Ltd.

These tabulations allow a comparison to be made between bulk and individual mineral analyses made in the course of this work. The average values of the bulk analyses were calculated and are represented in histograms Figs.7.1 to 7.5, Figs.7.6 to 7.10 show the average values of the individual mineral analyses determined by the electron probe-microanalyser from the different localities studied. Fig.7.11 to 7.15 represent the frequency distributions of platinum, iron, osmium, iridium and copper respectively, present in

grains analysed by the electron probe micro analyser.

During the micro-probe analyses for the natural platinoid minerals and alloys, fourteen analyses were made for the natural iridium-osmium and ruthenium alloys from the different localities studied. These analyses are tabulated in Table 11.1. In Table 6.2. is shown the microprobe analyses for two native iridium grains and the ferroplatinum matrix in which they are enclosed.

7.3 COMPARISON BETWEEN BULK ANALYSES AND ANALYSES BY ELECTRON MICRO-PROBE FROM THE LOCALITIES STUDIED.

Natural ferroplatinum usually occurs as minute, bright, isotropic grains of different shapes and size. They mainly occur as seperate grains but sometimes ferroplatinum is found as inclusions in other platinoid phases. The ferroplatinum grains are slightly different in colour, shape and size. These differences are due to difference in their chemical composition. The ferroplatinum grains were found to have elements such as iron, copper, iridium and osmium etc. These elements are dissolved in the grains as found from the electron micro-probe analyses (Tables 2.1, 3.1, 4.1, 5.1 and 6.1) , or intergrown and associated with the grains as found from the microscopic investigation. The presence of uniformly dissolved iron and copper in all the grains analysed, appears to be of genetic significance in all the concentrates studied.

ALASKA

The commercial bulk analysis of platinum concentrates from Alaska showed the lowest copper and iron content compared to other localities, (Fig. 7.2 and 7.3). This low content of copper and iron can be explained by the purity of the Alaskan concentrates i.e. no copper and iron minerals are intergrown or associated with the ferroplatinum.

Ruthenium, rhodium, palladium, silver, nickel and cobalt were not detected in the microprobe analyses. However, in the bulk analyses (Tables 7.1 and 7.3), there are small amounts of palladium and rhodium, which can be explained by the presence of small quantities of associated palladium and rhodium minerals.

CHOCO

From the microprobe analysis of Choco ferroplatinum it was found that it contained the highest platinum content of all the ferroplatinum natural alloys (Fig.7.6). However, the bulk analysis shows that the iron and copper content are high. This is because copper and iron occurs as discrete minerals intergrown and associated with the ferroplatinum e.g. magnetite (Fig. 3.6).

ETHIOPIA

From the microprobe analysis it was found that the dissolved osmium and iridium contents of the Ethiopian ferroplatinum are very close to those of Choco. However, the bulk analysis shows that the osmium content of the Ethiopian nuggets is higher. This is because of the intergrowth of native osmium in the ferroplatinum matrix as shown in Fig. 4.1.

WITWATERSRAND

Witwatersrand samples are the most interesting of the concentrates studied. During the microprobe analysis 50 grains have been analysed qualitatively, only 5 of them being ferroplatinum grains. The rest of the grains were alloys of iridium, osmium, ruthenium and rhodium etc. (Table 5.1). Ferroplatinum grains from Witwatersrand

contain dissolved iron and copper in high proportions. However, the bulk analysis show no copper and no iron . This is because little attention has been paid to determining copper and iron in the concentrates. The platinoid metal particles from the Witwatersrand concentrates often contain dissolved gold. This is a very rare case since gold is usually only associated with platinoid concentrates, as in the Choco deposits.

URALS

Electron microprobe analyses of the ferroplatinum from the Urals are tabulated in Table 6.1 . In the samples from Urals the content of iron and copper which are dissolved in the ferroplatinum are in contrast to the iron and copper content obtained from the bulk analysis. This is because of the presence of the intergrown and associated copper and iron minerals with the ferroplatinum. The Urals samples seem to be more close to the Alaskan samples with respect to platinum content, and higher in iridium content than the three localities studied except the Witwatersrand. This can be explained by the native iridium which has been found enclosed in the ferroplatinum matrix.

	Pt.	Pd	Rh	Ir	Os	Os-Ir	Fe	Cu	Au
Alaska	73.0	0.5	0.99	9.54	10.4	0.6	0.07	.03	
Choco	85.91	.72	1.9	1.54	0.57	2.11	7.03	.53	
Ethiopia	95.21	.43	.85	.92		2.59			
Witwaters rand.	12.86		.70	33.54	37.87				
Urals	74.62	.63	1.63	9.78		7.26	9.9	1.48	

(Table 7.1)

Shows commercial bulk analysis for platinum for the different alluvial and eluvial deposits studied.

	Pt	Pd	Rh	Ir	Os	Os-Ir	Fe	Cu	Au	Ag
1.	86.20	0.50	1.40	10.85		0.95	7.80	0.60	1.0	
2.	84.30	1.06	3.46	1.46	1.09		5.31	0.74		
3.	86.02	0.50	1.30	1.64	1.10	1.34	7.50	0.60		
4.	48.90	0.40	1.62			3.35	0.73	11.30	0.88	0.11
5.	86.10	0.30	2.16	1.19		1.19	8.03	0.40		

(Table 7.2)

Analysis for platinum from Choco according to Wokkitel (1960) obtained from Campilacion de los estudios geologicos en Columbia.

	Platinum	Palladium	Iridium	Rhodium	Osmiridium	Gold
Sierra Leone	77.10	1.41	0.65	1.13	2.70	0.03
Abyssinia	73.45	0.22	0.30	0.62	0.67	3.48
Yukon (USA)	73.15	0.29	1.76	0.96	7.48	2.33
Columbia	84.97	0.70	1.16	0.79	0.42	0.99
New South Wales	79.89	0.26	2.03	0.47	6.72	6.14
Russia	70.74	0.24	1.99	0.79	0.42	3.05

(Table 7.3.)

Average bulk analyses of platinum concentrates from the alluvial deposits kindly given by Messrs. Johnson Matthey and Co. Limited

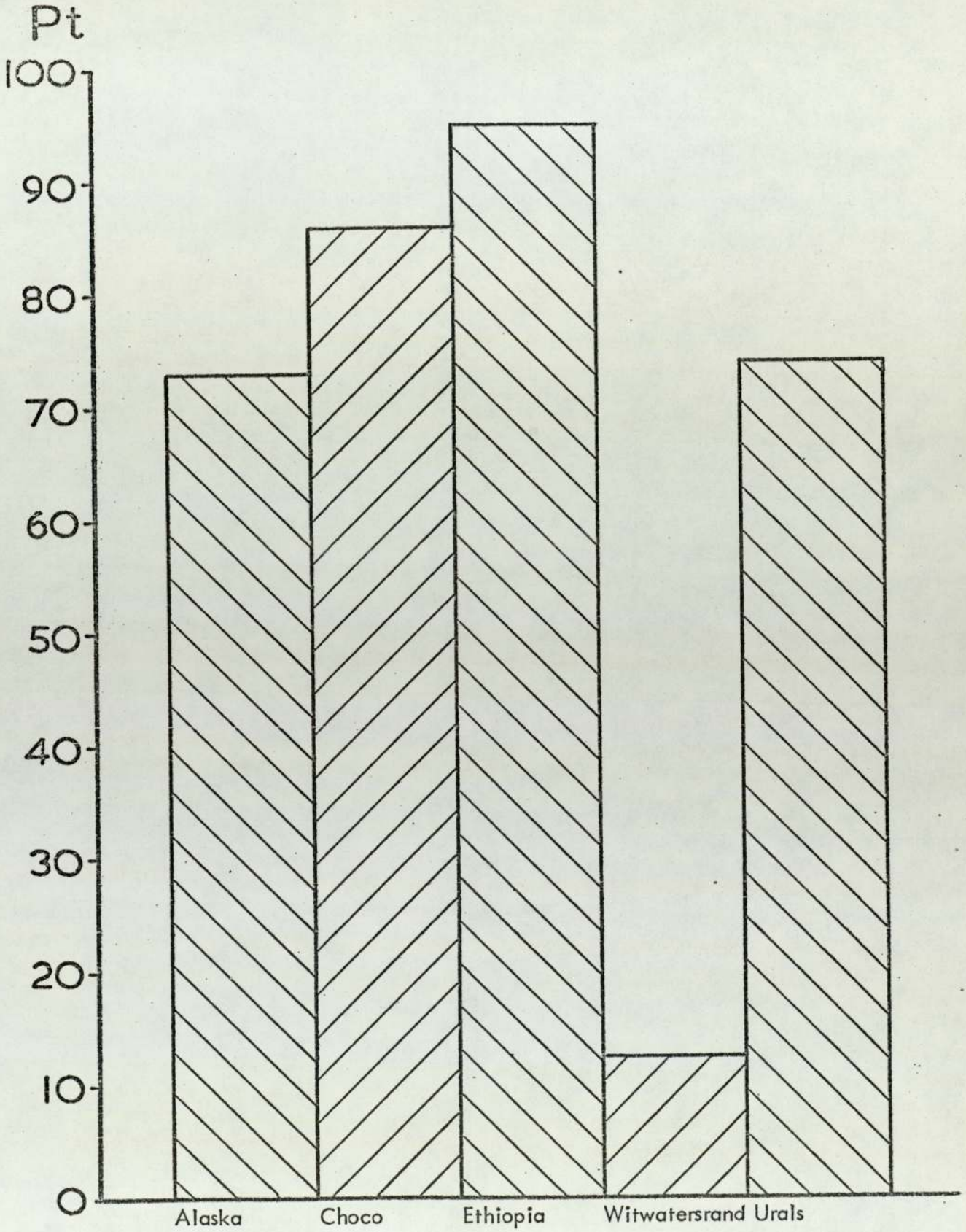

Histogram showing the average content of platinum, calculated from commercial bulk analyses, in the concentrates from the localities studied.

Fig. 7.1

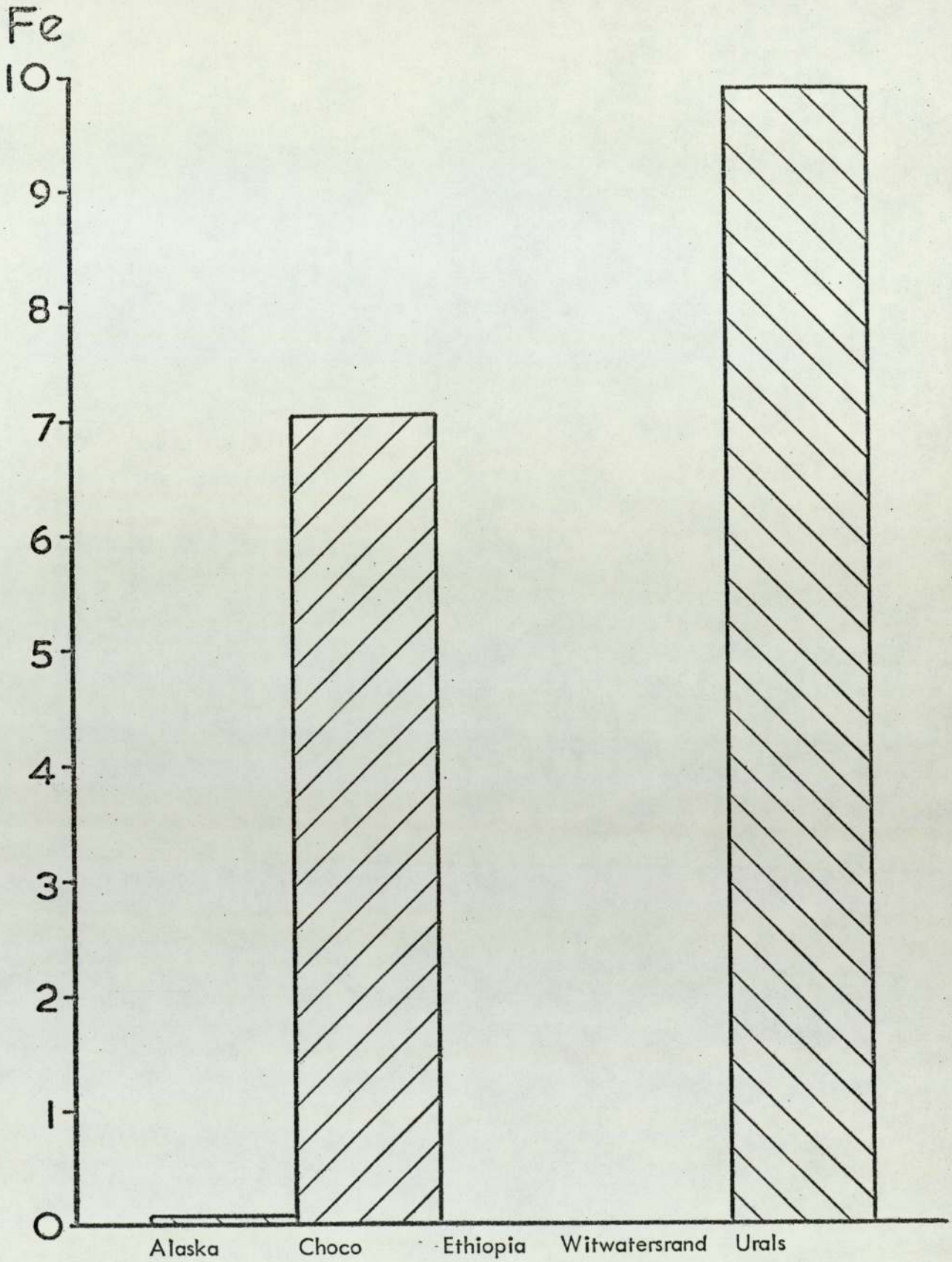

Histogram showing the average content of iron, calculated from commercial bulk analyses, in the concentrates from the localities studied.

Fig.7.2

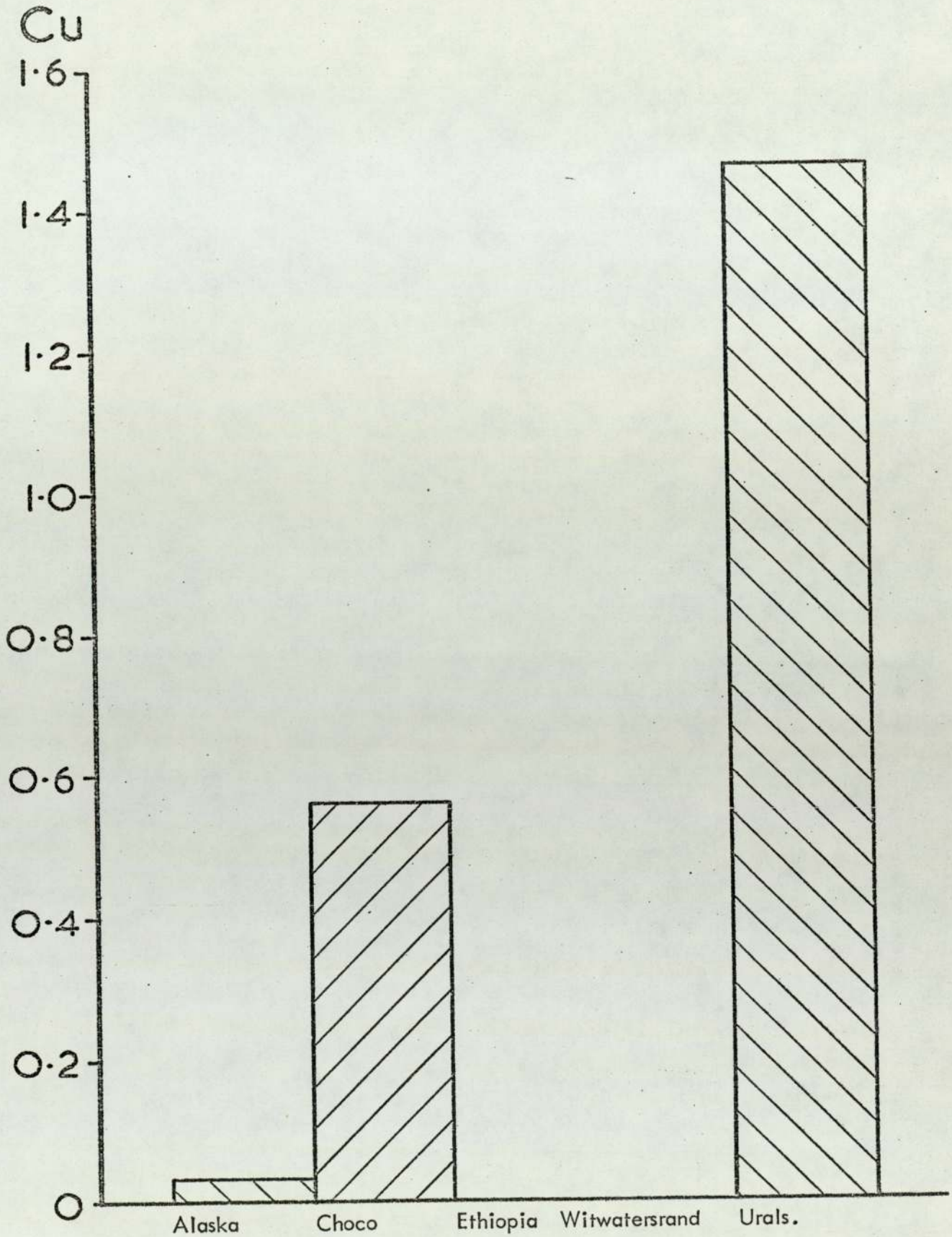

Histogram showing the average content of copper, calculated from commercial bulk analyses, in the concentrates from the localities studied.

Fig. 7.3

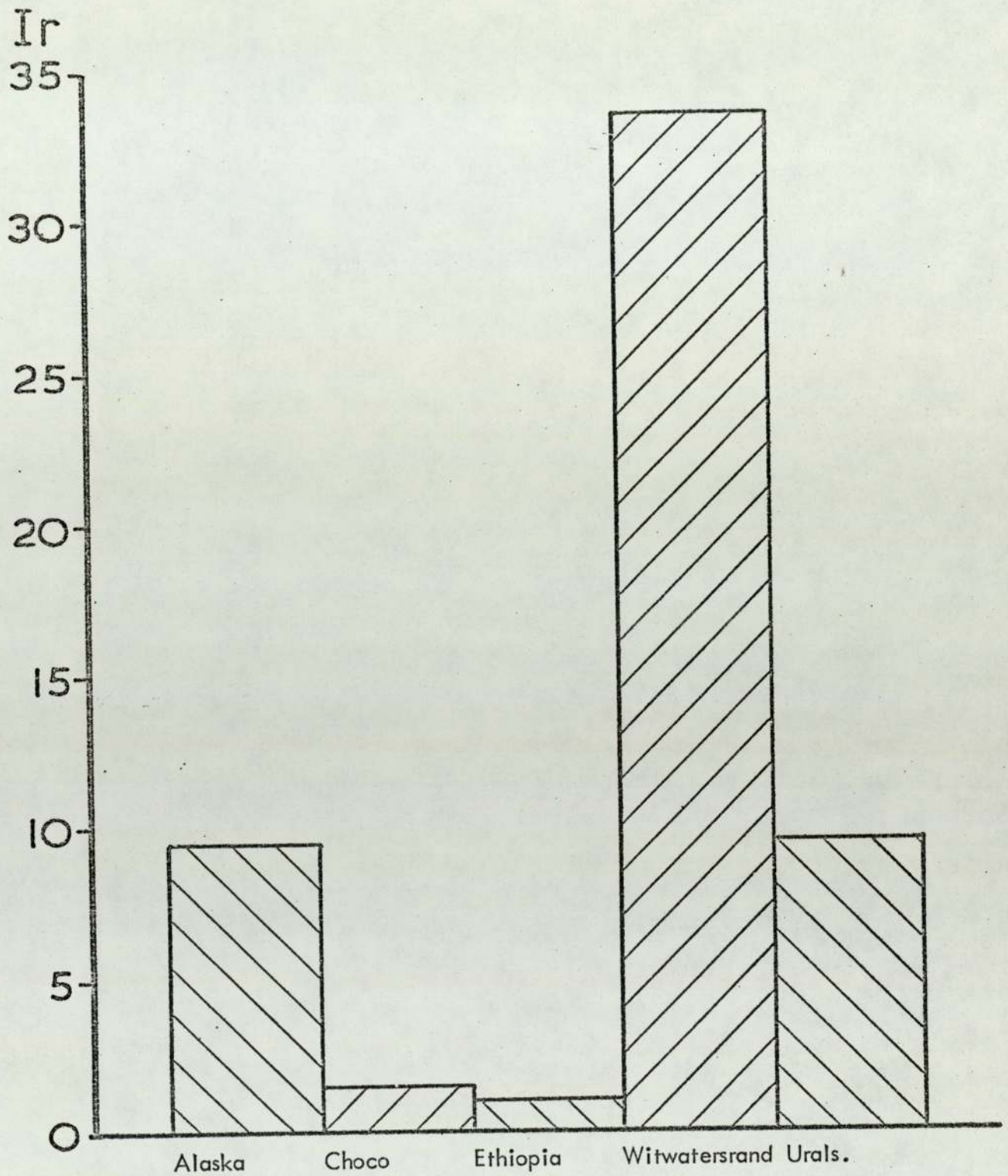

Histogram showing the average content of iridium, calculated from commercial bulk analyses, in the concentrates from the localities studied.

Fig. 7.4

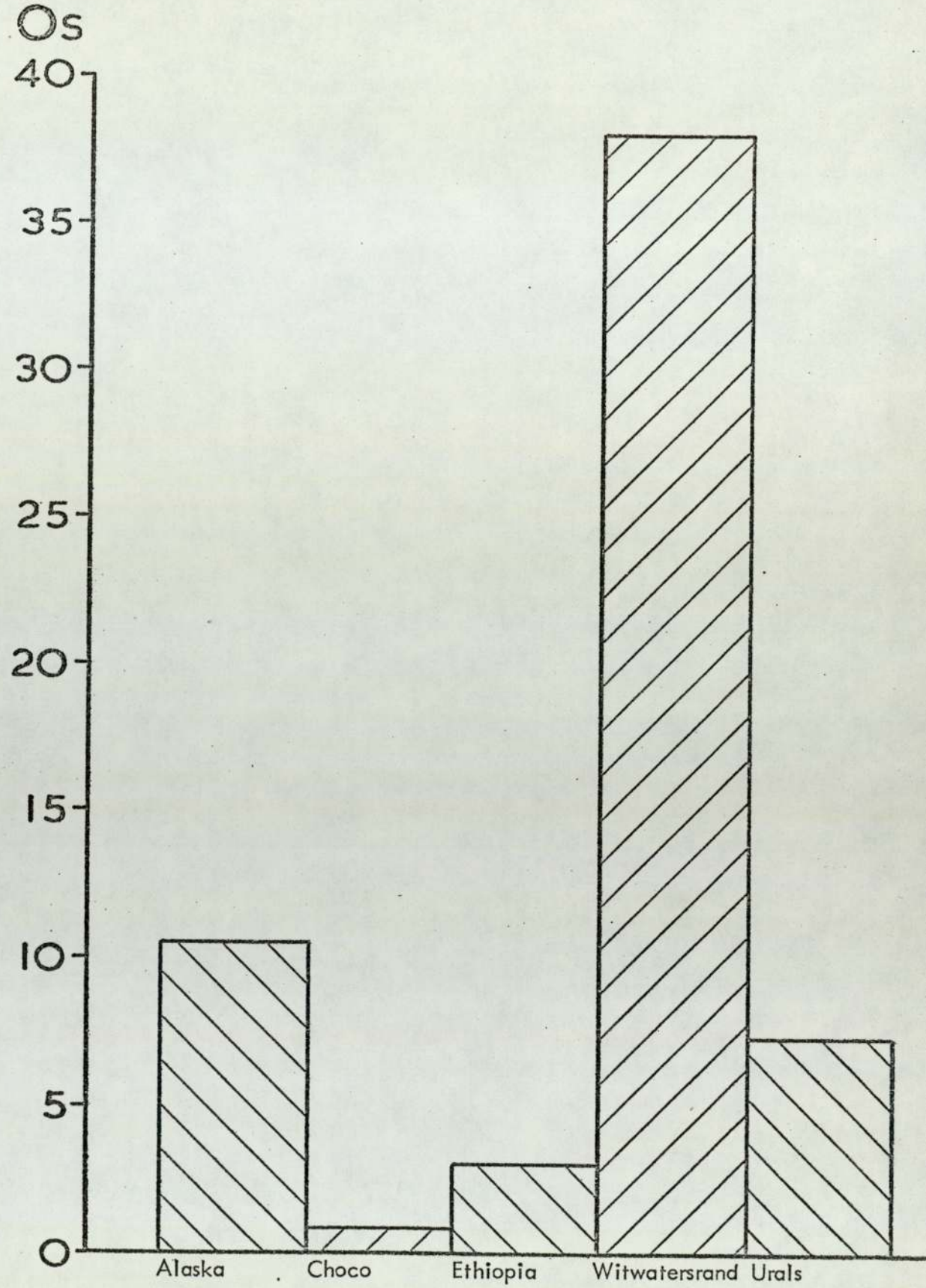

Histogram showing the average content of osmium, calculated from commercial bulk analyses, in the concentrates from the localities studied.

Fig. 7.5

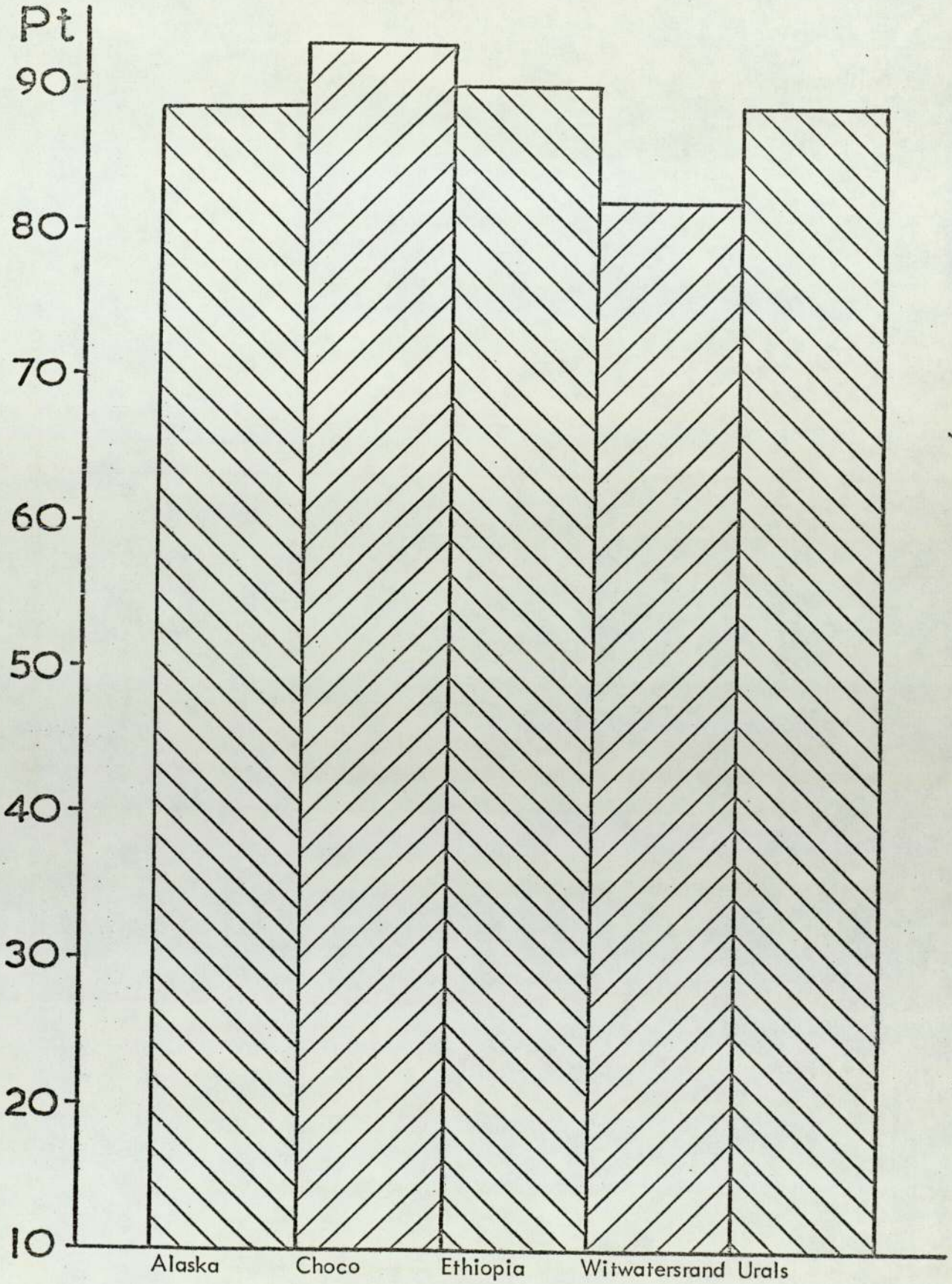

Histogram showing the average values of platinum content in the mineral analyses, determined by the electron-probe microanalyses from the different localities studied.

Fig. 7.6.

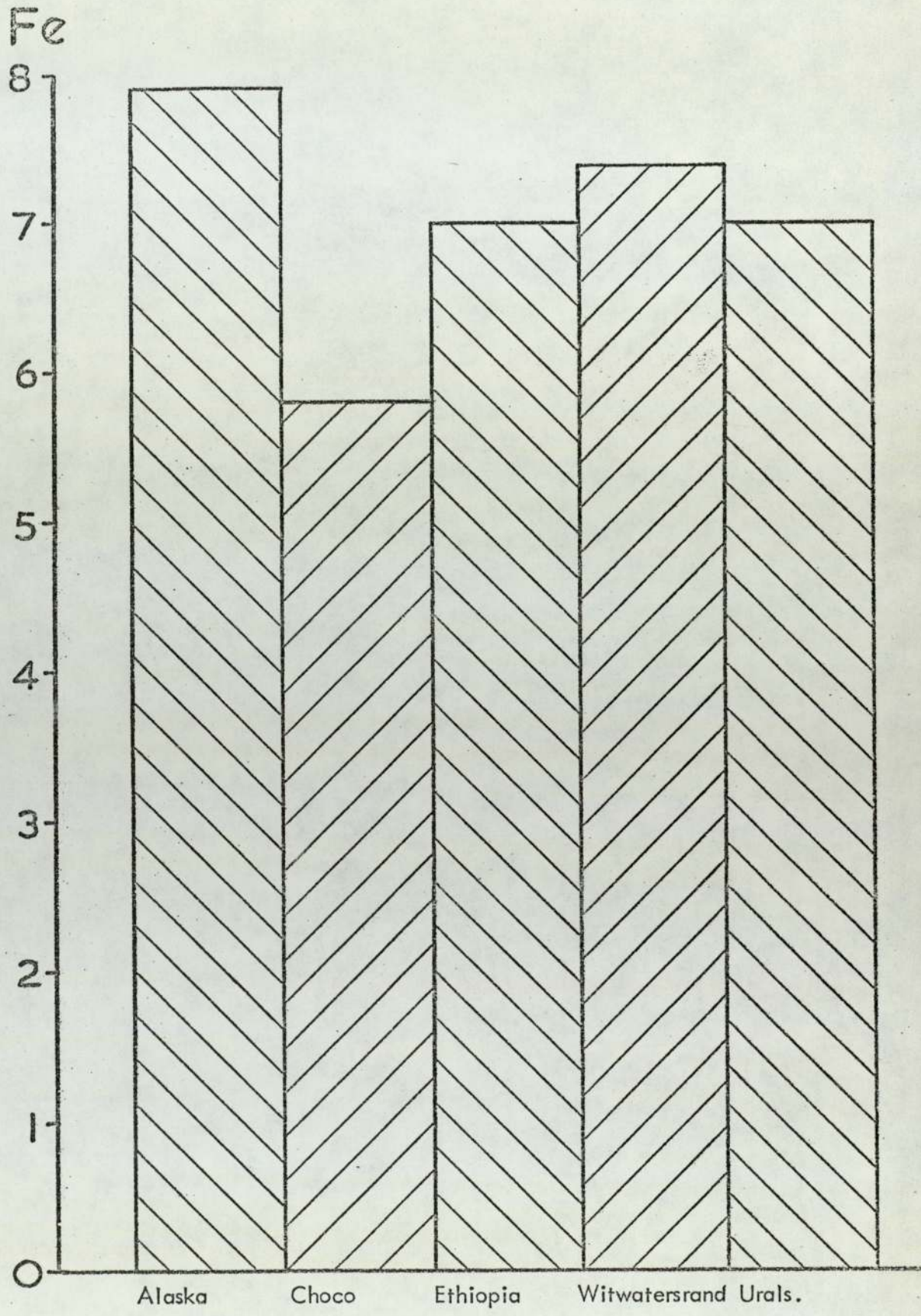

Histogram showing the average values of iron content in the mineral analyses, determined by the electron-probe microanalyser from the different localities studied.

Fig. 7.7

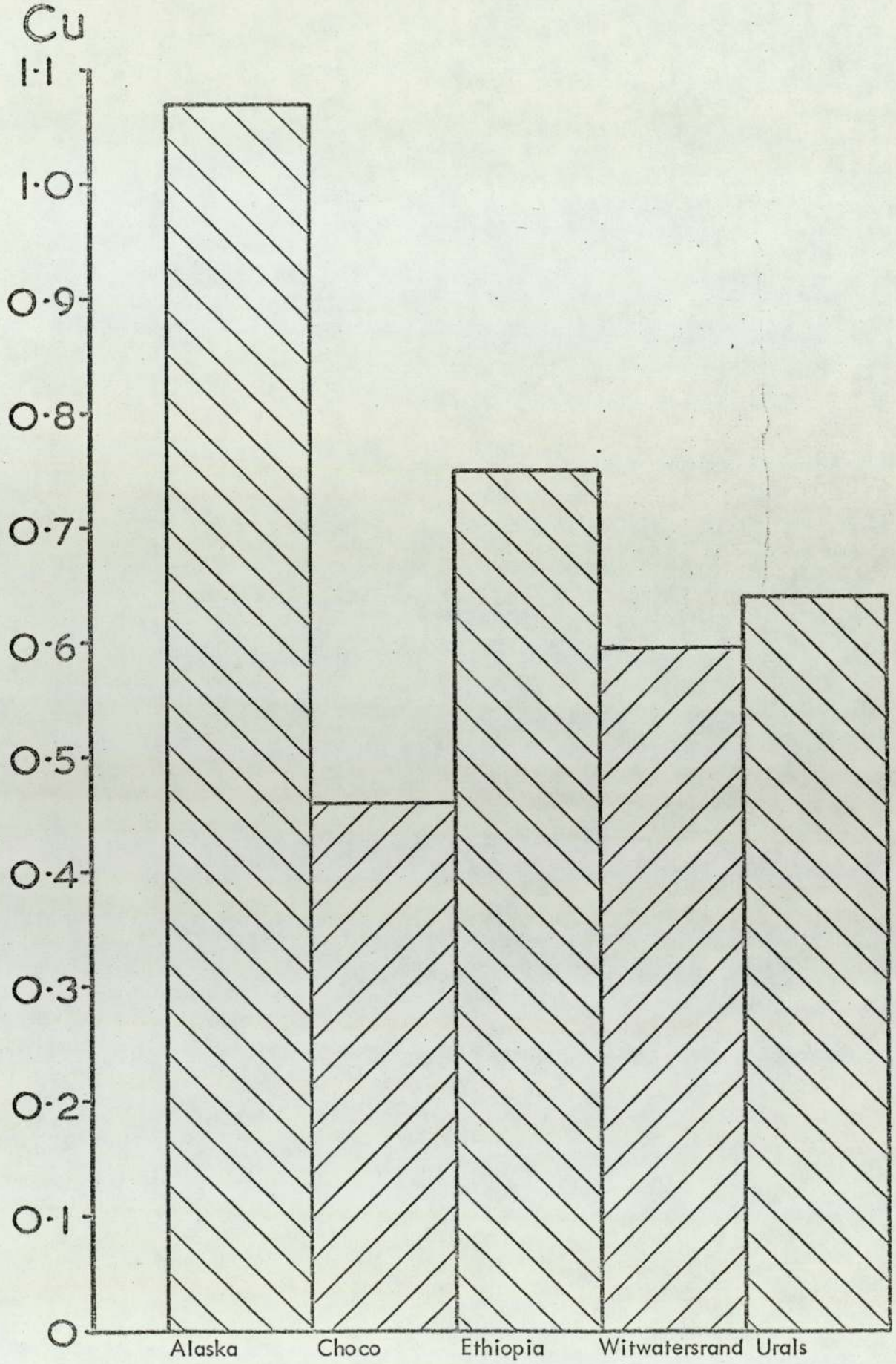

Histogram showing the average values of copper, content in the mineral analyses, determined by the electron-probe microanalyser from the different localities studied.

Fig. 7.8

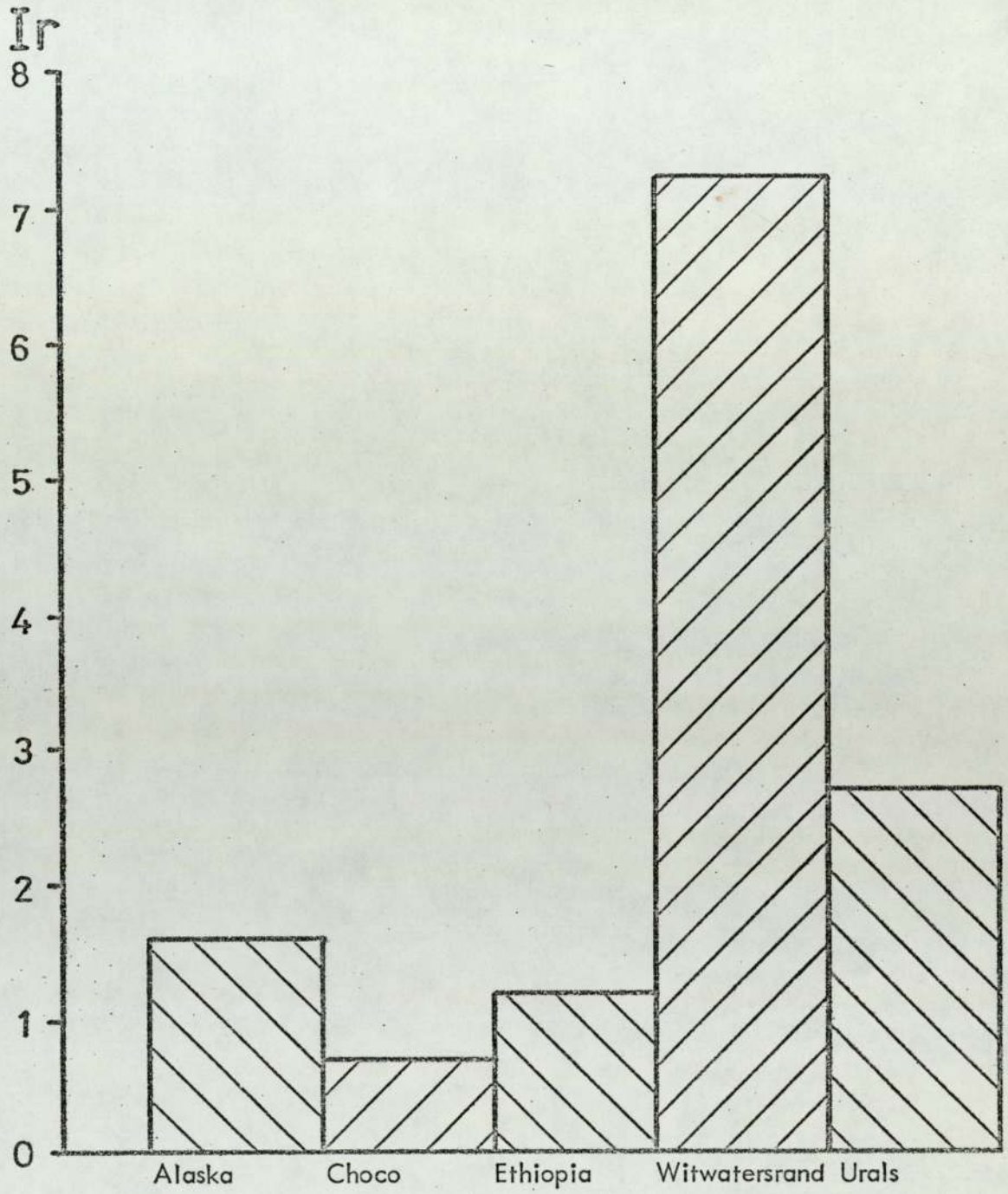

Histogram showing the average values of iridium, content in the mineral analyses, determined by the electron-probe microanalyser from the different localities studied.

Fig. 7.9

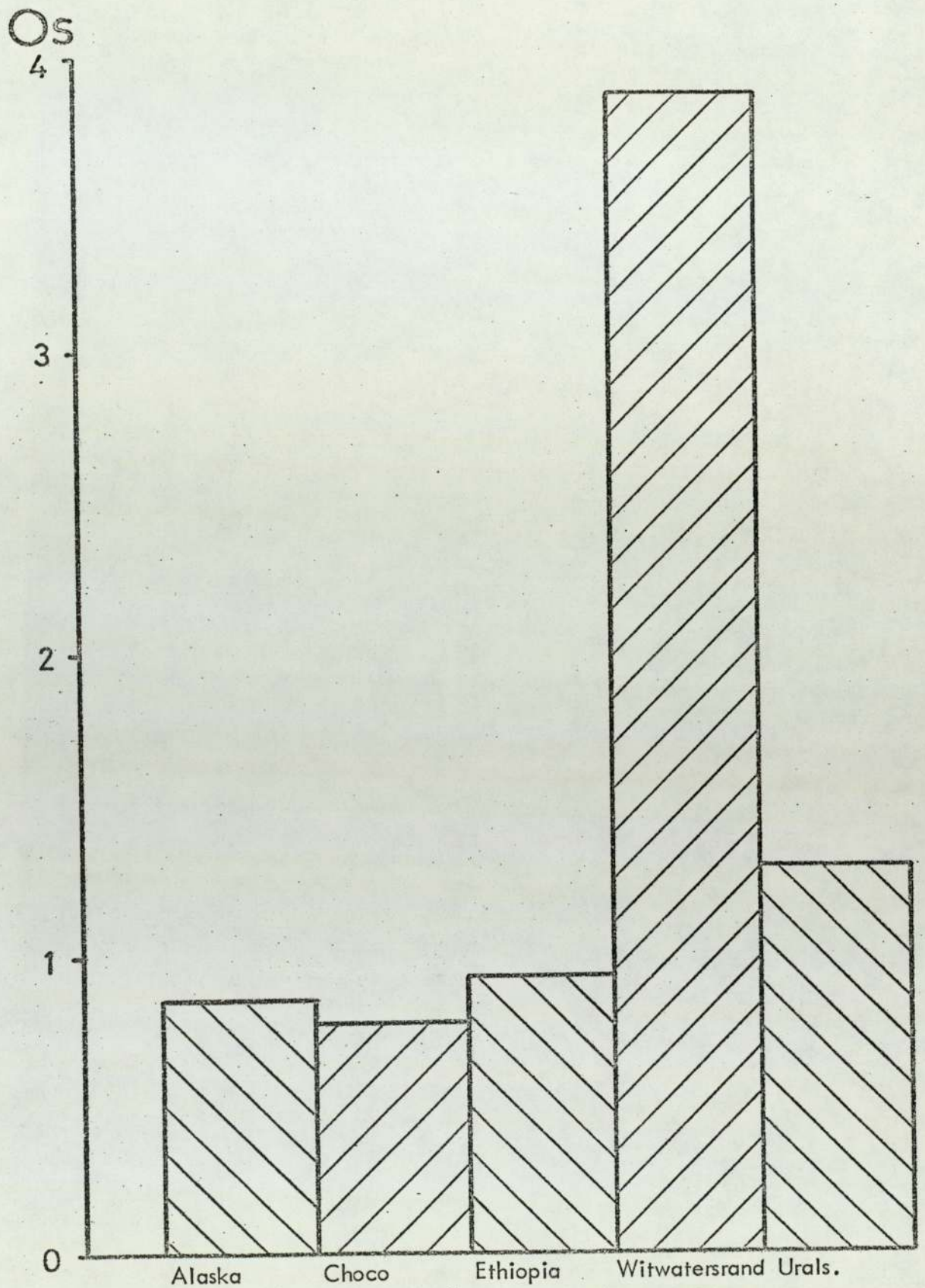

Histogram showing the average values of osmium, content in the mineral analyses, determined by the electron-probe microanalyser, from the localities studied.

Fig. 7.10

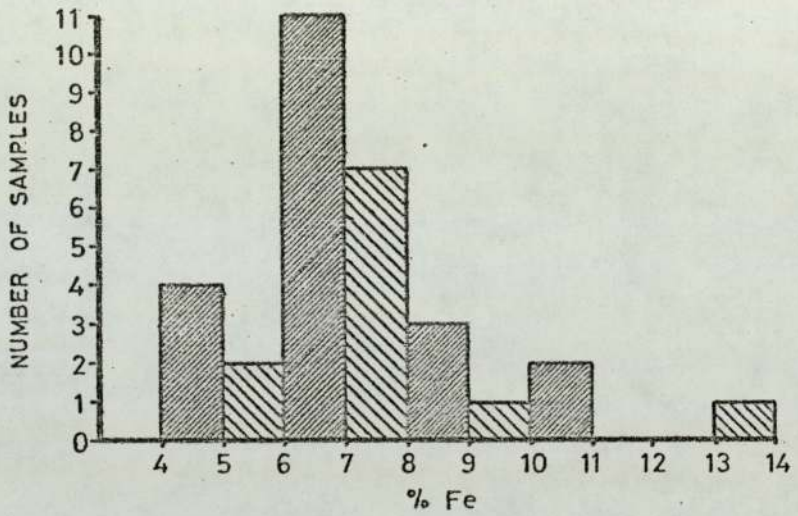

Fig. 7.12.

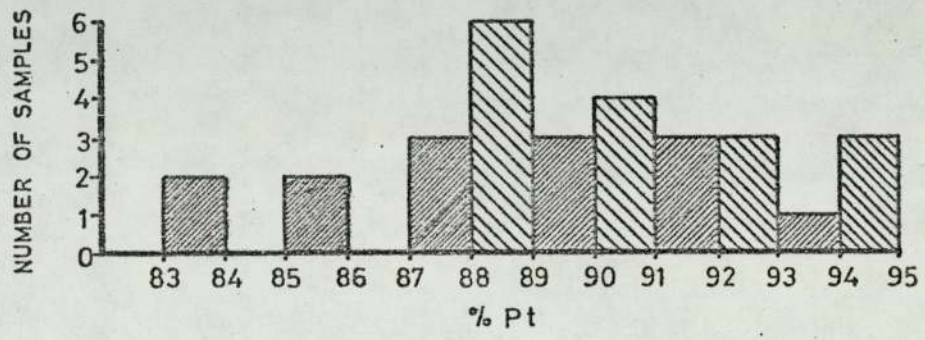

Fig. 7.11

Frequency distributions of platinum (7.11) and iron (7.12) in grains analysed by electron-probe microanalyser.

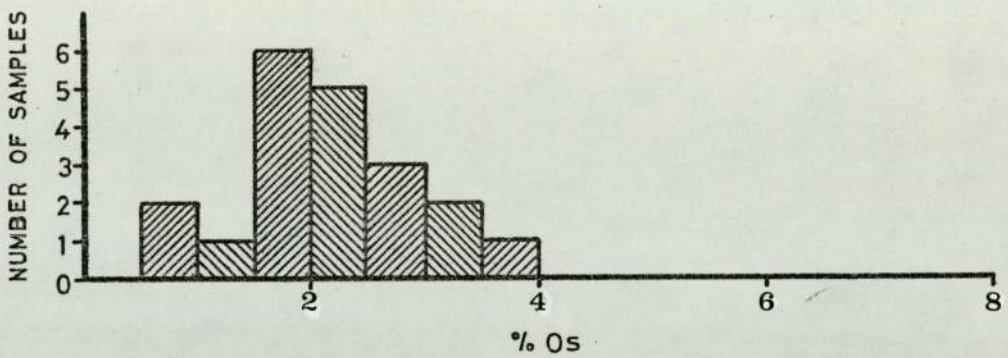

Fig. 7.13

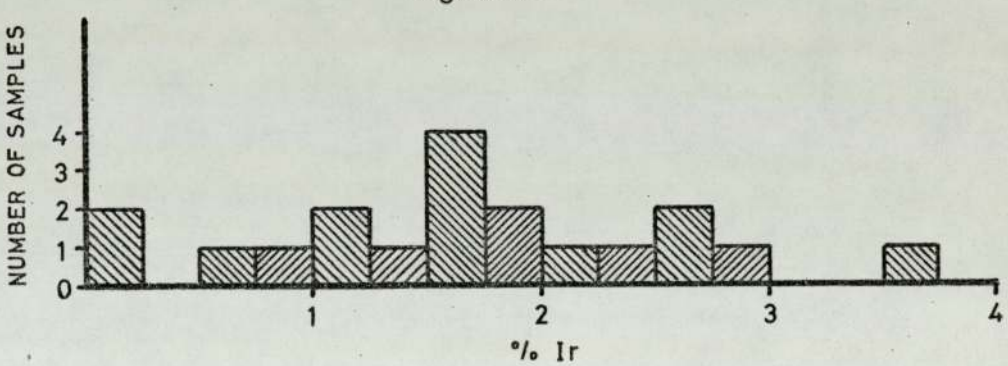

Fig. 7.14

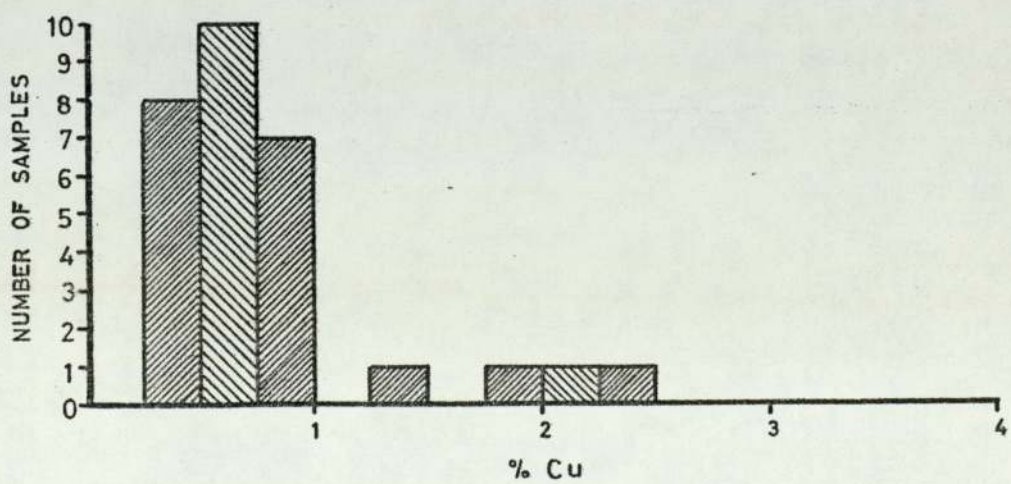

Fig. 7.15

Frequency distributions of osmium (7.13) iridium (7.14) and copper (7.15) in grains analysed by electron-probe microanalyser.

CHAPTER 8.

SYNTHETIC BINARY ALLOYS OF IRON AND PLATINUM.

Synthetic alloys were made up to allow a reliable correlation to be made between the optical properties and the composition of naturally occurring ferroplatinum alloys. A number of binary synthetic alloys of iron and platinum, prepared by Johnson, Matthey & Co. Ltd, were used. The chemical compositions of these alloy standards were as follows:-

90: 10 80: 20 70: 30 50: 50 platinum to iron.

These alloys were mounted in conducting bakelite and care was taken in the polishing to produce a perfect, flat, scratch-free surface. The synthetic alloys were analysed by the electron microprobe, using pure platinum and pure iron as standards. The count ratio obtained was plotted against the concentration ratio after correcting for the background (Fig. 8.1). This way of representation allowed the establishment of a correction procedure for natural platinum-iron alloys.

Measurements of reflectivity and microhardness were made on these alloys. The results of these measurements are tabulated with the microprobe analysis in Table 8.1.

Specimen	Prepared Composition		Microprobe Composition		Reflectance at 589.	Microhardness (VHN 100)	At % Fe.
	Pt.	Fe.	Pt.	Fe.			
1.	90	10	88.6	8.8	66.0	417	27.96
2.	80	20	76.3	17.9	60.5	563	46.6
3.	70	30	63.5	27.6	56.7	574	59.95
4.	50	50	40.4	49.0	54.0	412	77.75

(Table 8.1)

Analysis of Synthetic alloys of platinum and iron and their reflectance and microhardness.

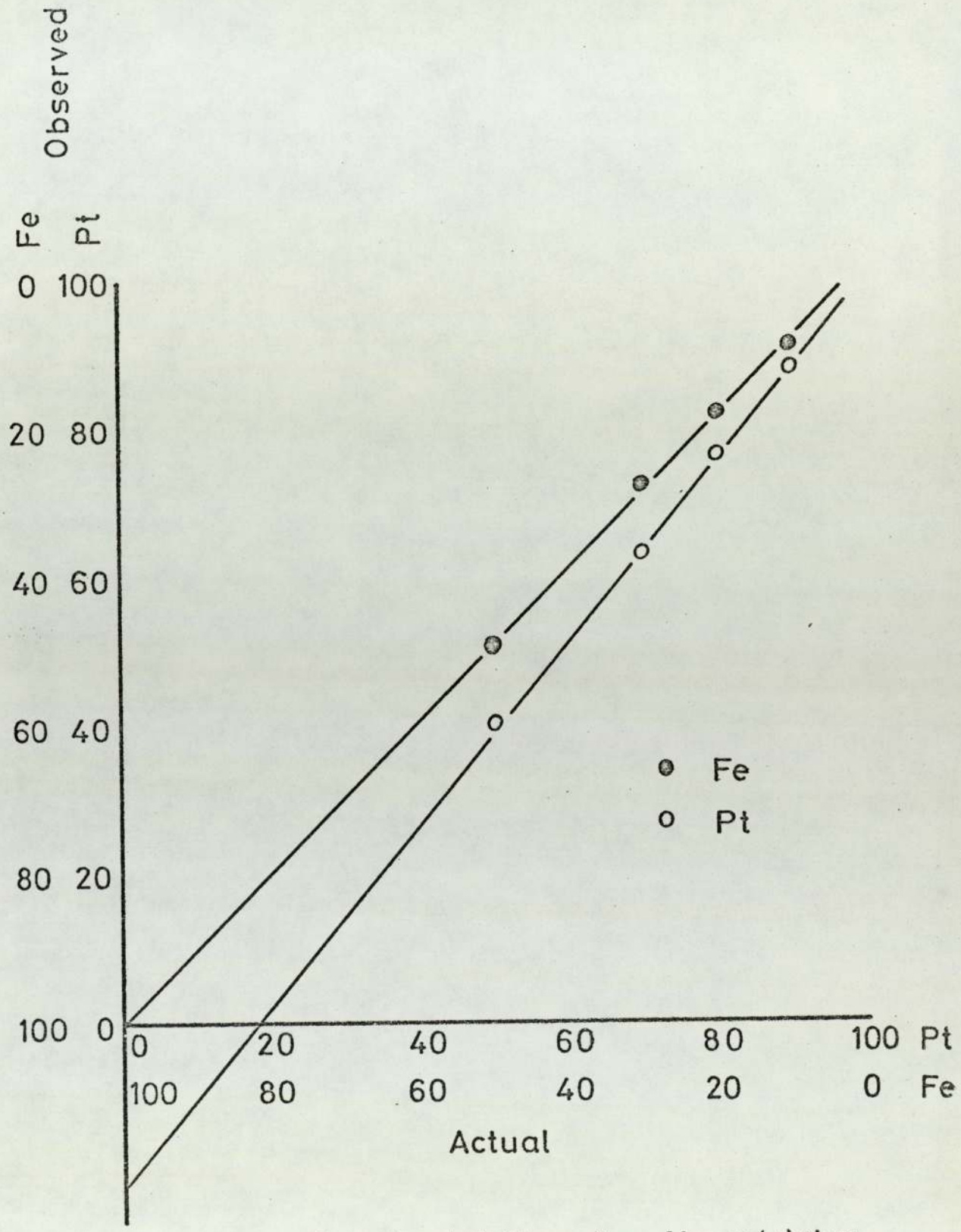

Micro-probe analyses of synthetic binary alloys of iron and platinum.

Fig. 8.1

CHAPTER 9.

REFLECTIVITY MEASUREMENTS OF FERROPLATINUM

9.1 REFLECTIVITY MEASUREMENTS OF NATURALLY OCCURRING FERROPLATINUM.

Quantitative measurements of reflectance at wave length 589 nm were made on more than 200 ferroplatinum grains and areas, 30 of them analysed by the microprobe. The results of the analysed grains are tabulated with the electron probe microanalysis results, Tables 2.1 3.1, 4.1, 5.1 and 6.1. It is noticed that the reflectivity decreases with increase in dissolved iron content of the ferroplatinum alloys. A wide range of reflectance was obtained during this study. Table 9.1 shows the range of reflectance obtained during this study and those results found in the literature.

9.2 REFLECTIVITY MEASUREMENTS OF BINARY SYNTHETIC IRON-PLATINUM ALLOYS.

Measurements of reflectance were made on the binary synthetic alloys of iron and platinum. The results of these measurements are tabulated in Table 8.1 It is found that the synthetic alloys show a linear variation of reflectance with iron content. This is illustrated in Fig. 9.1.

9.3 RELATION BETWEEN REFLECTANCE AND CHEMICAL COMPOSITION OF FERROPLATINUM.

All naturally occurring alloys of platinum contain dissolved iron, copper, and iridium which affect the reflectance of the ferroplatinum. The frequency distributions of these elements are shown in Fig. 7.11 to Fig. 7.15.

Table 9.1 shows the range of reflectance obtained in this study and those in the literature. The synthetic iron-platinum alloys show a linear variation of reflectance with iron content. The reflectivity of ferroplatinum decreases with increase of iron (Fig. 9.1.). Dissolved solute, especially iridium, has a large effect on the reflectivity values of naturally occurring ferroplatinum grains. Variations due to changes in the concentration of solutes others than iron, especially iridium, frequently outweigh the effect of iron. Fig. 7.14 shows a wide range of iridium content in a number of ferroplatinum grains, compared to a narrow range of osmium, and copper. This wide range causes the irregular variation of reflectance of ferroplatinum with iron content.

For this reason the correlation of reflectance with iron content shows no significant trend.

R% at 589 nm	Remarks
57.5 - 73.1	A general range obtained in this study.
64.0 - 71.3	Grey and Millman (1960) .
73%	Uytenbogaart (1951) in yellow light.
70%	Ramdohr (1969) in yellow light.
70%	Uytenbogaart (1971).
67.3	White light handbook of Metals (1961).

(Table 9.1)

Reflectance of natural platinum and ferroplatinum alloys.

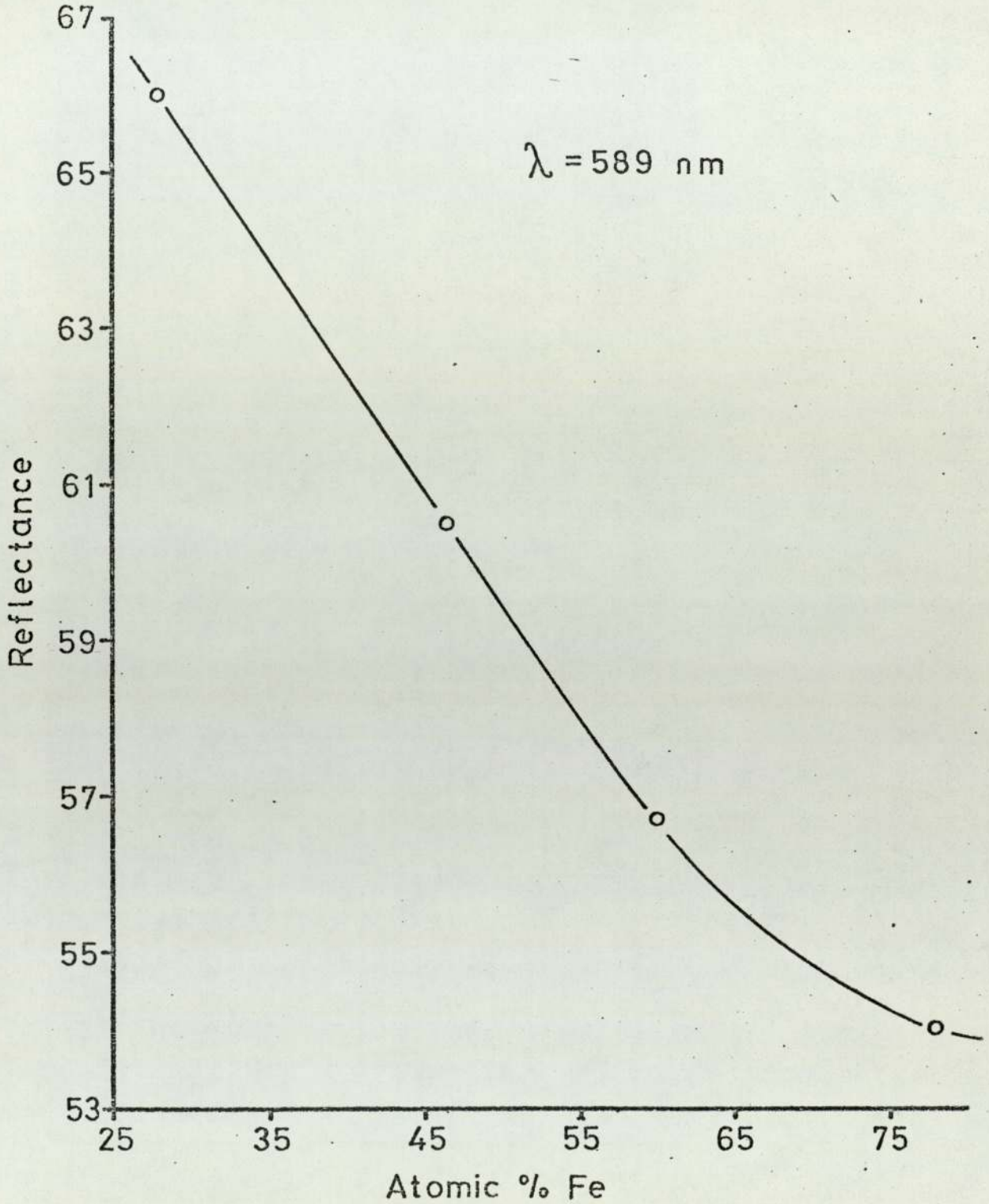

Variation of reflectance with iron content of synthetic binary iron-platinum alloys.

Fig. 9.1

CHAPTER 10.

THE MICROHARDNESS MEASUREMENTS OF FERROPLATINUM.

10.1 NATURALLY OCCURRING FERROPLATINUM ALLOYS.

Quantitative microhardness measurements were made on more than 200 naturally-occurring particles of ferroplatinum. The results are tabulated with the electron micro-probe results in Tables 2.1, 3.1, 4.1, 5.1 and 6.1. It is found that there is no clear relationship between microhardness and iron content of natural ferroplatinum, or indeed content of any element alone. This is shown by the Graph of Fig. 10.1, where the microhardness of natural ferroplatinum is plotted as a function of platinum content.

Also in Fig. 10.1, is a line showing the variation of microhardness with platinum content of iron-platinum synthetic alloys. This illustrates the trend to be expected in the natural alloys. The trend is present in the results, but a great deal of scatter is evident.

The range of values obtained during this study and results reported in the literature are included in Table 10.1. The behaviour of naturally occurring ferroplatinum alloys with regard to the relationship between iron-content and microhardness is unclear because of the many different impurity elements (Ir, Os, Cu, etc.), which affect the hardness of the ferroplatinum. Nevertheless, it is found that the microhardness increases with increasing iron content. The maximum iron-content for natural alloys obtained from the microprobe analyses is 13.6% Fe. Young and Millman (1963) observed the change of microhardness with Fe-content for naturally occurring ferroplatinum alloys, but did not give the compositions of the measured grains. Stumpfl and Tarkian (1973) found that VHN

increases with increasing Fe-content. Their results were confirmed by the results of Cabri (1973) on iron-bearing platinum from the Tulameen River area, British Columbia. The reported microhardness of naturally occurring alloys of iron-platinum show considerable variation. Uytenbogaardt and Burke (1971) quote Lebedeeva (1963) as giving VHN_{50} = 329-397 for polyxene (Pt with 6-11% Fe) and VHN = 114-274 for platinum.

They also state that "Fe-rich specimens show lowest hardness". Ramdohr (1969) provides a possible explanation for the widely varying VHN - values given by different authors. He remarks that platinum from placer deposits is significantly harder than commercially available platinum of identical composition. This is ascribed to "cold working" during transport in rivers.

It has been found during this study that the presence of Ir in naturally occurring platinum increases the hardness. These results agree with the result obtained by Nemilow (1932) on the synthetic Ir-Pt alloys that hardness of iridium-platinum alloys increases with increase of iriidum content to a maximum 50% Ir. There is insufficient data to assess the effect of Os content on the microhardness of Pt alloys.

10.2 SYNTHETIC BINARY IRON-PLATINUM ALLOYS.

Results of measurements of microhardness for the synthetic binary iron-platinum alloys are tabulated in Table 8.1. The synthetic binary iron-platinum alloys show an increase in hardness with the increase of iron content.

The variation of microhardness with iron content is shown in the diagram of Fig. 10.2. Maximum hardness occurs at approximately the composition of Fe Pt.

Interpretation of the hardness changes associated with the composition changes is complex, as the Fe - Pt system contains ordered phases based on Fe Pt_3 , Fe Pt and Fe_3 Pt. According to Crangle and Shaw (1962) Fe Pt_3 is cubic and extends over the range of 21-40 atomic % Fe. Fe Pt is tetragonal, the iron and platinum atoms occupying alternate 001 planes of a face centered tetragonal cell. The Fe Pt ordered phase extends from 36-62 atomic % Fe according to Vlausova and Sapozhkova (1970). The overlap of the reported Fe Pt_3 and Fe Pt phase fields indicates a discrepancy in the structural investigations of at least one of these workers, but does suggest that the Fe Pt_3 + Fe Pt phase field is small.

Neutron diffraction studies by Plaith, Kimball, Preston and Crangle (1969) have shown that as iron is added to platinum in the range of Fe Pt_3 to Fe Pt, the iron atoms replace the platinum atoms in particular structural positions, and result in a series of phases with different magnetic properties.

The ordered structures are shown in Fig. 10.3 . Finally another cubic phase based on Fe_3 Pt extends over the composition range from about 70-82. At% Fe (Vlasova and Sapozhkova (1970)). The Fe_3 Pt + Fe Pt phase field is narrow.

In such a system, where the ordered phases are separated by narrow, two-phase fields, the tendancy to order must not be very strong. It is probable that the anti-phase boundary produced by a moving dislocation will have a low energy. Pairing of dislocations is thus not expected to be strong and hardening will probably be due to the formation of an anti-phase boundary behind moving single dislocations, as in the case for Fe_3 Al (Flinn 1964).

The Goldschmidt atomic diameter of iron is 2.545 A° and that of platinum is 2.776 A° (Hume - Rothery 1956). The difference of 8.3% would suggest that the size effect would produce some hardening by the attraction of the iron atoms to the cores of the dislocations.

However, this could be in opposition to the ordering tendancy, which would at least restrict the number of energetically favourable sites to a relatively small proportion. Thus size effect hardening would probably be small. Since the valency of iron and platinum is the same, and the crystal structures are basically similar (face centered cubic), Suzuki locking and the shear modulus interaction would not be expected to contribute significantly to the hardening.

The major contribution to the variation of microhardness with composition therefore seems to be the ordering of iron and platinum atoms to produce the phases $Fe\ Pt_3$, Fe Pt and $Fe_3\ Pt$. The Fe Pt ordered alloy appears to exhibit the greatest microhardness.

MICROHARDNESS	REMARKS
VHN_{100} = 137.0 - 670	General range obtained in this study for natural alloys of platinum and ferroplatinum.
VHN_{50} = 423 - 655	
VHN_{100} = 412 - 574	Synthetic alloys of Fe pt Table 2.7 during this investigation.
VHN_{50} = 229 - 274	Young and Millman (1963)
VHN_{100} = 125 - 127	Young and Millman (1964)
VHN = 600	E.M. Wise (1948).
VHN_{50} = 329 - 397	Lebedeeva (1963)
VHN_{100} = 401 - 425	Stumpfl and Tarkian (1973) 54 grains 4-7% iron.
VHN_{100} = 503 - 572	Stumpfl and Tarkian. 68 grains 7-4% iron.
VHN_{50} = 553 - 588	Cabri & others (1973) 5 grains 10-83% Fe.
VHN_{50} = 580 - 633	Cabri (1973) 9 grains 11-99% Fe.

(Table 10.1)

Microhardness of platinum and ferroplatinum.

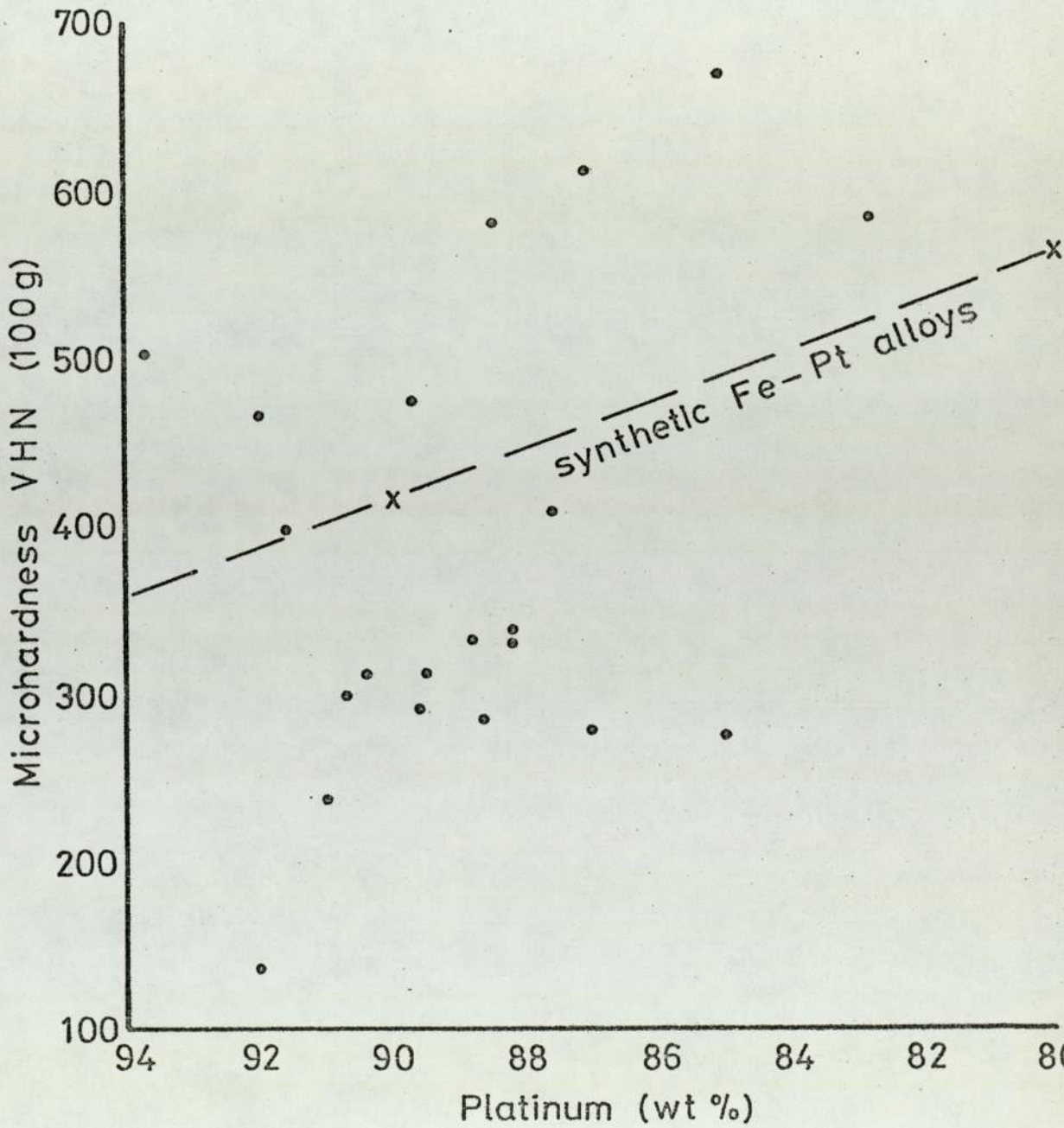

Variation of microhardness of naturally and synthetic alloys of platinum and iron, with platinum content.

Fig. 10.1

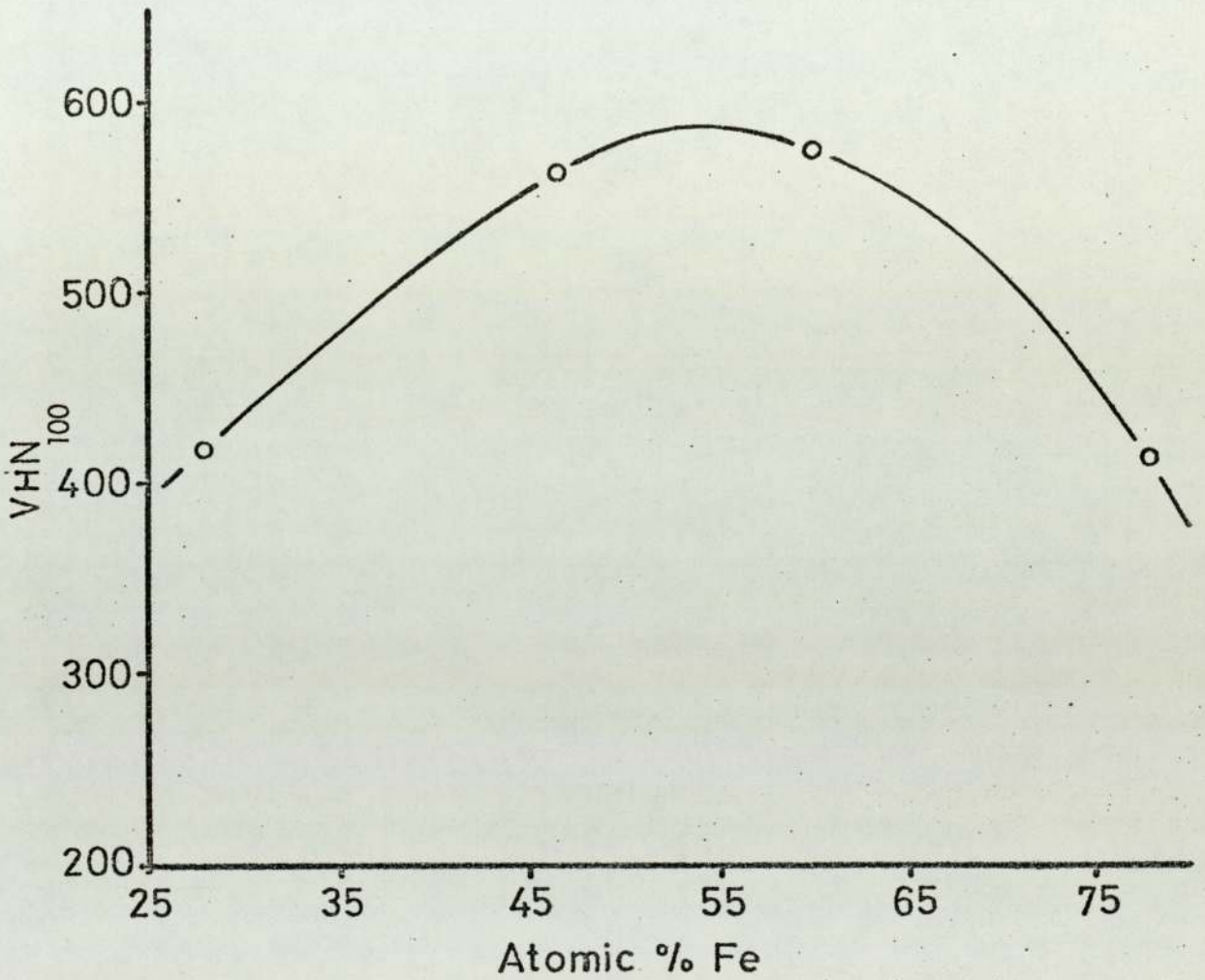

Variation of microhardness with iron content of the binary synthetic platinum-iron alloys.

Fig. 10.2

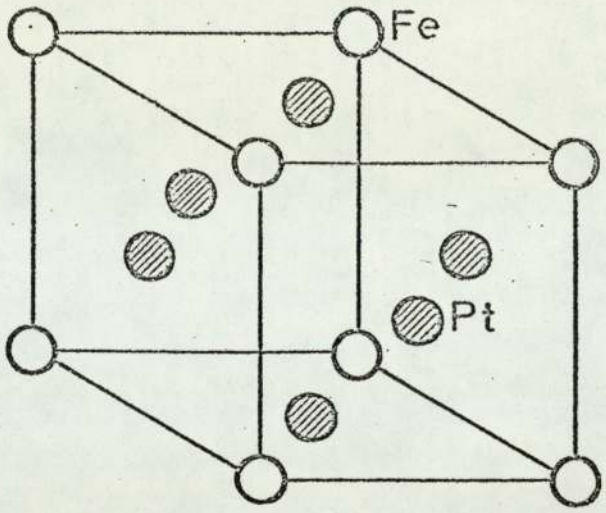

$FePt_3$
Cubic

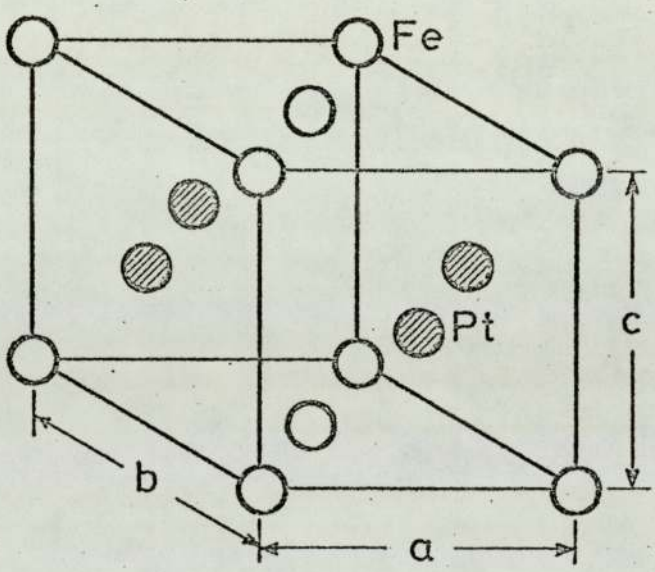

FePt
(Tetragonal)

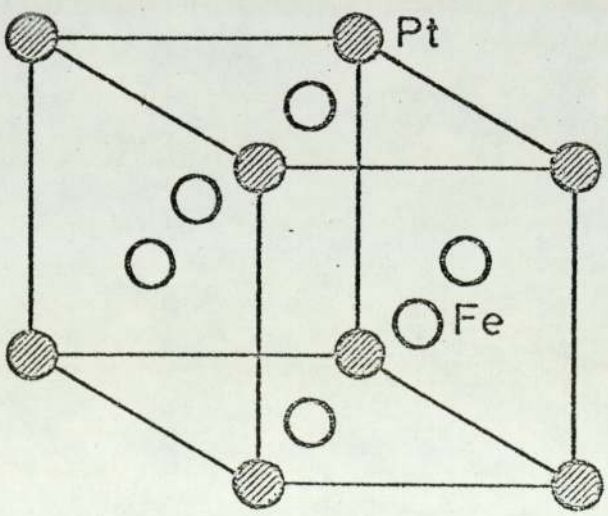

Fe_3Pt
Cubic

Fig. 10.3

Structure of ordered iron platinum phases.

CHAPTER 11.

NATURALLY OCCURRING IRIDIUM-OSMIUM-RUTHENIUM ALLOYS

11.1. MICROSCOPIC INVESTIGATION AND COMPOSITION.

Naturally occurring iridium and osmium alloys were first described by Wollaston (1805), as "ore of iridium" - although he knew that osmium was an important constituent. Subsequently they became generally known as osmiridium or iridosmine, the former being usually employed in the metal industry. Both alloy series, cubic and hexagonal have been differently named by various investigators. The composition of these alloys is very variable, and appreciable amounts of ruthenium, platinum and rhodium may also be present.

Svyaginter (1938 - 1943) studied natural iridium - osmium alloys and concluded that "alloys consisting of more than 32% Os have the close packed hexagonal structure of osmium, whereas those containing less than 32% osmium have the face-centred cubic structure of iridium". Analyses by Levry and Picot (1961) on material checked by X-ray diffraction show that the series covers nearly the entire composition range found in the iridium-osmium system, and they proposed that the name osmiridium be restricted to hexagonal (Ir Os) consisting of more than 50% Os. Hey (1963) suggested that the name osmiridium be used for cubic (Ir Os) alloys consisting of less than 32% Os, and iridosmine be used for hexagonal (Ir Os) alloys consisting of more than 32% Os . Hey's suggestion was based mainly on bulk chemical analyses of naturally occurring alloys given in the literature. Harris and Cabri (1973) summarised earlier work on natural alloys of Ir-Os-Ru and produced a paper on their nomenclature, which included electron-microprobe analyses of alloys from different localities.

In their diagram Fig. 11.1. they showed the Ir-Os-Ru composition diagram with the composition regions labelled according to their

nomenclature. No new names have been added to the names suggested in the literature, but their analytical results for naturally occurring Ir-Os-Ru alloys have allowed them to define more precisely the position of the miscibility gap in the Ir-Os-Ru system. Two 2-phase alloys near to the Ir-Os boundary allowed them to estimate this boundary with greater precision, but most of the analyses lie within the close packed hexagonal phase field, as pointed out by Cabri (1972) in his review of the mineralogy of the platinum minerals.

Stumpfl (1973) analysed a number of natural alloys from the Riam Kanan River area of Borneo. Most of the alloys lay near to the Os-Ir boundary in composition and a tendency for the alloy to have either a high Ru or high Pt content was noted.

Iridosmine, (hexagonal alloy phase), is a common mineral in alluvial deposits, and usually occurs as inclusions in the ferroplatinum matrix, and sometimes occurs as big laths or seperate grains (Fig. 3.2 and Fig. 5.2.) . In air, the colour of iridosmine is white with a bluish tint in some grains and creamy in others. In oil, the colour is much darker. The pleochroism of iridosmine is weak, but is more readily observed in oil. The anisotropy of the grains ranges from weak to distinct (orange-brownish-red). Optical properties of iridosmine vary with chemical composition (Fig.4.1.). Osmiridium,(cubic alloy phase), is less common than the hexagonal phase. It is the naturally occurring alloy of osmium and iridium in which iridium predominates. Osmiridium occurs in the alluvial deposits as small inclusions in the ferroplatinum matrix, or sometimes mantling iridosmine (Fig. 5.2.b). The colour of osmiridium in polished section is white (much whiter than iridosmine) with a very faint creamish tint. In oil it is slightly darker. It is isotropic and has higher reflectance and is much softer than the hexagonal iridosmine. The optical properties vary with chemical composition.

Electron microprobe analyses for naturally occurring alloys of iridium-osmium-ruthenium from the different localities studied are tabulated in Table 11.1.

In Alaska samples, iridosmine is found as hexagonal lamellae of different orientations included within a ferroplatinum matrix (c.f. Chapter 2). Some of these lamellae are very fine and are formed parallel to preferred crystallographic planes of the ferroplatinum. From the electron microprobe analyses, it was found that the Alaskan iridosmine is similar to the Choco material in chemical composition. The optical properties of iridosmine from these two localities were also very similar, although some iridosmine from Choco forms irregular shapes enclosed in the ferroplatinum (Fig. 3.1.).

Ethiopian iridosmine are strong anistropic (Fig. 4.1.) . The electron micro-probe analysis shows that the osmium content is very high comparing to other localities studied (60 to 70% osmium).

In placer deposits from Witwatersrand, iridosmine, is a major platinoid phase. Samples from Klerksdorp gold mine investigated in this study demonstrates this, and is confirmed by the bulk analyses which shows that the osmium content is higher than iridium. The analyses also show that the three major elements in the Witwatersrand samples are osmium, iridium and ruthenium. It is found as separate grains and not enclosed in ferroplatinum, unlike the samples from other localities. The grains are roughly spherical with a strongly anisotropic core indicating a high osmium and ruthenium content, surrounded by isotropic phase, and are low in osmium and rich in iridium and platinum. (c.f. Fig. 5.2. and 3.4.).

The Urals iridosmine is similar in shape from Choco and Alaska but differs in colour and exhibits weaker anistropy. Analyses show that they are higher in iridium than the Choco samples and consequently they are higher in reflectance and hardness.

Native iridium is a naturally occurring member of the iridium-osmium-ruthenium alloy group. It occurs as ex-solution bodies in ferroplatinum (Figs 11.2,3). In contrast to the ferroplatinum matrix it is isotropic. It exhibits higher reflectance and is harder

than ferroplatinum. The Urals samples are the concentrates which have the native iridium more than the other localities.

Electron micro-probe analyses for two grains from the Urals, together with reflectance and microhardness data are included in (Table 6.2.).

11.2 REFLECTIVITY MEASUREMENTS OF NATURALLY OCCURRING (Ir-Os-Ru) ALLOYS.

a. HEXAGONAL SERIES.

The reflectivity of randomly oriented grains from different localities was measured at 589 nm. The method used is described in Appendix 2. The main values obtained from various localities are shown in Table 11.2 and compared to other results quoted in the literature. It is interesting to note that the reflectivity increases with the increase of iridium content and decreases with the increase of osmium. This is in agreement with Stumpfl and Tarkian (1973). The variation of reflectance with chemical composition has been confirmed by the electron microprobe analyses for the measured grains which are included in Table 11.1. The reason for the reflectivity variation with chemical composition is far more complex and less well defined. It is associated with the free electron behaviour of the alloys. The presence of free electrons is characteristic of the type of bonding which is found in metals.

b. (Ir-Os-Ru) ALLOYS (cubic series).

The reflectivity values obtained from different osmiridium grains at a wave length 589 nm are included in Table 11.2 as are also those obtained by Stumpfl and Tarkian (1973).

11.3. MICROHARDNESS DATA FOR NATURALLY OCCURRING IRIDIUM-OSMIUM-RUTHENIUM ALLOYS.

a. IRIDOSMINE

The microhardness has been measured for grains from various localities. The method used is described in Appendix 3. Indentation marks are usually symmetrical and without fracture, but sometimes with a 50g load, one of the sides of the indentation is slightly deformed. The results obtained are given in Table 11.3 and compared with those in the literature.

b. OSMIRIDIUM

Microhardness measurements were made on different grains at 50 g. load; for the samples from the Witwatersrand, microhardness was measured at 50 and 100g. load. The indentation marks were well developed without fractures or cracks.

The hardness of the naturally occurring iridium-osmium-ruthenium alloys varies with chemical composition. It is found that the hexagonal series are higher in hardness than the cubic series. The variation in hardness will be explained in the synthetic alloys of iridium-osmium-ruthenium in Chapter 12.

Most grains used for measuring the reflectance and microhardness data were analysed by the electron probe. These analyses are included in Table 11.1.

No.	Os	Ir	Ru	Pt	Pd	Rh	Fe + Cu	Total	Locality
1.	55.5	35.0	-	8.8	-	-	.46	99.76	Choco
2.	65.4	16.6	9.7	8.0	-	-	-	99.7	Ethiopia
3.	41.9	16.5	18.16	23.3	-	-	-	99.86	Alaska
4.	25.5	13.97	2.8	19.3	2.6	34.9	.82	99.89	Alaska
5.	22.36	51.21	-	26.4	-	-	-	99.97	Chaco
6.	29.49	36.87	15.05	18.58	-	-	-	99.99	Witwatersrand
7.	18.76	42.5	16.9	23.0	-	-	-	101.15	Witwatersrand
8.	65.6	16.6	9.67	8.07	-	-	-	99.94	Ethiopia
9.	21.2	63.3	-	13.77	-	-	.1+.86	99.95	Urals
10.	41.9	16.57	18.16	23.34	-	-	-	99.97	Witwatersrand
11.	31.65	29.5	-	38.8	-	-	-	99.95	Witwatersrand
12.	25.5	13.96	2.8	19.34	2.6	34.89	.83	99.92	Witwatersrand
13.	5.09	14.9	33.2	15.78	1.23	-	29.77	99.97	Witwatersrand
14.	21.4	18.77	34.8	20.8	2.29	1.84	-	99.9	Witwatersrand

(Table 11.1).

Electron microprobe analyses for natural alloys of osmium-iridium-ruthenium and platinum from the localities studied.

LOCALITY	R% - 589	REMARKS
Ethiopia	56.5 - 58	Very high content of Os
Alaska and Choco	59 - 62	Samples have similar content of Os and Ru
Urals	61.9 - 64	Higher Ir and lower Os than Ethiopia, Choco and Alaska.
Witwatersrand	55.8 - 61.9	Wide range of chemical composition
	70.7 - 71.8	Isotropic - Osmiridium
	71.7	Levy and Picot (1961) at wave length 4722A° for 49% Os
	65.1	Cabri (1972) at wave length 583 nm.
S.E. Borneo	61.5 - 64.2	Stumpfl and Tarkian (1973) at wave length 583 nm.
S.E. Borneo	68 - 68.6	Stumpfl isotropic osmiridium.

(Table 11.2)

Reflectance of natural iridosmine and osmiridium alloys from the localities studied, and those in the literatures.

MICROHARDNESS	REMARKS
VHN_{50} = 794-976	Samples from Ethiopia.
VHN_{50} = 476-592	Samples from the Urals.
VHN_{50} = 587-683	Samples from Choco.
VHN_{50} = 571-583	Samples from Alaska.
VHN_{50} = 962-1038	Samples from the Witwatersrand.
VHN_{50} = 1505	Core of iridosmine surrounded by a mantel of osmiridium from the Witwatersrand.
VHN_{50} = 739-466	Osmiridium from Witwatersrand.
VHN_{100} = 514-464	Osmiridum from Witwatersrand.
VHN_{50} = 549-396 VHN_{100} = 572-297	Young and Millman (1963).
VHN_{100} = 762-946.	Stumpfl and Tarkian (1973) for samples from S.E. Borneo.

(Table 11.3)

Microhardness of natural alloys of iridosmine and osmiridium.

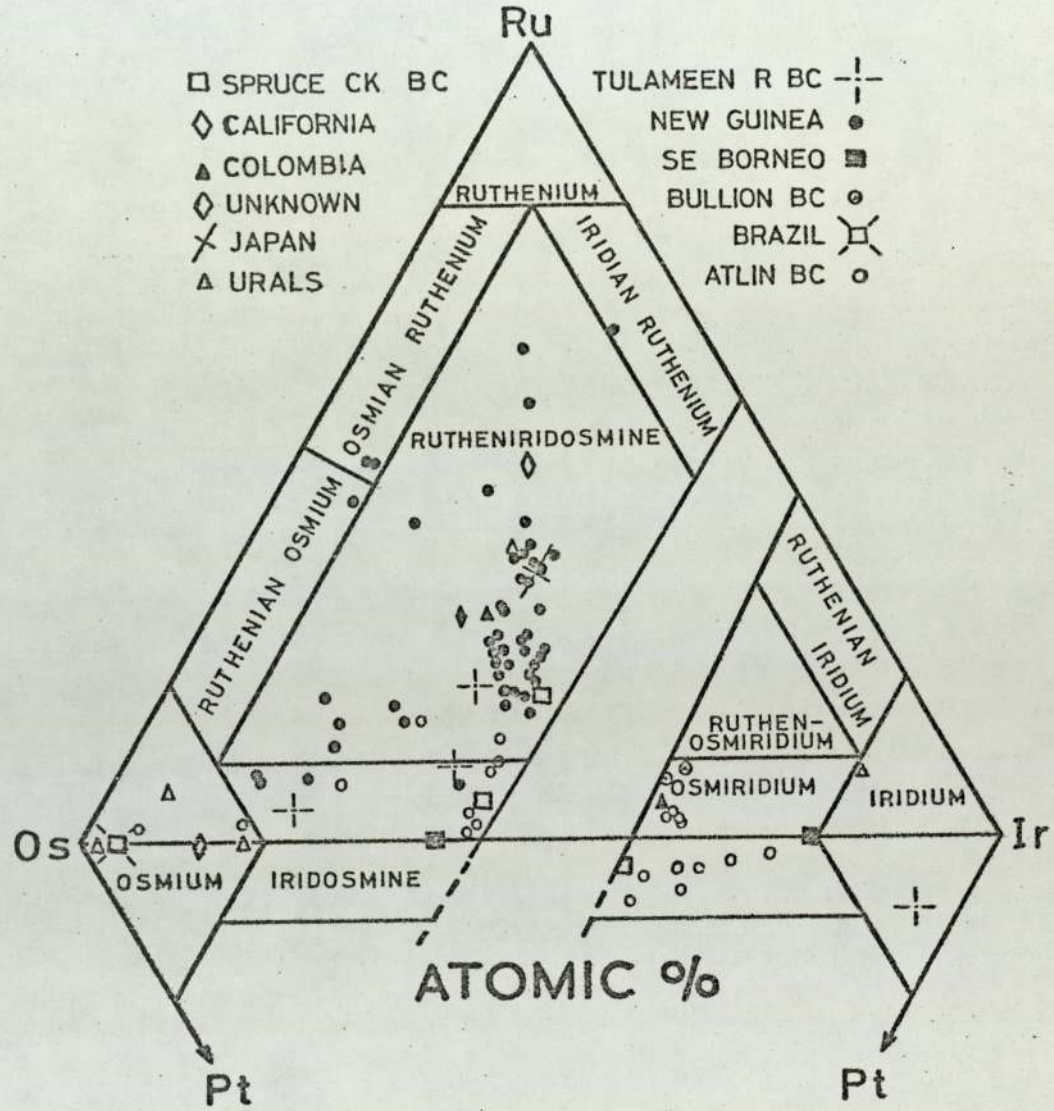

Composition diagram of naturally occurring iridium-osmium-ruthenium produced by Harris and Cabri (1973).

Fig. 11.1

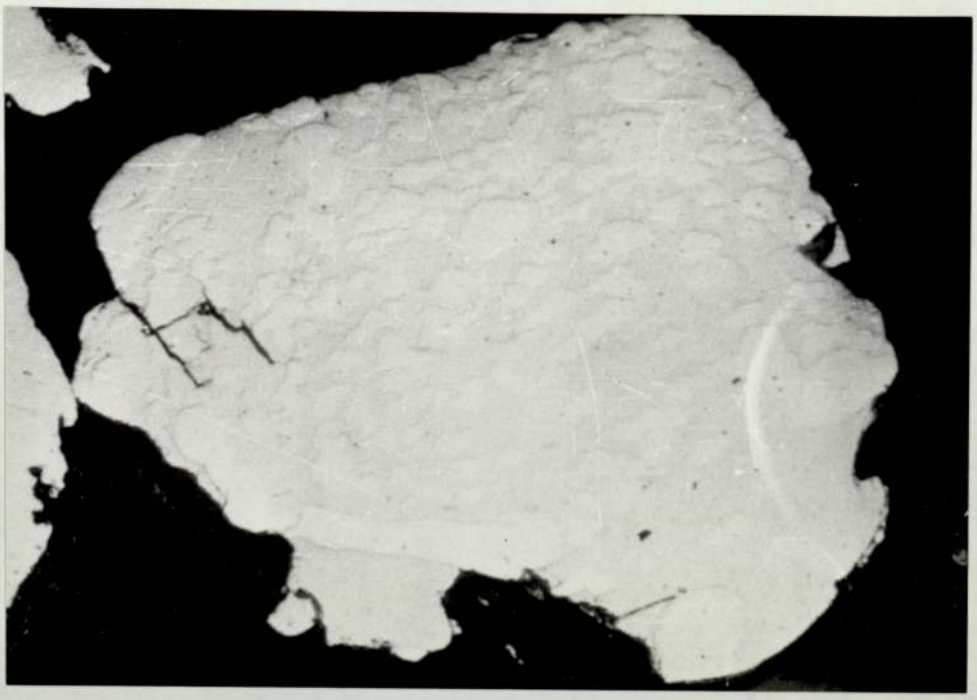

Fig. 11.2

Reflected light photomicrograph, showing ex-solved native iridium in the ferroplatinum matrix.

Locality : Choco.

Magnification X 560.

Fig. 11.3

Reflected light photomicrograph, showing small ex-solved bodies of native iridium in ferroplatinum matrix.

Locality : Urals.

Magnification X 480.

CHAPTER 12.

PHASE RELATION OF IRIDIUM-OSMIUM-RUTHENIUM ALLOYS.

12.1 BINARY PHASE DIAGRAMS.

The binary phase diagrams for osmium-ruthenium, iridium-osmium and iridium-ruthenium systems are shown in Fig. 12.1, 12,2. and 12.3 .

According to Raub (1959) osmium and ruthenium are isomorphous and are mutually soluble in all proportions below the solidus temperature. The formation of a miscibility gap in the solid state at lower temperatures was not observed, but the conditions are unfavourable for the observation of an exsolution process at lower temperatures.

The iridium-osmium phase diagram is less well established. However, it was found by Reiswig and Dickinson (1964) that a peritectic reaction occurs at 266 0 ∓ 35°C.

Liquid + c.p.h. solid solution (β) = f.c.c. solid solution (α).

The mutual solid solubilities of (Ir) and (Os) change very little with temperatures and they form nonequilibrium structures.

The iridium-ruthenium phase diagram is largely unknown, but it has been proposed by Raub (1959) (1964) that a peritectic reaction occurs between the liquid and the f.c.c. Ir-rich phases.

Liquid + f.c.c. solid solution (α) = c.p.h. solid solution (β)

The limits of the $\alpha + \beta$ phase field are partially known between 1000°C and 2000°C.

12.2. TERNARY PHASE DIAGRAM.

Only limited data on the phase relations in the osmium-iridium-ruthenium system are available.

Cabri (1972) summarised the literature on natural and synethic alloys of Os-Ir-Ru from which he proposed a diagram for the Os-Ir-Ru alloys which approximates to a solid-state isothermal reaction. Here a two phase field between hexagonal and cubic alloys is approximately defined (Fig. 12.5.). Subsequently Harris and Cabri (1973) introduced their paper on the naturally occurring alloys which included further analyses and a revised scheme of nomenclature for the alloys. The miscibility gap which was defined by Vacher, Bechtoldt and Maxwell (1954) in Os-Ir system and by Rudman (1967 , 1964) in the Ir-Ru system was therefore extended to the ternary system using analytical data mainly on natural samples. No synthetic study of the Os-Ir-Ru system has been previously attempted.

The object of this part of the investigation was to establish experimentally the limits of the two phase field running from the Os-Ir binary edge to the Ru-Ir binary edge. For this purpose a number of synthetic alloys were prepared from pure sponge osmium-iridium and ruthenium supplied by Johnson, Matthey and Co. Ltd. The method of preparation is described in the Appendix 4.

Since the synthetic alloys were prepared by fusion of a molten bead, which was rapidly cooled by contact with the water cooled base of the apparatus (Appendix 4), the phase relations are taken as applying to temperature conditions just below the solidus in the osmium-iridium-ruthenium system. The two phase field located in the study of natural ternary alloys was found experimentally by electron probe microanalysis during this study as shown in Fig. 12.6, at a temperature higher than 2000°C.

DISCUSSION OF THE Os-Ir-Ru PHASE DIAGRAM.

The boundaries of the two phase region in the Os-Ir-Ru system are

shown in Fig. 12.6. It appears that the width of the two phase region is much narrower than indicated by previous workers. This may in part be due to the higher temperature used or due to the electron beam spot overlapping a second phase during microanalysis of the two phase alloys, which would tend to contract the tie-line joining the compositions of the separate phases. However, the analyses indicated are themselves thought to be reasonably accurate, as is shown by the good correspondence between the prepared compositions of the alloys and those determined by microprobe analysis (Table 12.1). In the case of the two-phase ternary alloys (alloys composed of Ir-Os-Ru), it was found that the mean composition of the alloy lay on the tie-line joining the individual compositions of the two phases, thus confirming the accuracy of the phase analyses.

Outside limits of the width of the two phase region are set by the alloys which were found by optical microscopy and X-ray structural analysis to be single phase. However, it is considered that overlap could only produce a slight contraction of the tie-line in the case of the two-phase alloys as irradiated volume was kept as small as possible by the use of low operating potential and a small beam current (15 KV, 50 nA). Thus it is most probable that the narrow $\alpha + \beta$ phase field is a real effect and not a function of the analytical method. The slope of the tie-lines increases across the $\alpha + \beta$ phase field as the ruthenium content of the alloys is increased. This effect, although strange at first sight, is readily explained in terms of the cooling process.

It should be noted that a true ternary equilibrium reaction cannot be determined exactly from the data as no attempt was made to achieve isothermal equilibrium. The exact form of the ternary equilibrium diagram is not known, but one may presume that the inflection in the liquidus surface at the liquidus peritectic temperature on the Os-Ir binary edge must swing over and descend towards that on the Ru-Ir edge, if the latter binary phase diagram is correct. There is a

possibility that the inflection line moves into the diagram from the Ru-Ir edge, with decreasing temperatures, resulting in a ternary peritectic reaction. However, the simplest case is that the inflection in the liquidus surface moves steadily with decreasing temperature from the Os-Ir edge down to the Ru-Ir edge. The freezing of alloys which are two phase at low temperature will be completed by movement of the $L + \alpha + \beta$ phase field across their composition point. These phase triangles are shown in the diagram of Fig. 12.7. This mechanism predicts that the $\alpha + \beta$ tie-line will slant across the phase field in the manner observed but that a reversal of the trend must occur as the three phase triangle approaches the Ru-Ir edge. Finally, the tie line must be parallel to the binary edge. Inspection of the diagram of Fig. 12.7 shows that the slant of the tie-line of alloy 14 is somewhat less than that of alloy 15 which is in accordance with the predicted shift. The positions of the tie-lines are those imposed by the freezing process and are not necessarily the same as those in an alloy which has been equilibrated at some temperature below the freezing point. The experimentally observed slant in the tie-lines of the two phase field provides strong evidence that the suggested Ir-Ru phase diagram is essentially correct, in that the peritectic liquid composition lies on the Ru-rich side of the solid-phase compositions.

On the basis of the results obtained in this study and the data available from the binary phase diagram, it was possible to construct sections through the ternary phase diagram which show the probable mechanism of solidification of ternary alloys not too near the Ru-Ir binary edge. These sections are shown in the diagrams of Fig. 12.8, 9, 10, 11 and 12.

At 2,800° C (Fig. 12.8), solidification has started by the separation of an Os-rich alloy from the liquid. At 2,660°C (Fig. 12.9), which

is the peritectic temperature of pure Ir-Os alloys, liquid containing 27% Os is reacting with solid β containing 62% Os (B) to produce the solid αα phase of composition 45% Os (A).

In (Fig 12.10), the result of this peritectic reaction is the formation of a triangular phase field on the ternary section in which three phases of composition A, B, and S derived from the line BAS on the binary edge are in equilibrium. Assuming that the Ru-Ir diagram is correct, S must follow the curved path shown as a dotted line on Fig. 12.10, from the binary Os-Ir edge to the Ru-Ir edge as cooling proceeds. Experimentally, the tie-line AB has a pronounced tilt relative to the β-Ir line and is shown this way on the isothermal section. This is consistent with rapid movement of S towards the Ru-rich end of the Ru-Ir binary edge, but is not a requirement of this mechanism. At a later stage in freezing (Fig. 12.11), AB is more nearly parallel to BS, exact parallelism (and superposition) occurring when the peritectic point on the binary Ru-Ir edge is reached at 2,300° C, (Fig. 12.12).

A and B define the composition of the αα and β phases at a particular temperature at the instant of freezing. Subsequently, at a lower temperature, the compositions of the αα and β phases in equilibrium may change. In this work, equilibrium was not achieved and it is probable that the tie-lines define the compositions represented by A and B at the freezing point of the alloy. A slanted tie-line is not necessary for the mechanism of freezing suggested above. It is however, consistent with it. Furthermore, a slanted tie-line would be difficult to explain by any other mechanism except that brought about by the presence of a liquidus surface which slopes from osmium to iridium on one binary edge and from iridium to ruthenium on the other.

12.3 X-RAY STUDIES OF SYNTHETIC Ir-Os-Ru ALLOYS.

The X-ray results are collected in Table 12.1 The volume-per-atom is a convenient measure of the lattice parameter changes produced by alloying and allows a direct comparison of the f.c.c. and c.p.h. structures. This volume-per-atom (or specific volume) was calculated from the measured lattice parameters (Fig.12.12) and is included in Table 12.1 The specific volumes of pure osmium ruthenium and iridium were calculated from the unit cell dimensions given in the ASTM Powder Index File and are shown together with the data from this work in Fig.12.13.

CLOSE PACKED HEXAGONAL PHASE.

From Fig.12.14 it appears that the volume changes produced by substituting osmium atoms for ruthenium atoms are as would be expected from the different atomic sizes. The Goldschmidt Atomic diameters Co-ordination No.12 for osmium and ruthenium are 2-71A° and 2.68A° respectively (Hume-Rothery and Raynor 1956). The volume change brought about by completely substituting osmium for ruthenium would be 3.39%. The actual change from the pure element lattice parameters is 3.02%. This agreement is good considering the uncertainties in the values of the atomic diameters. No experimental data were available for the binary osmium-ruthenium system but the data for alloys on the close-packed hexagonal side of the two phase field with an approximately constant iridium content of about 40% can be used to indicate the effect of replacing osmium by ruthenium. The result is shown in the lower line of Fig.12.15. Within the experimental scatter a small linear decrease in specific volume is shown. Extrapolation of this line to 60% ruthenium (i.e. the composition on the binary edge (Ru-Ir) gives a better estimate of the effect of adding iridium to ruthenium than is provided by the single data point of alloy 16 on Fig.12.13. From the atomic diameters of the pure

the atomic diameters of the pure elements, the specific volume at 40% iridium should be 13.75A^{o3}/atom, where as that derived from Fig. 12.15 is approximately 13.84A^{o3}/ atom . This result shows that the cell volumes of ruthenium-iridium alloys are largely determined by atomic diameter but that some second order effects dilate the lattice a little. The iridium atom (Goldschmidts Atomic Diameter 2.714A^{o}) is only fractionally larger than the osmium atom so the specific volumes of osmium-iridium alloys ought to be similar. From Fig. 12.13, it appears that this is the case for both the close packed hexagonal and face centred cubic phases. Actually, the c.p.h. phase of alloy 1 appears to be slightly smaller than pure osmium, but this may be a calibration effect rather than a real one as the cell dimensions of pure osmium were taken from the literature, not measured. Certainly there is no significant difference in specific volume between the c.p.h. and f.c.c. phases of the binary alloys 1 and 2, which are similar in composition.

The above evidence suggests that the specific volume of the c.p.h. phase in the iridium-osmium-ruthenium system is determined largely by the atomic diameters of the atoms concerned.

FACE-CENTRED CUBIC PHASE.

The specific volume of iridium-osmium-ruthenium alloys containing an approximately constant iridium content of about 50% were calculated from the data of Table 12.1. and the result is shown in the upper line of Fig. 12.15 . The coincidence of this line with that of the c.p.h. phase at 40% iridium and zero ruthenium emphasises the fact that osmium has little or no effect on the specific volume of either f.c.c. or c.p.h phases. However, contrary to expectation, the specific volume of the f.c.c. phase is greatly increased by the substitution of the smaller ruthenium atom for osmium. The effect is approximately a linear function of ruthenium content, and must be due in some way to the second nearest-neighbour effects which determine which of the two close-packed structures is actually adopted. Since ruthenium is monovalent and osmium

and iridium are divalent then the effect may be a result of a tendancy to directed bonding.

Since the two lines of Fig.12.15 diverge, it is inferred that in the case of binary ruthenium-iridium alloys, there is a large change in specific volume across the two phase field. The sharp increase in volume which must take place when ruthenium is substituted for iridium in the f.c.c. lattice suggests that the free energy of the f.c.c. lattice is increased to a greater extent by the addition of ruthenium than by osmium. However, extensive solid solubility of both osmium and ruthenium in iridium is shown by Fig.12.15 and hence this effect is of minor importance.

12.4 MICROHARDNESS STUDY OF SYNTHETIC OSMIUM-IRIDIUM-RUTHENIUM ALLOYS.

The microhardness data are shown in graphical form in Fig.12.16. Data on the microhardness variations in the binary systems are only available for osmium-iridium alloys. For the single phase alloys, the microhardness is a linear function of osmium content (Fig.12.17). The 50% and 53% osmium alloys are two-phase and give no useful information on the hardening effect of dissolved osmium. Fig.12.18, shows the variation in microhardness of a series of osmium-iridium-ruthenium alloys at two approximately constant iridium contents. One at 40% iridium lies in the c.p.h phase field. The other at 50% iridium lies in the f.c.c. field. Both curves show maximum at 20% ruthenium. Such a maximum in hardness versus composition curves is a common phenomenon in many alloy systems, for example Cu-Ni or Au-Ag.

The shape of such a hardness curve may be determined by the mechanisms by which solute atoms obstruct dislocation movement. There are many such mechanisms of which some may apply to the system iridium-osmium-ruthenium. Some important mechanisms are listed:-

a. Suzuki locking. This occurs in close packed structures which have a low stacking fault energy. Solute atoms are preferentially attracted to the stacking fault and thus pin the dislocations, increasing the yield-strength of the alloy. Suzuki, H. (1957)

b. Size-effect. If the radius of the solute atom differs from that of the solvent, the solute atom will be attracted to the dislocations and will pin them. Even if the dislocation is freed from the solute, they exert a strong retarding force on it.

c. Modulus effect. A solute atom will locally change the elastic modulus of the matrix. This allows the solute to interact with the dislocations to slow down their movements.

d. Local ordering. If there is a tendency to short-range order, the passage of a dislocation will upset that order across the slip-plane. This effect provides a retardation force to appose dislocation movement.

In the case of both close-packed hexagonal and face centred cubic phases, there is no data in the literature concerning the stacking-fault energy. However, the extensive solid solubility shown in the phase diagram demonstrates that the free energies of both c.p.h and f.c.c. structures are not too dissimilar and extensively dissociated dislocations may be formed, particularly in the region of the two-phase field, especially near the osmium-iridium edge where size effect and modulus effect are negligible. However, the hardness curves of Fig. 12. 18 are at a constant ratio of c.p.h. atoms to f.c.c. atoms, so these hardness changes are independent of Suzuki locking. Since the specific volume changes as shown in Fig. 12. 15 are small, it is unlikely that these large hardness changes are due to a size effect. However, modulus changes due to valency difference are known to have a large effect on hardness of an alloy, and since ruthenium is monovalent whereas osmium and iridium are divalent,

the large changes in hardness are probably due to the modulus effect.

Similar large changes would be predicted near the ruthenium osmium edge, for the same reasons. Near the ruthenium-iridium edge the mechanisms will be more complicated. Within the c.p.h. phase field size effects are small, but Suzuki locking and a valency effect would be expected. In the f.c.c. phase field a small size effect would also contribute to the hardness. However, the hardness data required to test these hypotheses are not available, since the object of this study was to investigate the immediate region of the two-phase field.

Alloy No.	% wt. before melting Os	Ir	Ru	Microscopic Investigation	E.M.P. Results for the phases. Os	Ir	Ru	Structure	Lattice parameter Å a	c	c/a	Specific Volume Å^3	VHN (100 g)
1.	50	50	-	2 phases	43.8	56.2	-	f.c.c.	3.836	-	-	14.111	909
					53.0	47.0	-	c.p.h.	2.728	4.352	1.595	14.024	803
2.	40	60	-	1 phase	41.7	58.3	-	f.c.c.	3.828	-	-	14.029	634
3.	32	68		1 phase	33.4	66.6	-	f.c.c.	3.828	-	-	14.029	425
4.	31	69	-	1 phase	33.5	66.5	-	f.c.c.	3.830	-	-	14.045	406
5.	58	42	-	1 phase	64.3	35.7	-	c.p.h	-	-	-	-	934
6.	55.5	45.5		1 phase	55.4	44.6		c.p.h	-	-	-	-	634
7.	53	44	3	2 phases	49.2	45.0	5.8	f.c.c.	3.836	-	-	14.119	888
					53.0	41.9	5.1	c.p.h	2.728	4.363	1.599	14.059	925
8.	32	65	3	1 phase	31.6	62.7	5.7	f.c.c.	3.836	-	-	14.119	464
9.	10	50	40	1 phase	7.3	38.6	54.1	c.p.h	2.722	4.332	1.591	13.898	681
10.	20	50	30	1 phase	14.0	41.2	44.8	c.p.h	2.718	4.332	1.593	13.857	783
11.	40	50	10	2 phases	33.2	48.5	18.3	f.c.c.	3.839	-	-	14.145	980
					39.5	44.2	16.3	c.p.h.	2.728	4.346	1.593	14.004	1080
12.	34	46	20	1 phase	25.3	42.1	32.8	c.p.h	2.729	4.343	1.591	14.004	987
13.	20	60	20	1 phase	16.9	51.4	31.7	f.c.c.	3.866	-	-	14.448	760
14.	10	60	30	2 phases	6.8	51.9	41.3	f.c.c.	3.866	-	-	14.448	885
					15.6	46.8	37.5	c.p.h.	2.726	4.320	1.585	13.900	933
15.	25	55	20	2 phases	13.2	50.4	36.4	f.c.c.	-	-	-	-	
					25.4	46.9	27.7	c.p.h.	2.729	4.338	1.590	13.988	475
16.	-	65	35	1 phase		52.0	48.0	c.p.h.	2.722	4.328	1.590	13.885	965
17.		58	42	1 phase		31.0	69.0	c.p.h.					518

Results of the microprobe analyses microhardness and X-ray diffraction study for the synthetic alloys of iridium-osmium-ruthenium
The X-ray lines in samples 5, 6, 15 (f.c.c.) and 17 could not be measured accurately and are omitted from the table.

(Table 12.1)

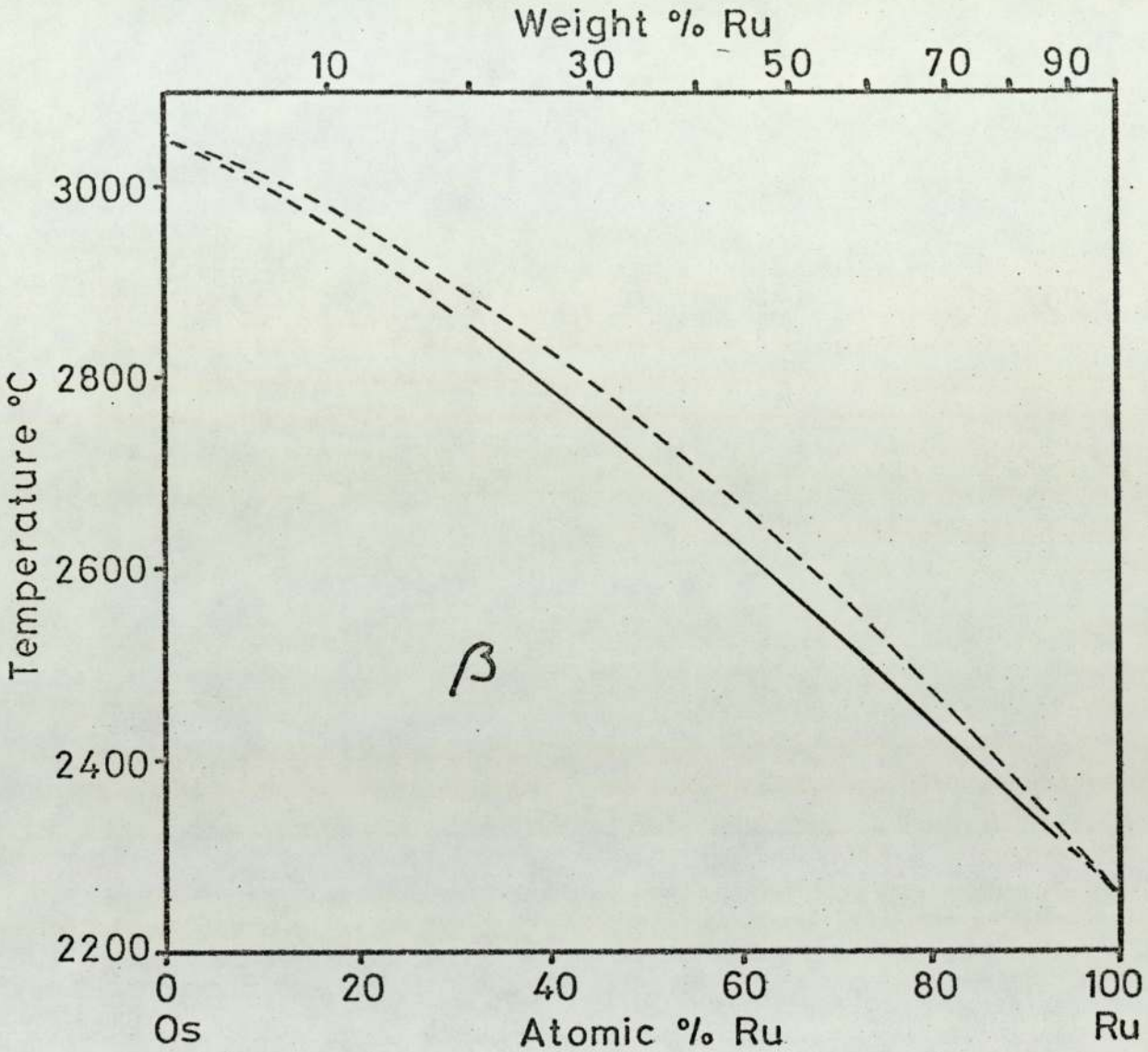

Osmium-Ruthenium binary phase diagram.

Fig. 12.1

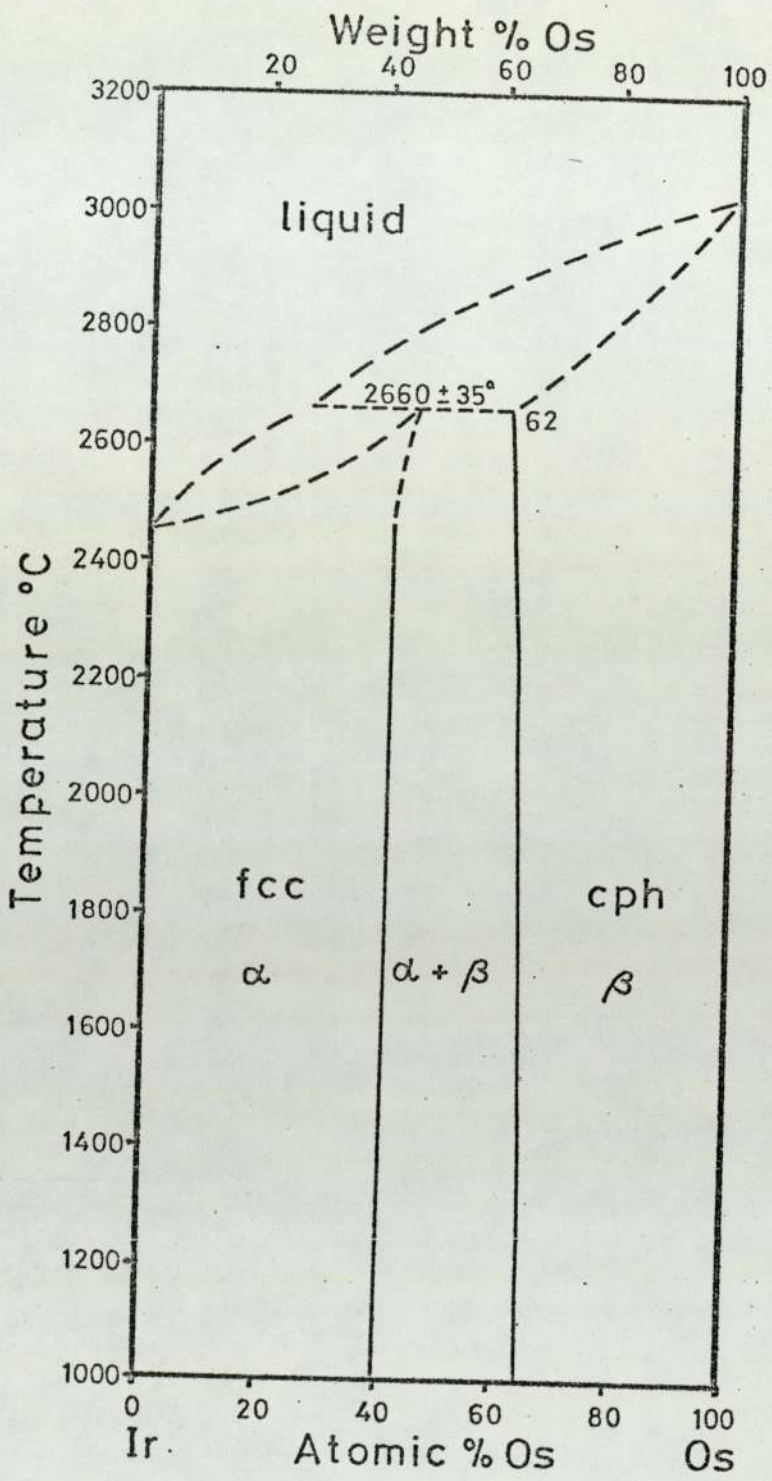

Iridium-Osmium binary phase diagram.

Fig. 12.2

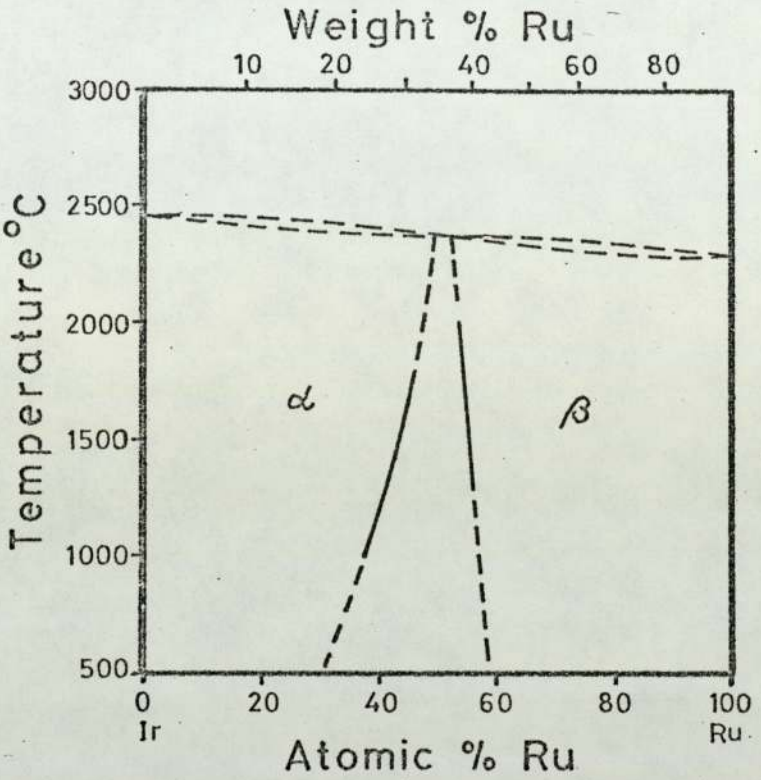

Iridium-Ruthenium binary phase diagram.

Fig. 12.3

Fig. 12.4

Reflected light photomicrograph showing synthetic osmium-iridium alloy consisting of two phases one hexagonal and the other cubic. (sample 1. in the phase-diagram Fig. 12.6.).

Magnification X 400.

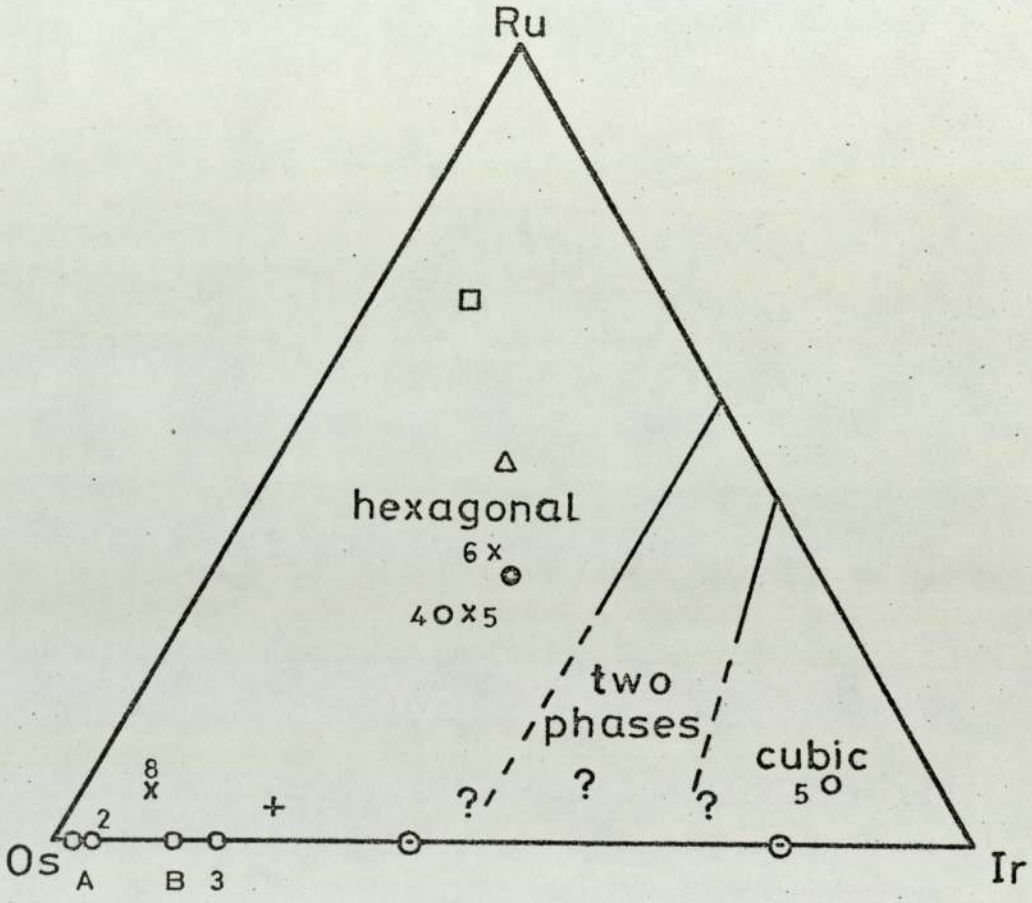

Ternary phase diagram proposed by Cabri (1972) at 1300°C.

Fig. 12.5

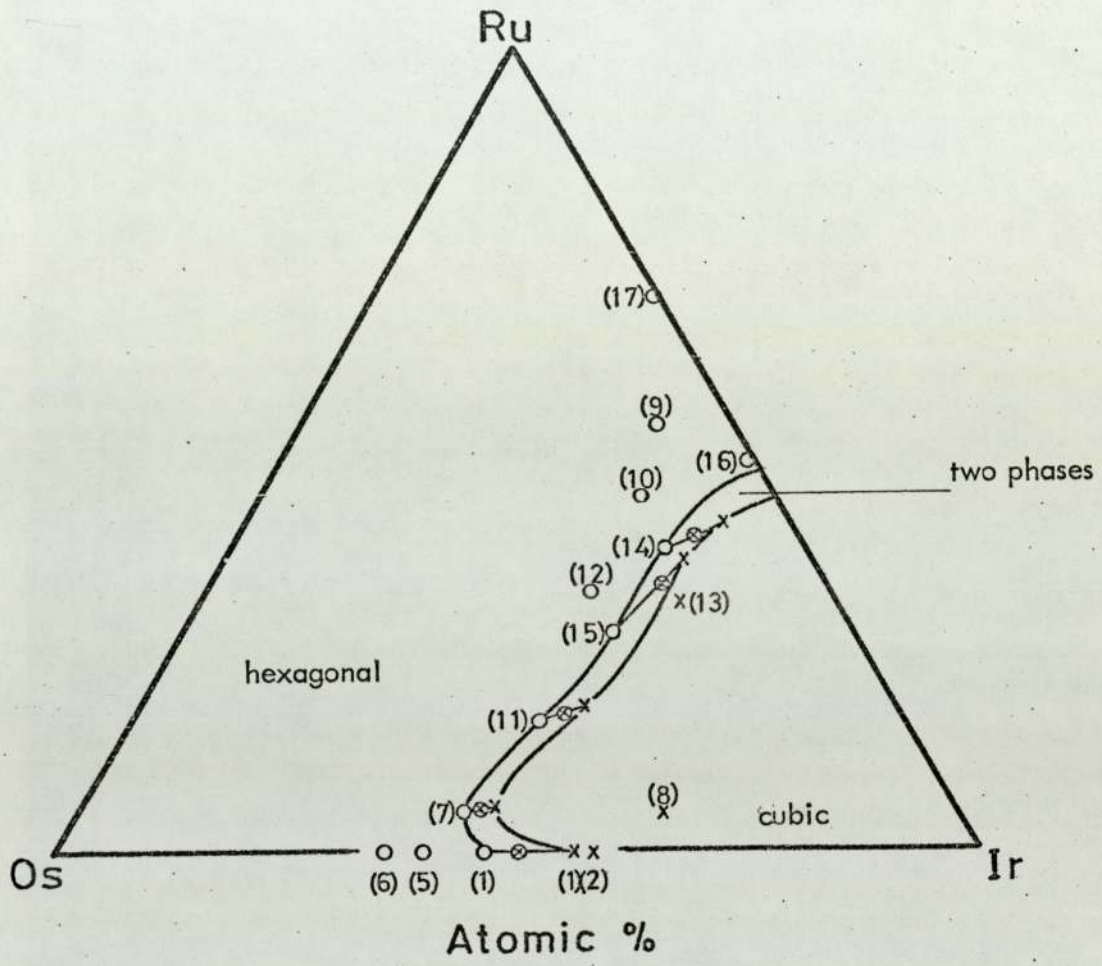

Ternary phase diagram determined in this study from Electron-probe microanalyses for the phases in the alloys studied, at a temperature higher than 2000° C.

Fig. 12.6

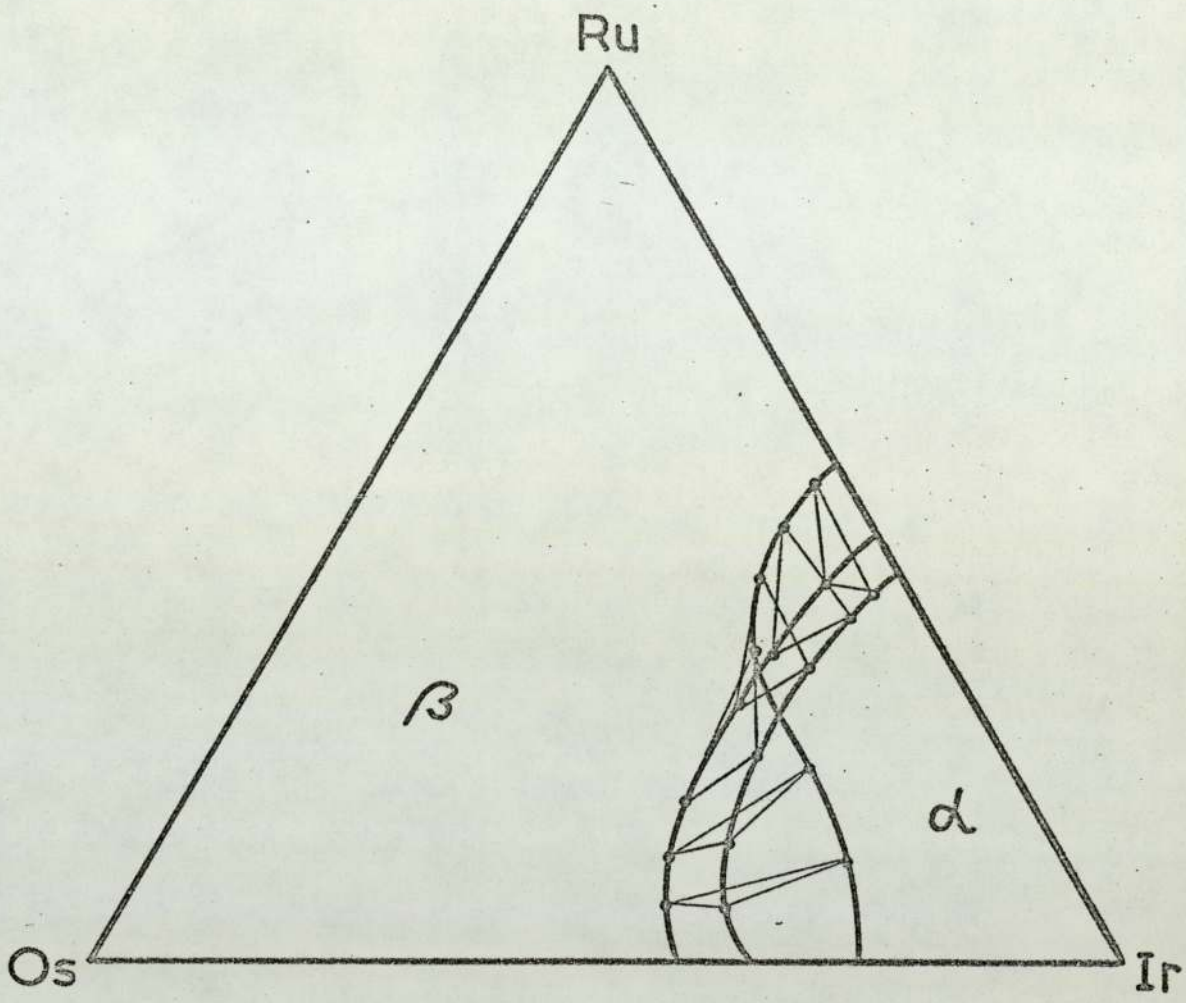

Hypothetical ternary section showing the change in shape and position of the 3 phase-field during solidification.

Fig. 12.7

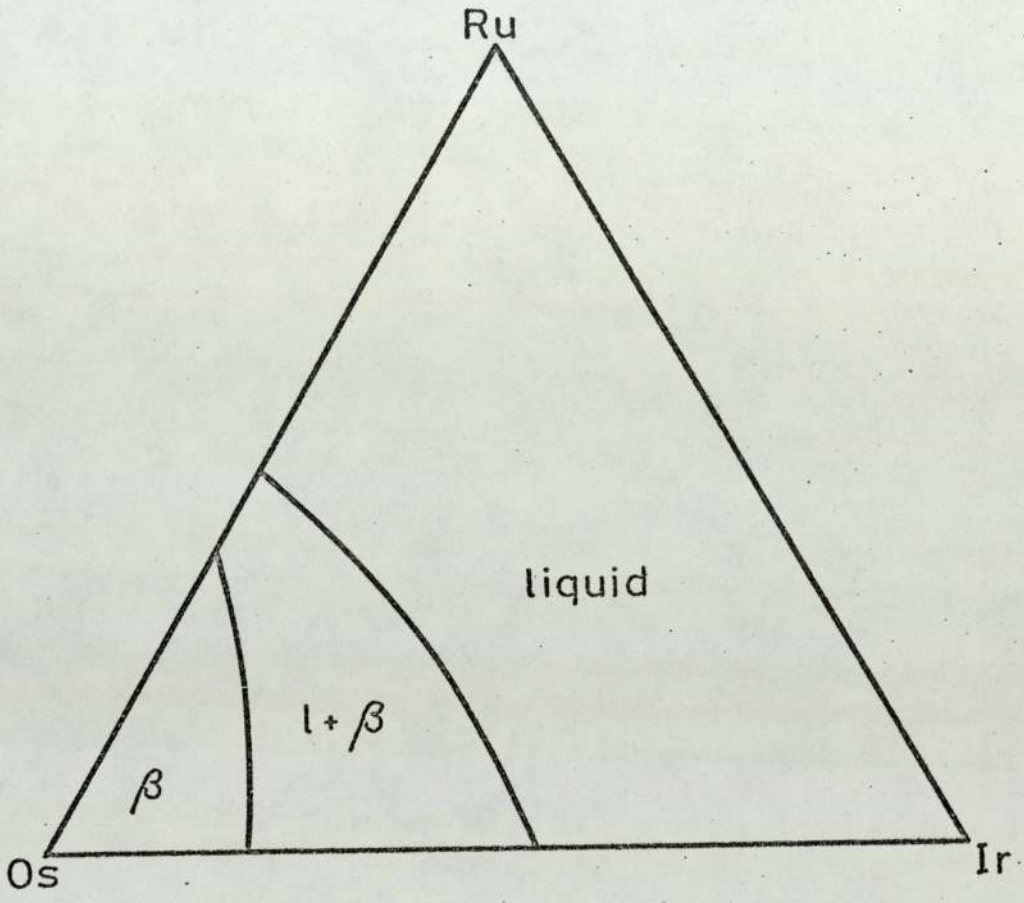

Hypothetical section through the ternary phase diagram showing the probable mechanism of solidification of ternary alloys not too near the ruthenium edge at 2800 °C.

Fig. 12.8

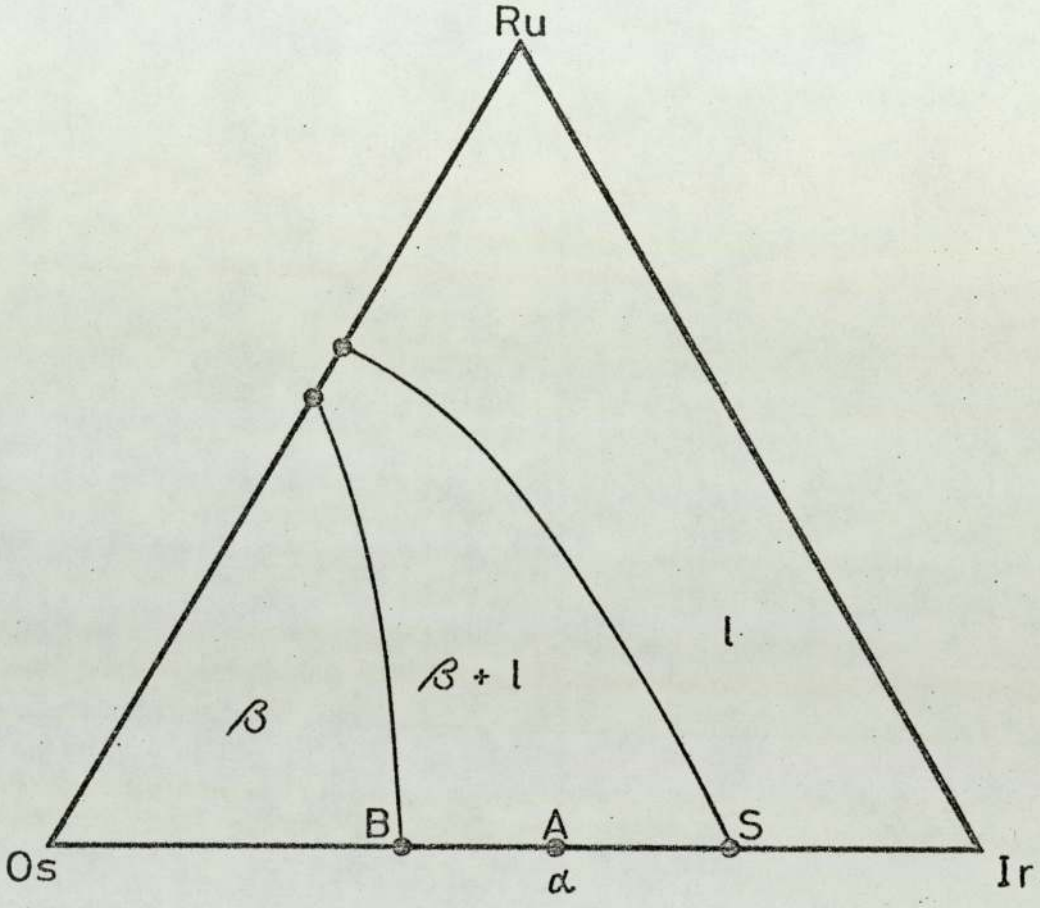

Hypothetical Section at 2,660°C.

Fig. 12.9

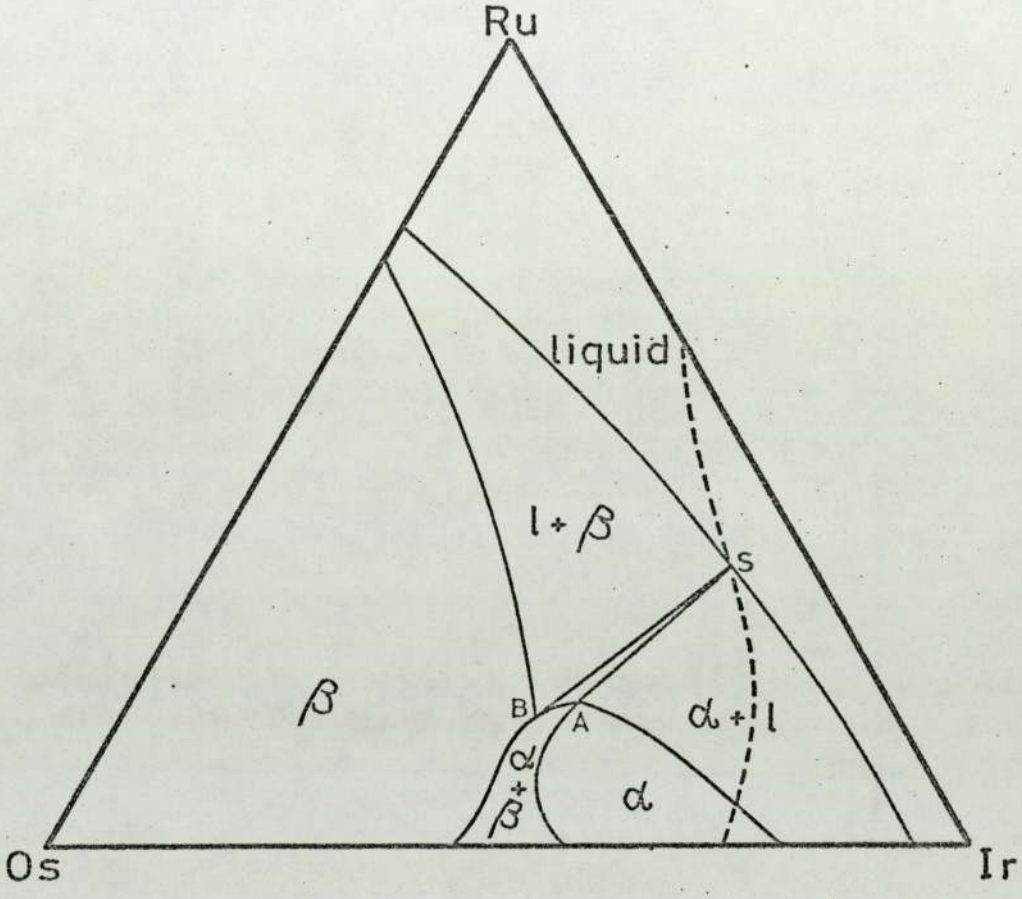

Hypothetical section at 2,500°C.

Fig. 12.10

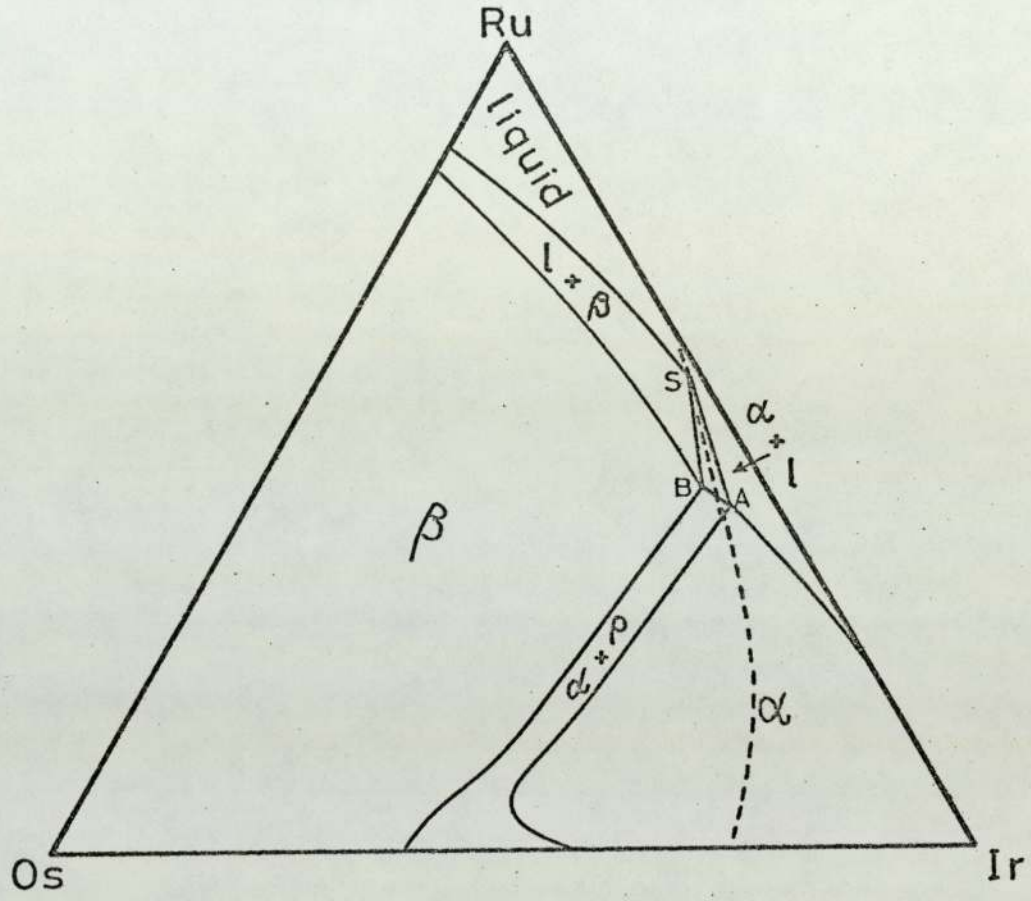

Hypothetical section at 2,400°C.

Fig. 12.11

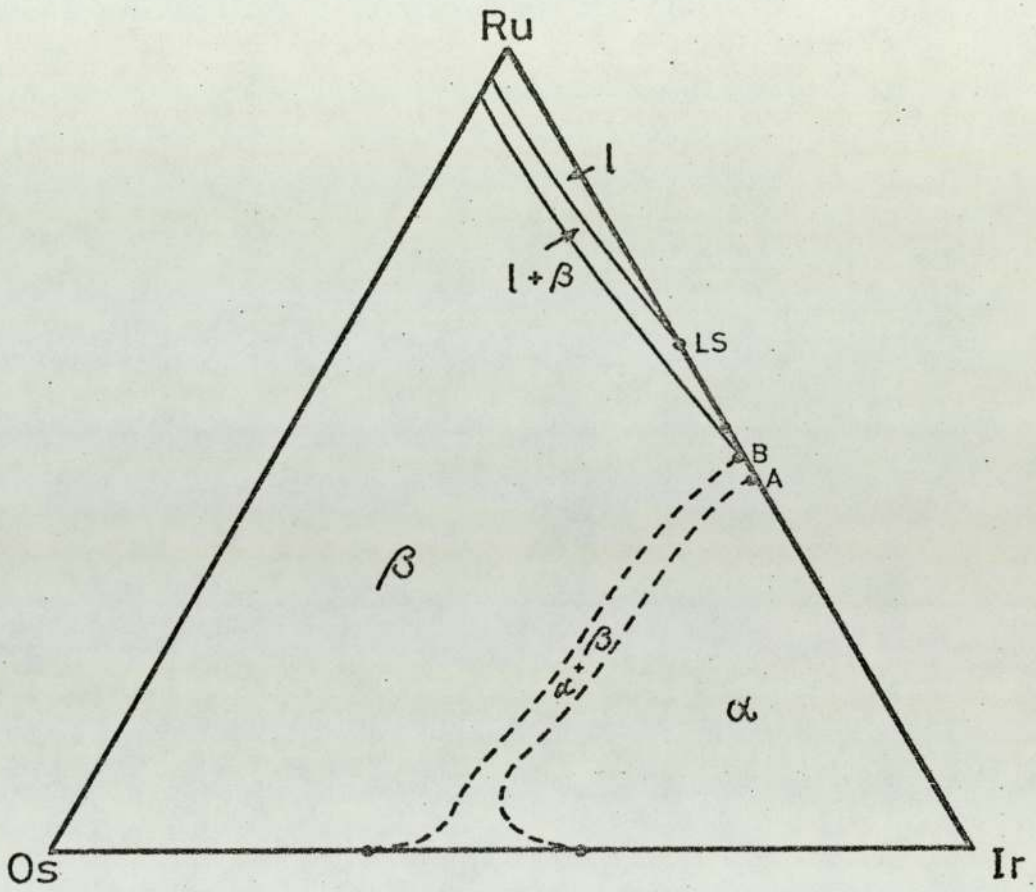

Hypothetical section at 2,300°C.

Fig. 12.12

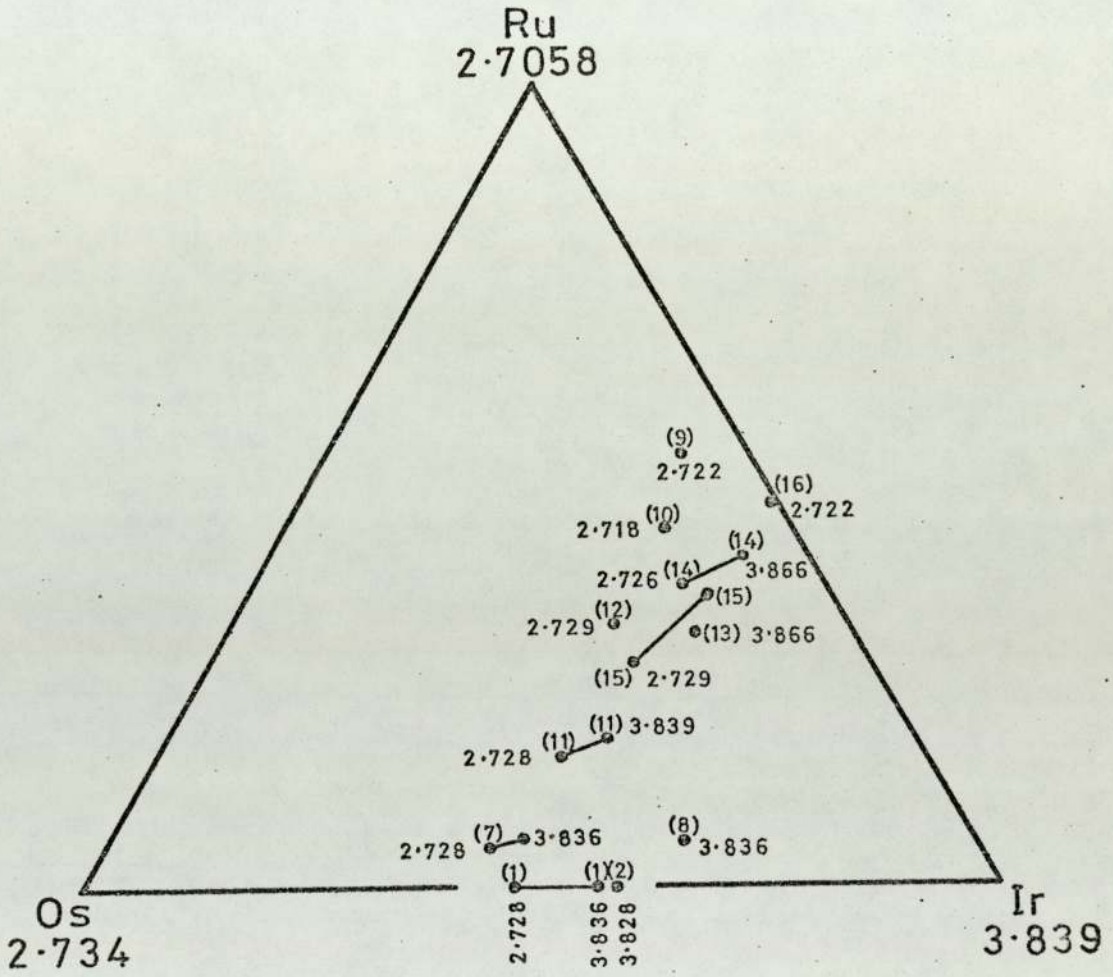

Lattice parameters of synthetic Ir-Os-Ru alloys.

Fig. 12.13

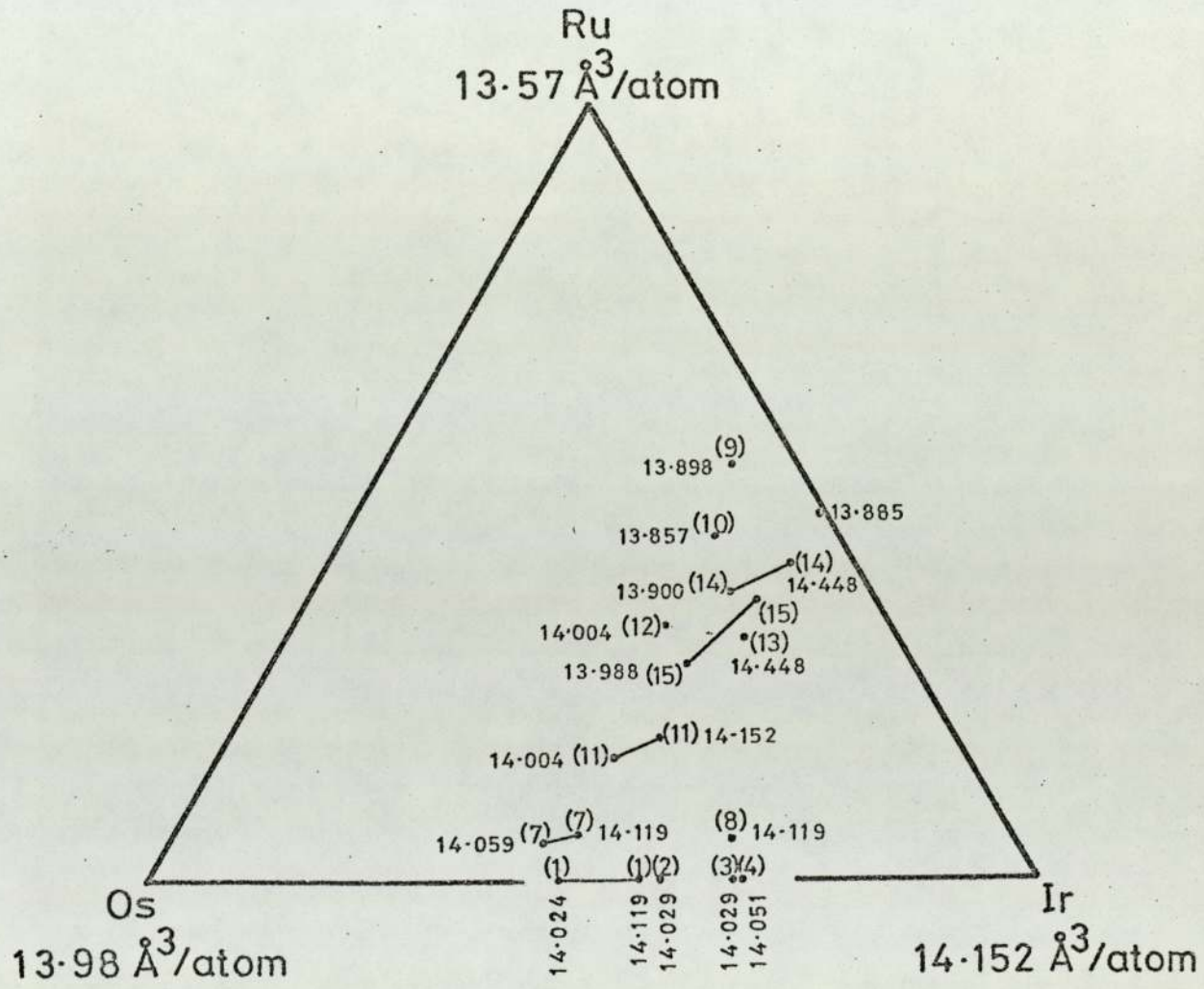

Specific volume of the phases in synthetic alloys Ir-Os-Ru.

Fig. 12.14

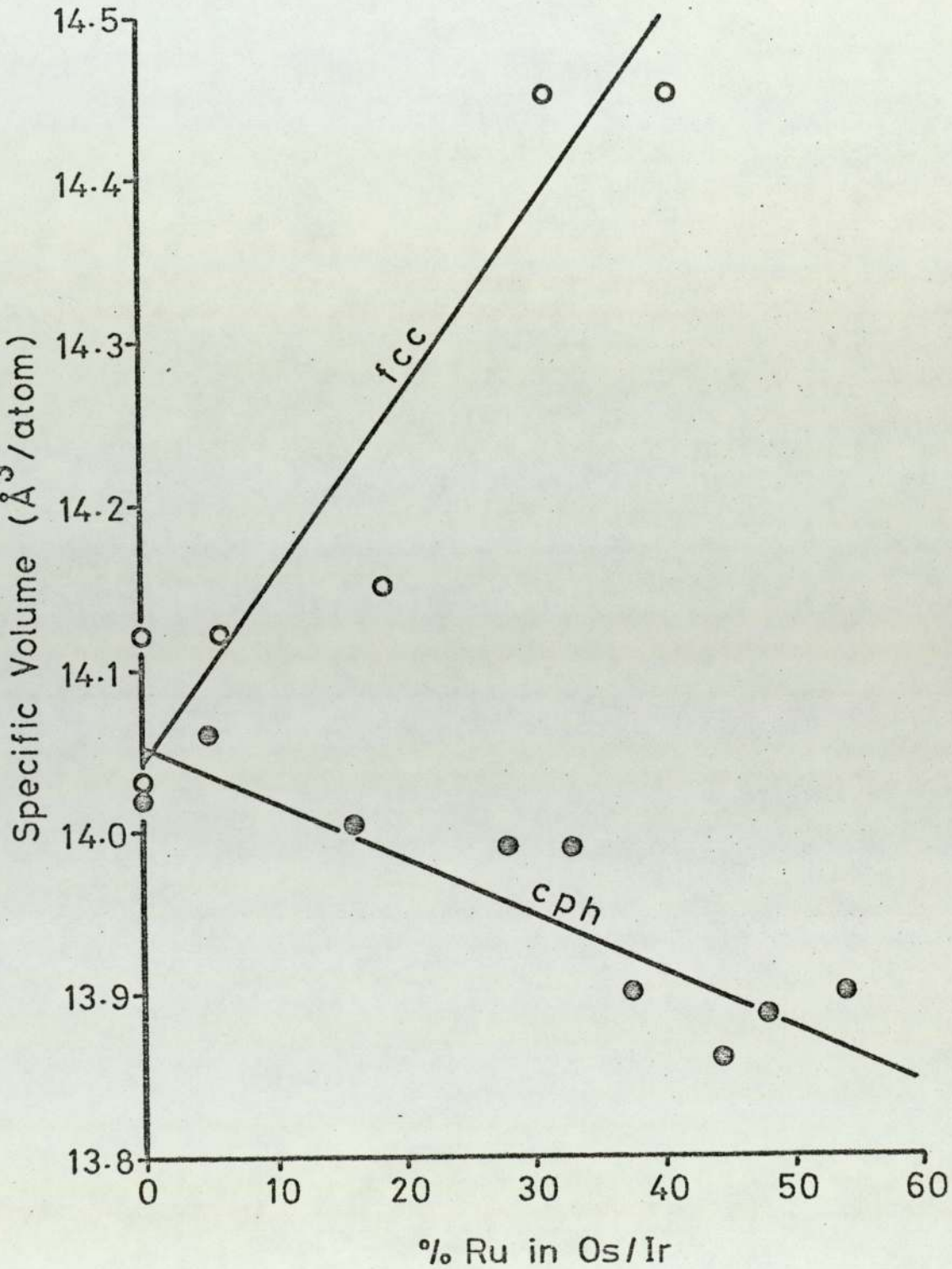

Relationship between the specific volume of iridium-osmium-ruthenium alloys and the percentage of ruthenium in these alloys with a constant iridium content (of approximately 50%).

Fig. 12.15

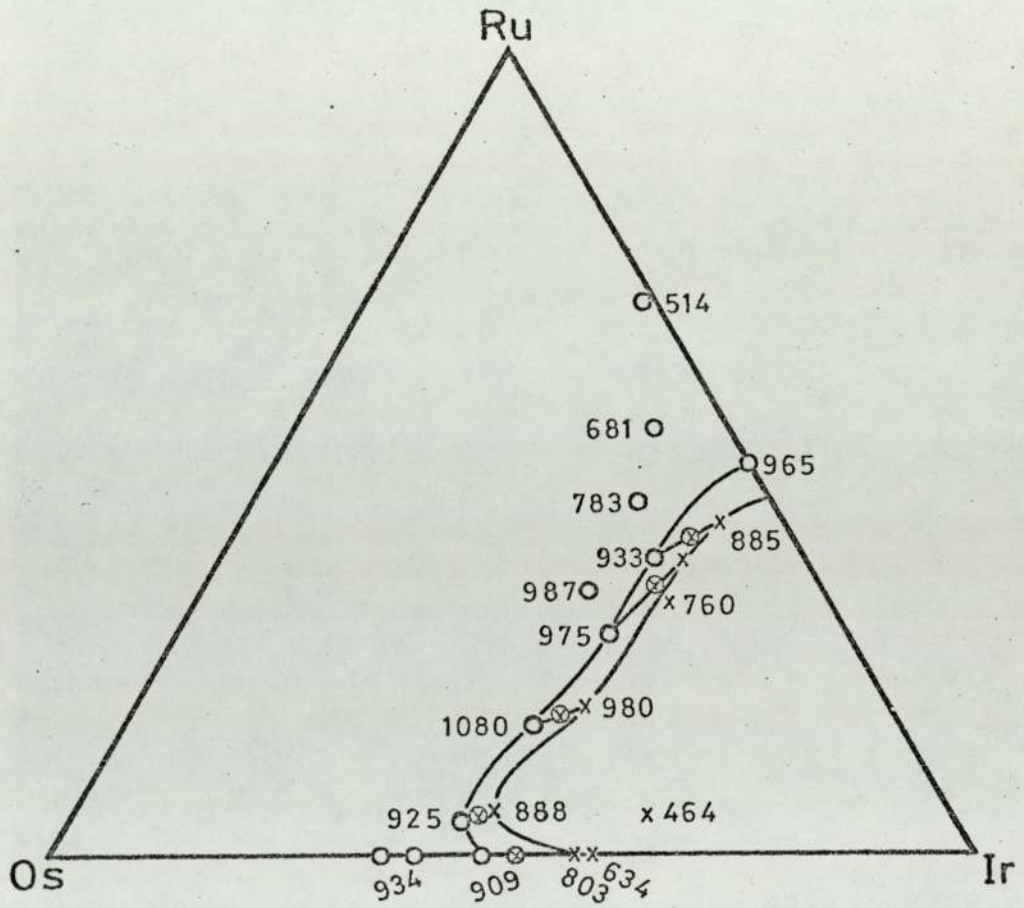

Microhardness data for the Iridium-Osmium-Ruthenium synthetic alloys.

Fig. 12.16

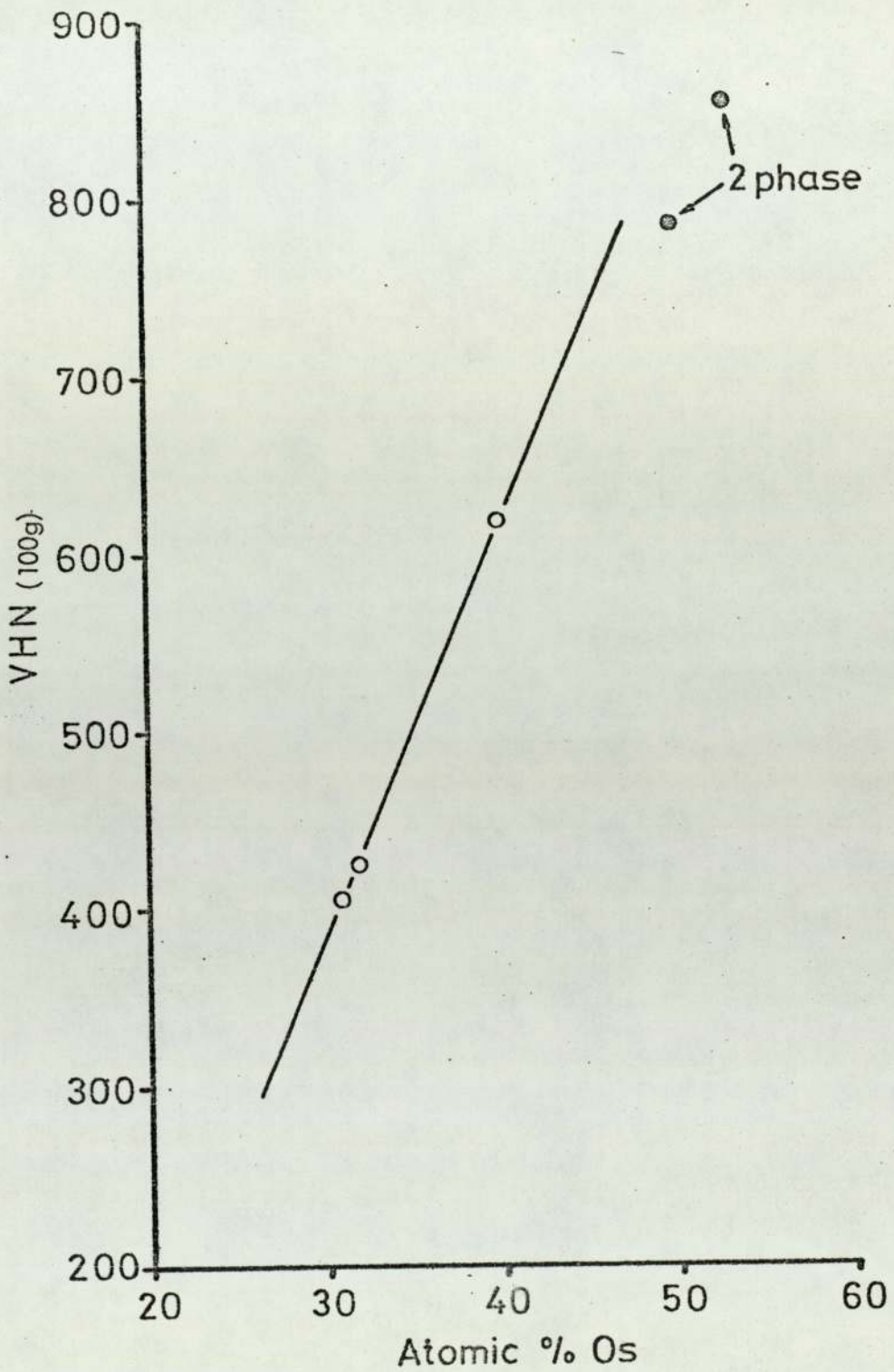

Variation of hardness with osmium content of single phase alloy.

Fig. 12.17

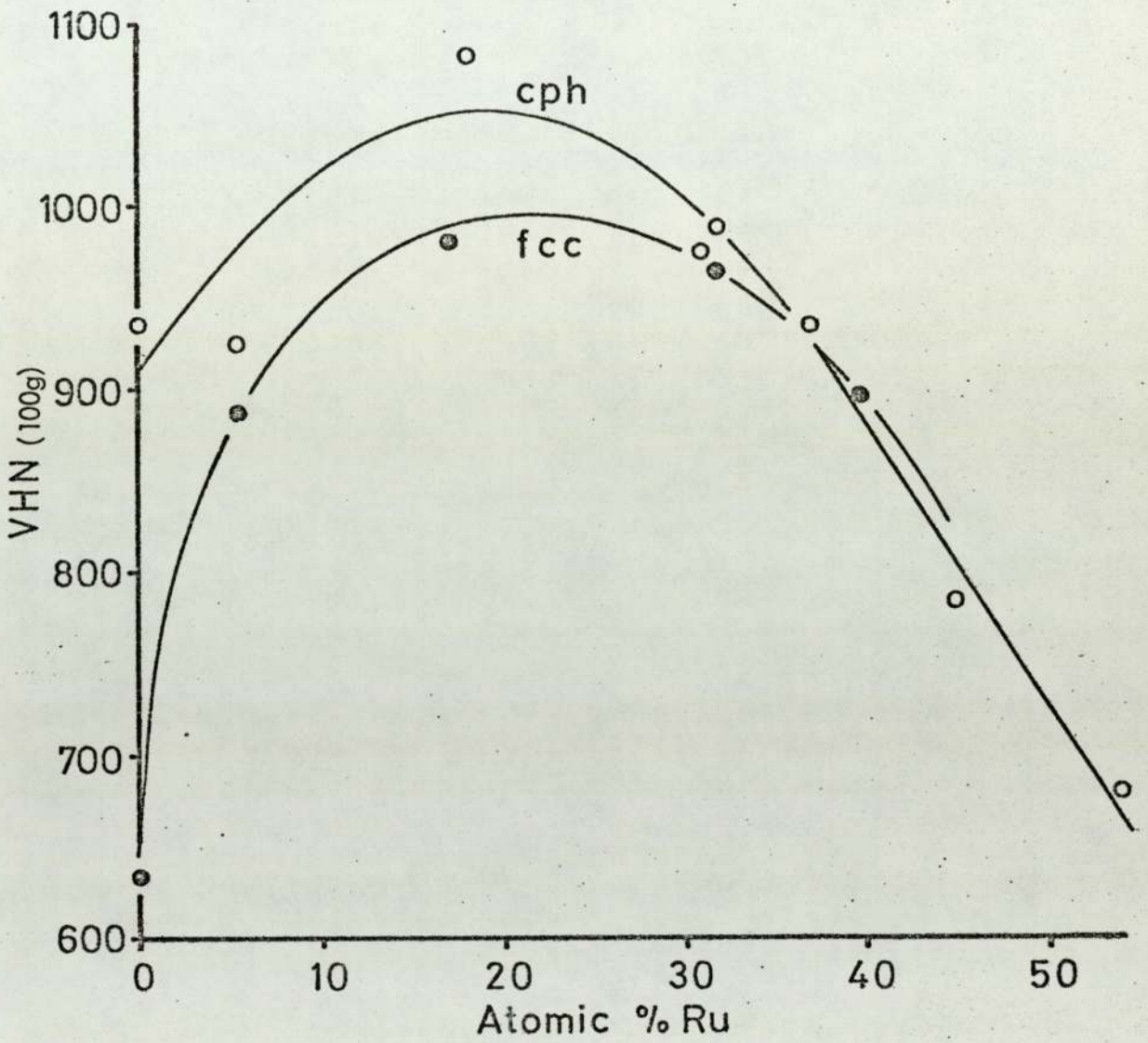

Microhardness measurements of synthetic alloys of iridium-osmium-ruthenium.

Fig. 12.18

CHAPTER 13.

CONCLUSIONS

Placer ferroplatinum usually occurs as minute, bright, creamy-white, isotropic grains of different shapes and sizes, mainly as separate grains. The ferroplatinum grains from different localities are slightly different in colour and also they are different from one grain to another owing to the differences in chemical composition. All natural alloys of platinum contain dissolved iron and copper. Natural platinum should be classified as ferroplatinum, as platinum with less then 4% iron does not occur naturally. The frequency distributions of the different elements in platinum show that typically a ferroplatinum grain has the approximate composition :-

Platinum = 88-89% Iron = 6-7% Iridium = 1.5-1.75%
Osmium 0.75-1.0% Copper = 0.5-0.75%.

The iridium is most likely to differ appreciably from the range quoted above. For this reason reflectance and microhardness values are found to differ very considerably from one grain of ferroplatinum to another. Dissolved solute, especially iridium, has a large effect on the reflectivity values of naturally occurring ferroplatinum grains. Variations due to change in the concentration of solutes other than iron thus frequently outweighed the effect of iron. For this reason the correlation of reflectance with iron content shows no significant trend. The synthetic binary iron platinum alloys show a straight variation of reflectance with iron content. This increase reaches a maximum at the composition of Fe Pt. The relationship between iron content and microhardness of naturally occurring ferroplatinum alloys is unclear. This is due to the many different dissolved elements, such as iridium which affects the hardness of the ferroplatinum.

Iridium-osmium alloys , both hexagonal and cubic phase are found intergrown in the ferroplatinum. Alaska iridosmine is similar to Choco iridosmine in chemical composition. Also the optical properties from these two localities are very similar. Iridosmine from Urals is slightly different from the Choco and Alaska iridosmine, having weaker anisotropy. It is higher in iridium content, and has higher reflectance and lower hardness. In contrast iridosmine from Ethiopia is strongly anisotropic and is high in osmium content. Witwatersrand concentrates contain all the variety of iridosmine and osmiridium, as separate grains or as inclusions.

The microscopic study of the alluvial and eluvial deposits showed that some of the minute inclusions are base metal minerals, in which iron and copper are the principal cations, such as chalcopyrite, pyrite and pyrrhotite .

Laurite (RuS_2), braggite (Pt, Pd, Ni), cooperite (Pt S) and other sulphides such as sulphides of rhodium, iridium and osmium are found enclosed in ferroplatinum. In some cases they are found replacing ferroplatinum and other platinoid minerals.

Gold is found associated or intergrown with the ferroplatinum grains. It is found as segregated grains in samples from Chaco and intergrown and dissolved in samples from Witwatersrand.

Magnetite, chalcopyrite and pyrrhotite are found as inclusions in the ferroplatinum and in other platinoid minerals. Sometimes they are found associated with the ferroplatinum.

Chromite is found commonly either attached to, or intergrown with the ferroplatinum.

In the study of iridium-osmium-ruthenium synthetic alloys, the system of solidification agrees with the experimental results,

Particularly in the sloping tie lines in the ternary system. The width of the two phase region between hexagonal and cubic phases is much narrower than indicated by previous workers. The X-ray studies of synthetic iridium-osmium-ruthenium alloys allow the volume per atom to be calculated and this is used to demonstrate that the lattice dimensions of the close-packed hexagonal phases are mostly determined by the sizes of the atoms. In the face centered cubic alloys the lattice dimensions are not directly determined by the sizes of the atoms. i.e. the volume per atom is a convenient measure of the lattice parameters produced by alloying and allows a direct comparison of the face centered cubic and close packed hexagonal structure. The microhardness of the phases is very dependant upon the composition and their dependance can be interpreted in terms of the mechanism of hardening of metallic solid solutions. The hardness of hexagonal iridium-osmium-ruthenium alloys both natural and synthetic is greater than the cubic alloys. The results obtained from the ternary phase diagram are used to explain that the Witwatersrand platinoids, have more than one origin.

Banded grains demonstrate a magmatic origin for some particles. Banding itself can arise from difference in platinoid concentration during solidification of the magma.

Selective sulphidisation produces platinoid and base metal sulphides and sometimes liberate native gold. This is explained by the reaction of the sulphur with the platinoid metal grains after their deposition. It is possible that displacement of sulphur from associated sulphide minerals by hydrothermal action produced the sulphide replacement.

The mineralogy of the other concentrates from Alaska, Choco, Ethiopia and Urals is consistent with little transportation and no subsequent chemical changes.

APPENDICES

EXPERIMENTAL METHODS, TECHNIQUES AND PROCEDURES.

Some of the samples used in this study were kindly supplied by the "Compania Minera Choco Pacffice, Columbia". Others were lent by other workers from their own collections. The synthetically prepared alloys were prepared from the pure elements which were purchased from Johnson Matthey & Co. Limited.

The samples from the alluvial concentrates were divided mechanically into four fractions, non-magnetic, weakly magnetic, strong magnetic and the raw concentrates. They were selected with the aid of a stereoscopic microscope and a hand magnet. Grains from each fraction were mounted in Cold-setting plastic, (Ceemar fluid 100 cc + tea spoonful of hardner + 18-20 drops of accelerator). When the section polymerised it was removed from the mould, and ground for 5 minutes on a glass plate using 500 mesh Carborundum and water. This step was repeated using 850 mesh Carborundum and water. Samples were polished using the following method :-

Sections were polished on a "metcloth" - Covered Lap. Using 12 microns diamond dust in oil for about 60 minutes, till the section is uniform and perfectly flat. This was followed by using another "metcloth" - covered lap with 6 micron diamond dust in oil till the grains in the sections start to take a high shine. Time was about 45-60 minutes. The same methods were repeated using 2 micron diamond dust in oil and finished with $\frac{1}{2}$ micron diamond dust in oil. Final polish was made using nylon covered lap (shiney side) to remove final scratches with $\frac{1}{2}$ micron diamond dust in oil. No weights resting on specimens have been used.

For synthetic alloys and the electron probe standard, special attention was paid to polishing and cleaning using Ultrasonic method of cleaning.

APPENDIX 1

MICROSCOPIC EXAMINATION AND PHOTOMICROGRAPHY.

Microscopic studies of polished sections were undertaken using a Reichert Zetopan ore microscope (Nr. 353908). Most of the minerals were examined in air and under oil immersion. Colours were compared in contrast to the platinum grains when the other mineral phases are found as inclusions in the ferroplatinum matrix.

With regards, to photomicrographs a Zeiss photomicroscope II with fully automatically operated Cameras was used. The film used was 35mm film, speed 125. For coloured photographs a high speed Ektachrome ASA 125, 22 DIN was used.

APPENDIX 2.

QUANTITATIVE REFLECTANCE MEASUREMENTS.

Quantitative reflectance values were determined by means of a Reichert Zetopan ore microscope equipped with reflex spectral microphotometer. A full description of it is given by Singh (1965). It's main features are the use of a narrow band width monochromator instead of filters that produce errors in the measurements, especially regarding the spectral dispersion produced by some minerals at different wave lengths. It has also a system of secondary emission of electrons for the amplification of the photo-current. It's spectral response has been found to be very close with this of the human eye; its accuracy and other features were fully investigated by Singh and Squair (1965). Measurements were made at 589 nm (Na-Line). All values were obtained in air and related to a pyrite standard. The standard pyrite used is a polished crystal face (100) calibrated at 10 wave lengths by the National Physical Laboratory, Teddington. The reflectance of the pyrite standard is 51.0% at 589 nm. Necessary precautions were taken to ensure that the microscope is perfectly centred and precisely adjusted to give normal incident plane polarized light. Standard and specimen are cleaned and levelled and relatively flawless areas are selected. The instrument is switched on 15 minutes, before measuring the 'warming up' time recommended by the manufacturers. The recording instrument is set at Zero using the dark Current Compensator and the light source connected to the battery. The aperture diaphragm is adjusted to give the image clarity and optimum contrast. This adjustment minimizesdazzle and 'flare'. The collimator field diaphragm is stopped right down to reduce stray light.

The reflectivity is calculated using this formula.

$$R\% \text{ of mineral} = \frac{\text{Deflection value of unknown}}{\text{Deflection value of standard}} \times K$$

where K = Calibrated reflectivity of standard.

APPENDIX 3

QUANTITATIVE MICROHARDNESS MEASUREMENTS.

The microhardness values were obtained by means of a Vicker indenter fitted to a Leltz microscope, manufactured by E. Leitz Ltd, Wetzlar. Vickers hardness (HV) is determined from Vickers conversion tables which is based mainly on the following equation :-

$$HV\ (Kg/mm^2) = \frac{1854.4 \times t}{d^2}$$

where HV = Vickers hardness in Kg/mm^2

t = weight in grams

* d = length of the diagonal in microns.

The data obtained are expressed as Vickers Hardness Number (VHN) with the load in grammes as a subscript (i.e. VHN_{100} = Vicker microhardness measured at 100 grammes).

(* one micron = .001 mm.).

APPENDIX 4.

PREPARATION OF SYNTHETIC IRIDIUM-OSMIUM-RUTHENIUM ALLOYS.

The carefully weighed elements were mixed together, then pressed to make a bead, in a cold press. The bead was melted using a tungsten arc in an atmosphere of high purity argon. The melting chamber was made of stainless steel with a water cooled copper base, (Fig. 4 A.). A thoriated tungsten melting electrode was used.

The chamber was initially evacuated to 10^{-4} TORR using an oil diffusion pump, backed by a rotary pump. The argon was admitted into the chamber which was again evacuated to 10^{-4} TORR. Argon was then admitted into the box to achieve a positive pressure and a side valve on the box was opened to achieve a flow-through of pure argon. An argon flow rate of 15 L/min was used throughout. The arc was initially struck on the water cooled base before it was moved over the specimens. In this way, the alloys were melted three times for periods of 0.5 mins. in order to ensure complete homogenisation. A current of 300 amps, and a voltage of 11 volts (approximately) was used throughout. The water cooled copper base ensured that the arc melted buttons solidified rapidly when the arc was switched off. Weighing the alloys before and after the melting revealed that the weight loss during arc melting was negligible (> 0. 01Wt. %).

An attempt was made to measure the temperature of the alloys during melting using a disappearing filament pyrometer observed through a glass window in the apparatus. The highest indicated mean temperature reached greater than the upper scale limit. (the scale reached 2000°C).

After preparation, the alloy buttons were mounted in bakelite and polished for optical examination, microhardness determination and electron-probe microanalysis. After probe analysis, the buttons were removed from the bakelite for X-ray examination.

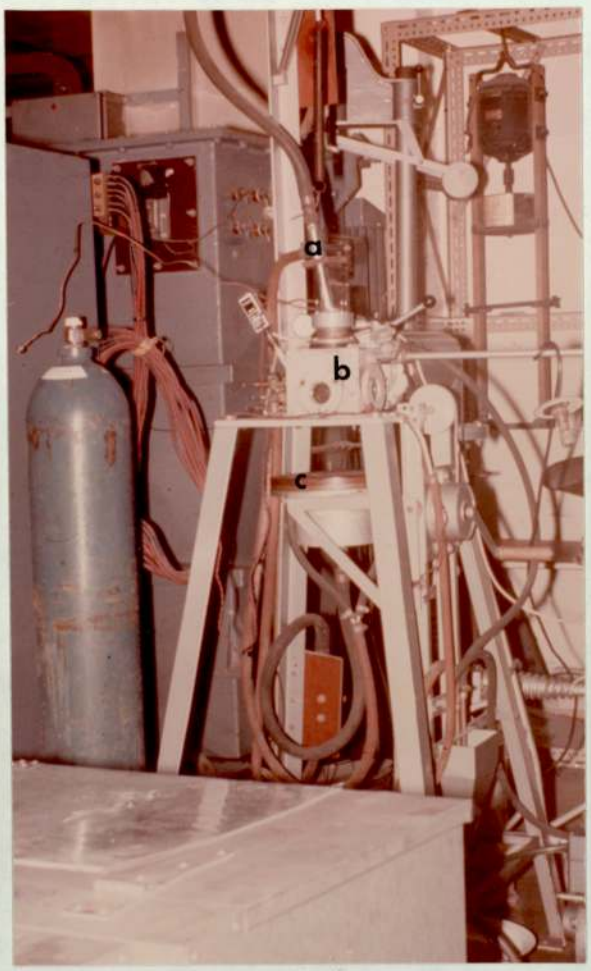

Fig. 4.A

Shows the apparatus used in the preparations of the synthetic alloys of iridium-osmium-ruthenium.

a. Tungsten arc.

b. Melting chamber.

c. Water cooled copper base.

APPENDIX 5.

ELECTRON PROBE MICRO ANALYSIS FOR SYNTHETIC IRIDIUM-OSMIUM-RUTHENIUM ALLOYS.

This was carried out on flat, polished sections mounted in conducting bakelite. The instrument used was a Cambridge Microscan Five microanalyser. Analyses were carried out at 15 KeV and a beam current of 50 nA. Under these conditions an electron spot size of approximately 0.2 μm is achieved, but since the electrons diffuse into the metal under the surface the iradiated volume is greater than this. The electron range can be estimated from the Thompson Widdington Law :-

$$X\,r = a\,\frac{(AV^2)}{(Z\rho)}\quad (Cm)$$

where a is 10^{-12}

A is the atomic weight

Z is the atomic number

V is the accelerating potential (V)

ρ is the density.

The results are tabulated below.

ELEMENT	ATOMIC No.(Z)	ATOMIC Weight (A)	DENSITY	ELECTRON range (μm)
Ru	44	101.1	12.2	0.42
Os	76	190.2	22.48	0.25
Ir	77	192.2	22.42	0.25
Pt	78	195.1	21.45	0.26

Since the distance is so small the analysed volume will be less than 0.5μin diameter. Hence the different phases initially divided two phase alloys could be analysed separately.

An adequate flux of fluorescent X-rays were produced despite the low operating potential. The L $\alpha_{1,2}$ line was used for osmium, iridium and platinum. Since the critical excitation energy for these lines lies in the range 1.91 KeV to 2.84 KeV, the overvoltage ratios at 15 KeV range from 5.29 to 7.85. Such overvoltage ratios give an adequate X-ray flux without stimulating too much Bremstralung radiation.

The analyses were carried out using PET diffracting crystal and a sealed, Xe-filled proportional counter. The intensity ratios were calculated by comparison with the pure elemental standards. Full ZAF (Atomic number, atomic weight, flourescent) correction procedures were made to the results using the standard university correction programme (1969). The mass absorption coefficients used are of Heinreich (1966), and Bishops (1968). Back scattering and stopping power Coefficients were used.

For electron probe microanalysis of natural platinum iron alloys, series of alloys had been prepared by Johnson Matthey and Co. Limited. The chemical composition of these alloys were as follows :-

90: 10, 80:20, 70: 30, 50: 50 platinum: iron.

These alloys were analysed using pure platinum (99.999% and pure iron 99.999%). The count ratio obtained was plotted against the true ratio after correction for the back ground. The values obtained are tabulated in the table below, and graphically represented in Fig. 8.1.

Analysis of Synthetic alloys of platinum and iron.

Specimen.	Prepared Composition		Microprobe analysis composition	
	Pt	Fe	Pt	Fe
1	90	10	88.6	8.8
2	80	20	76.3	17.9
3	70	30	63.5	27.6
4	50	50	46.4	49.0

APPENDIX 6

X-RAY DIFFRACTION.

A Philips diffractometer (Model PW 1050) was used in this investigation . The specimens from the microprobe analysis work were broken out of their plastic mounts and imbedded in plasticene for X-ray examination. All the work was carried out using a Cu X-ray tube with a nickel filter at 40 KeV potential and 20 μA current. The size of the Collimated X-ray beam was about 3mm x 1mm, and since the alloys were frequently smaller than this the diffraction pattern always contained lines due to plasticene (calcite) or aluminium. These were however, sufficiently far away from the important lines of the alloy as to pose no problem of interpretation.

Calibration of the diffractometer with gold standard showed that the angular error was not more than 0.03° 20' in the angular range used in this investigation.

BIBLIOGRAPHY

Agustithis, S. (1965) — Mineralogical and geochemical studies of the platiniferous dunite-birbirite-pyroxenite complex of Yuobdo (Abyssinia). VEB Fischer Verlag, Jena Band 24, Heft 2.

Betechtin, A.G. (1961) — Mikroskopische Untersuchungen an platinerzen aus dem Ural. N. Jb. Miner. Abh. 97 (German).

Bishop, H. (1968) — Brit. J. App. Physics (D) P673.

Cabri, L.J. (1972) — The mineralogy of the platinum-group elements. Minerals Sci. Engng. 4 3-29.

Cabri, L.J., Owens, D.R. & Laflamme, J.H.G. (1973). — Tulameenite, a new platinum-iron-copper mineral from placers in the Tulameen River area, British Columbia. Can. Miner. 12. pp. 1, 21-25.

*(see footnotes)

Castaing, R. (1960) — Electron probe microanalysis. In "Advances in Electronics and electron physics." Ed. L. Marton, Vol. 13, p. 317. Academic, Press, New York.

Cotezee, C.B. (1960) — The geology of the Orange Free State gold-field: South Africa Geol. Survey Mem. 49, 198p.

Cousins, C.A. (1973) — Platinoids in the Witwatersrand system. J.S. Afr. Inst. Min. Metall., Vol. 73, pp. 184-199.

Cousins C.A. (1973) — Notes on the geochemistry of the platinum group elements. Trans. geol. Soc. S. Afr., Vol. 76, pp. 77-81.

Crangle J. and Show J.A. (1962) — phil. Mag. 7 p. 207.

Davidson C.F. (1953) — The gold-uranium ores of the Witwatersrand. Mining Mag. V 90 p. 73-85.

Davidson C.F. (1955) — The mineralization of the Witwatersrand: Mining Mag. V92 p. 152-156.

Duparc C.L. (1925) — Les gites platiniferes de l' Oural en relation avec ceux du Transaal : Schweizer. Mineralog. u. Petrog. Mitt. V.5 . p. 147-172.

Duparc C.L. (1927) — Sur la birbirite, une roche nouvelle: Soc. phys. et historie nat. Geneva Compte rendu. V. 44 p.137-139.

Duparc C.L. and Molly E. (1927) — Sur les gisements platiniferes du Birbir (Ethiopia) : Schweizer. Mineralog u petrog. Mitt. V.8 p240-257.

Duparc C.L. and Tikonowitch M.N.(1920) — Le platine et les gites platiniferes de l'Oural et du monde. Geneve Soc. Anonyme des Editions Sonor p. 542.

Flinn and Peckner (1964) — The strengthening of metals. p.226.

Furon Raymon. (1963) — Geology of Africa (English ed). New York, Hafner publishing Co. 377p.

Graton L.C.(1930) — Hydrothermal origin of the Rand gold deposits. Econ. Geology V.25 supp. to no.3. p.185.

Genkin A.D. (1959) — Conditions of occurrence, and features of the compositions of minerals of the platinum group in ores of the Noril'sk deposits Akad. Nauk SSSRI Inst. Geol. Rudnykh Mestorozhdeniy, No. 6 p.74-84 (In Russian).

Genkin A.D. and Basova G.V.(1965). — New data on minerals of the U.S.S.R. Tr. Mineral Muzeya no.16 p.209 (In Russian).

Genkin A.D. and Korolev N.V. (1961) — On methods of determining small grains of minerals in ore, Akad. NaukSSSSR, Geol. Rudnykh Mestorozhdeniy no. 5 p64-69 (In Russian).

Genkin A.D. and Murav'eva I.V. and Troneva N.V. (1966) — Zvyagintsevite, a natural intermetallic compound of palladium, platinum, lead and tin. Akad. Nauk SSSR. Geol. Rudnykh Mestorozhdeniy no.5. p64-69 (In Russian).

Genkin A.D. Zhuravlev N.N. and Smirnova E.M. (1963) — Moncheite and Kotulskite, new minerals, and the composition of michenereite: Vses. Mineralog. Obshch Zapiski v.92 no.1, p.33-50 (In Russian).

Genkin A.D. Zhoravlev NN and Troneva N.V. and Murav'eva I.V. (1966) — Irarsite, a new sulfoarsenide of iridium, rhodium, ruthenium and platinum. Vses. Mineralog. Obshch. Zapiski v. 95 p700-712 (In Russian).

Genkin A.D. and Zvyagintes O.E.(1962) &(1963) — Vystoskite, a new sulphide of palladium and nickel. Vses. Mineralog. Obshch. Zapiski v. 91 no.6 p-718-925 (In Russian).

Gray I.M. and Millman S.P. (1960). — Spectral reflectivity of ore minerals. Nature 187,

Gray I.M. & Millman AP. (1962) — Reflection characteristics of ore minerals. Econ. Geol. 57 May

Grimaldi F.S. and Schnepfe MM (1969). — Mode of occurrence of Pt, Pd and Rh in chromitite. Washington U.S. Geol. Surv. Handbook of Metals (1961).

Harris D.C. and Cabri L.J. (1973). — The nomenclature of the natural alloys of osmium, iridium and ruthenium based on new compositional data of alloys from worldwide occurrences. Can. Mineralogist, Vol.12 pp 104-112.

Hawley J.E. (1962) — The sudbury ores. Their mineralogy and origin. Can. Mineralogist. Vol.7 pp 1-207.

Hawley J.E and Berry L.G. (1958) — Michenerite and froodite, palladium bissmuthide minerals. Can. Mineralogist. Vol.62 pp.59-74.

Heinreich F.G. (1966) — Proc. symp on electron microprobe, New York. John Wily p 296.

Hey M.H. (1963) — The nomenclature of the natural alloys of osmium and iridium . Mineral. Mag. 33, 712-717.

Hume-Rothery and Raynor G.V. (1956). — The structure of metals and alloys.

Kingston G.A. (1966) — The occurrence of platinoid bismuthotellurides in the Merensky Reef at Rustenburg platinum mine in the western Bushveld. Mineralog. Mag. Vol.35, pp.438-450.

Koen G.M. (1964). — Rounded platinoid grains in the Witwatersrand banket. Trans. geol. Soc. S. Afric. Vol. 67, pp139-148.

Kunz G.F. (1921) — Platinum. Bull. Pan American Union .

Lebedeeva S.I. (1963) — The determination of the microhardness of minerals Izdatelstvo Nauka SSSR Moskva pp. 122. (In Russian)

Lipson H. Shoenberg D and Stupart G.V. (1941) — The relation between atomic arrangement and coercivity in an alloy of iron and platinum. T. Inst. Metals. Vol.58 pp. 1137-1140.

Mardgraff. (1757) — Johnson, Matthey and Co. Limited . London.

Macdonal R. Donland (1960) — A history of platinum. Johnson, Matthey and Co.Ltd. London.

Mertie J.B. (1940) — The goodnews platinum deposits, Alaska. Washington U.S. Geol. Survey. Bull 918.

Mertie J.B. (1969) — "Economic Geology of the platinum metals". U.S. Geol. Survey. Professional paper 630, Washington.

Mihalik, P. Jacobsen J.B.E. and Hiemstra S.A. (1974) — Platinum-group minerals from a hydrothermal environment. Economic Geology Vol. 69, pp257-262.

Molly E.W. (1959) — Platinum deposits of Ethiopia. Economic Geology. Vol. 54, pp.467-477.

Nemilov V.A. (1932) — Z Onorg. Chem. Vol. 204, pp.41-48 (In Russian).

Ottemann J. and Augustithis S.S. (1967) — Geochemistry and origin of "platinum-nuggets". in lateritic covers from ultrabasic rocks and birbirites of W. Ethiopia. Mineralium- deposits Vol.1 pp.269-277.

Plaith D. Kimball, Preston and Crangle (1969) — Phys. Rev. 178 (2) pp.795-799.

Ramdohr P. (1960) — Die Erzmineralien und ihr Verwachsungen . 3 Aufl. Berlin, Akademie.

Ramdohr P. (1969) — The ore minerals and their intergrowths. London Pergamon, p.1174.

Raub E. (1959) — Metals and alloys of the platinum group. J. Less-common metals Vol.1. pp.3-18.

Raub E. (1964) — Die Ruthenium-Iridium-Legierungen Z. Metallkde. Vol. 55, pp.316-319.

Reiswig. R.D. and Dicknson J.M.(1964) The Osmium-Iridium-Equilibrium Diagram. Tras. Met. Soc. Amer. Inst. Min. Met. Eng. Vol.230, pp.469-472.

Rucklidge J.C. (1969) Electron microprobe investigations of platinum metal minerals from Ontaria. Can. Mineralogist, Vol.9, pt.5 pp.617-628.

Rudman P. S. (1967) Lattice parameters of some h.c.p. binary alloys of rheniumand osmium. Re-W, Re-Ir, Re-Pt, Os-Ir, Os-Pt J. Less-common Metals, Vol.12 pp.79-81.

Singh D. S. (1965) Measurement of spectral reflectivity with the Reichert Microphotometer . Trans. Inst. Min. and Met. Vol. 74 pp.901-931.

Singewald Q.D.(1950) Mineral resources of Columbia (other than petroleum) U.S. Geol. Survey Bull. 964B, pp.53-204.

Snetsinger K.G. (1971) A platinum nugget from Trinity county, California Am. Mineralogist. Vol.56 pp.1101-1105.

Snetsinger K.G. (1971) Erlichmanite (OsS_2), a new mineral Am. Mineralogist, Vol. 56, 1501-1506.

Stumpfl. E.F. (1961) Some new platinoid-rich minerals, identified with the electron micro-analyser. Minerall Mag. Vol.32. pp.833-847.

Stumpfl. E.F. & Clark A. M. (1965) Hollingworthite, a new rhodium mineral identified by electron-probe microanalysis. AM. Minerlog. Vol. 50 pp.1068-1074.

Stumpfl. E.F. and Clark A.M. (1966) Electron-probe microanalysis of gold-platinoid concentrates from southeast Borneo. Trans. Inst. Min. Metall. Vol.74, pp.933-946.

Stumpfl. E.F. and Tarkian M. (1973) Natural osmium-iridium alloys and iron-bearing platinum, new electron probe and optical data. N. Jb. Miner Mh. h. 7/8 pp 313-322.

Stumpfl. E.F. (1974) The ganesis of platinum deposits. Further thoughts. Minerals. Sci. Engng. Vol. 6 no.3 July.

Uytenbogaardt. W. and Burke E.A.J. (1971)	Tables for microscopic identification of ore minerals . New York, Elsevier.
Uytenbogaardt. W. and Burke E.A.J. (1951)	First edition.
Vacher H.C. Bechtoldt C.J. & Maxwell E (1954)	Structure of some iridium-osmium alloys J. Metals Vol.6. p.80.
Vlausova YE.N. and Sapozhkoval T.P.(1970)	"Ordering in Fe-Pt alloys". Phys. of Met. and Metall 30. (5) pp.85-89 . UDC 66.15.539.26.
Walaston.WH. (1805)	Phil. Trans. Vol. 95. p.316.
Wise E.M. (1948)	Handbook of Metals.
Wanger P.A.(1929)	The platinum deposits and mines of South Africa London Oliver and Boyd.
Wright T.L. and Fleischer M. (1965)	Geochemistry of the platinum metals, U.S. Geol. Survey. Bull. 1214-A. Washington.
Westland A.D. and Beamish F.E. (1958)	The chemical analysis of iridosmines and other platinum metal minerals. Am. Mineralogist, Vol.43 pp.503-516.
Young B.B. and Millman. A.P. (1964)	Microhardness and deformation characteristics of pre minerals.Trans. Inst. Min. Metall Vol,73 pp.437-466.
* Cahn, R.W. (1970)	Physical Metallurgy. North Holland p.1020.
Suzuki, H (1957)	Dislocations and Mechanical properties of crystals. J.C. Fisher et al, eds. (John Wiley and Sons, New York).

(ZAF) Programme. Duncumb and Jones (1969) Tube Investments.